UNIVERSITY OF CALIFORNIA SAN DIEGO

HSP27 regulation of GPCR-induced vascular inflammation

A dissertation submitted in partial satisfaction of the
requirements for the degree
Doctor of Philosophy

in

Biomedical Sciences

by

Cara Coleen Rada

Committee in charge:

Professor JoAnn Trejo, Chair
Professor Richard Daneman
Professor Silvio Gutkind
Professor Tracy Handel
Professor Tony Hunter
Professor Alexandra Newton

2020

The dissertation of Cara Coleen Rada is approved, and it is acceptable in quality and form for publication on microfilm and electronically:

_____

_____

_____

_____

_____

_____

Chair

University of California San Diego

2020

DEDICATION

To:

My Mother and Father, who have been a resounding supportive presence from 2000 miles away, despite no direct flights.

TABLE OF CONTENTS

Signature Page . . . iii

Dedication . . . iv

Table of Contents . . . v

List of Figures . . . vii

Acknowledgements . . . viii

Vita . . . x

Abstract of the Dissertation . . . xi

Chapter 1 Introduction: GPCR-induced vascular inflammation and its effectors . . . 1
1.1 Introduction . . . 1
1.1.1 Mechanisms of vascular inflammation . . . 2
1.1.2 GPCR-activated endothelial barrier disruption pathways . . . 4
1.1.3 Thrombin generation and PAR1 canonical signaling pathways . 6
1.1.4 p38 MAPK canonical and non-canonical activation . . . 7
1.1.5 HSP27 activity and phosphorylation . . . 9
1.1.6 Cytokine response to GPCR stimulation . . . 12
1.2 References . . . 13
1.3 Figures . . . 21

Chapter 2 PAR1-induced p38 activation causes specific phosphorylation of HSP27 through kinases MK2 and MK3 . . . 25
2.1 Introduction . . . 26
2.2 Results . . . 28
2.3 Conclusion and Discussion . . . 36
2.4 Materials and Methods . . . 39
2.5 Acknowledgements . . . 44
2.6 References . . . 45
2.7 Figures . . . 50

Chapter 3 PAR1 induced endothelial barrier recovery is mediated by HSP27 . . . 59
3.1 Introduction . . . 60
3.2 Results . . . 61
3.3 Conclusion and Discussion . . . 67
3.4 Materials and Methods . . . 68
3.5 Acknowledgements . . . 73
3.6 References . . . 74
3.7 Figures . . . 77

Chapter 4 GPCR regulation of non-canonical p38 and HSP27 IL-6 cytokine production 82
4.1 Introduction . . . 83
4.2 Results . . . 84
4.3 Conclusion and Discussion . . . 85
4.4 Materials and Methods . . . 86
4.5 Acknowledgements . . . 88
4.6 References . . . 90
4.7 Figures . . . 92

Chapter 5 Conclusion: Impact of GPCR-induced vascular inflammation resolution for therapeutic potential. . . . 94
5.1 Delineation of novel GPCR signaling pathway . . . 95
5.2 HSP27 function in controlling endothelial barrier properties . . . 96
5.3 Future Directions of HSP27 regulation of Barrier Resolution . . . 97
5.4 Final thoughts . . . 98
5.5 References . . . 99

Bibliography . . . 101

LIST OF FIGURES

Figure 1.1: Vascular Inflammation. 21
Figure 1.2: Gα12/13 and Gαq/11 signaling upon PAR1 activation. 22
Figure 1.3: p38 canonical and non-canonical signaling 23
Figure 1.4: HSP27 structure and activity 24

Figure 2.1: Thrombin-induced p38 signaling is not integrated with the RhoA/MLC pathway and promotes HSP27 phosphorylation 50
Figure 2.2: GPCR agonists stimulate p38-dependent HSP27 phosphorylation in multiple endothelial cell types. 52
Figure 2.3: PHOXTRACK computational software results selecting MAPKAPK2 (MK2) and MAPKAPK3 (MK3) as causal HSPB1 (HSP27) kinases 54
Figure 2.4: MK2 and MK3 are required for thrombin-induced HSP27 phosphorylation . . 55
Figure 2.5: GPCR-induced HSP27 activity requires p38, MK2 and MK3. 57
Figure 2.6: PAR1 signaling pathway through HSP27 58

Figure 3.1: Loss of HSP27 enhances thrombin-induced endothelial barrier permeability *in vitro* 77
Figure 3.2: HSP27 phosphorylation is required for endothelial barrier recovery 79
Figure 3.3: Disruption of HSP27 oligomerization enhances PAR1-induced vascular leakage in vivo. 80

Figure 4.1: Thrombin and histamine induced IL-6 production requires non-canonical p38 92
Figure 4.2: Thrombin induced IL-6 production requires HSP27 93

ACKNOWLEDGEMENTS

This dissertation is a collection of my unique contribution to the scientific field over the last six years. And with each new advancement and discovery in my project, there were a plethora of other scientists and mentors who brought me there. I would specifically like to thank my mentor Professor JoAnn Trejo for encouraging my development of scientific autonomy, analytical interrogation, and exceptional guidance to disseminate my discoveries.

I would also like to thank the diverse group of scientists in my day-to-day activities for providing unique and creative insight. The Trejo lab and department of Pharmacology provided a supportive and ever resilient environment amongst my numerous failed experiments. So many lab members were ever present to provide a coffee or laugh to bridge me until the next successful experiment. I will forever be grateful for sharing their love of science with me, whether it be through a heated debate in the tissue culture room or staring at westerns until it felt like our eyes would bleed. So many of these interactions have helped me become the scientist I am today and I thank each of you immensely.

Chapter 2 and 3 is material submitted for publication in: **Rada CC**, Mejia-Pena H, Grimsey NJ, Canto-Cordova I, Olson J, Wozniak JM, Gonzalez DJ, Nizet V, Trejo J. “Heat Shock Protein 27 activity is linked to endothelial barrier recovery induced by GPCR pro-inflammatory mediator.” The dissertation author was the primary author.

A portion of chapter 4 figures are published as: Grimsey NJ, Lin Y, Narala R, **Rada CC**, Mejia-Pena H, Trejo J. “G protein-coupled receptors activate p38 MAPK via a non-canonical TAB1-TAB2- and TAB1-TAB3-dependent pathway in endothelial cells.” Journal of Biological Chemistry. 2019 Apr 12;294(15):5867-5878. This dissertation author is a co-author of the

manuscript and performed and designed experiments used in this dissertation.

VITA

2010	Bachelor of Arts in Biology, Wartburg College, Waverly, IA
2020	Doctor of Philosophy in Biomedical Sciences, University of California San Diego

PUBLICATIONS

Harrod JS, **Rada CC**, Pierce SL, England SK, Lamping KG. Altered contribution of RhoA/Rho kinase signaling in contractile activity of myometrium in leptin receptor-deficient mice. Am J Physiol Endocrinol Metab. 2011 Aug; 301(2):E362-9.

Rada CC Pierce SL, Nuno DW, Zimmerman K, Lamping KG, Bowdler NC, Weiss RM, England SK. Overexpression of the SK3 channel alters vascular remodeling during pregnancy, leading to fetal demise. Am J Physiol Endocrinol Metab. 2012 Oct 1; 303 (7):E825-31.

Odibo AO, **Rada CC**, Cahill AG, Goetzinger KR, Tuuli MG, Odibo L, Macones GA, England SK. First-trimester serum soluble fms-like tyrosine kinase-1, free vascular endothelial growth factor, placental growth factor and uterine artery Doppler in preeclampsia. J Perinatol. 2013 Sep; 33(9):670-4.

McCloskey C, **Rada CC**, Bailey E, van den Berg HA, Atia J, Rand DA, Shmygol A, Chan Y, Quenby S, Brosens JJ, Vatish M, Zhang J, Denton JS, Taggart MJ, Kettleborough C, Tickle D, Jerman J, Wright P, Dale T, Kanumilli S, Trezise DJ,Thornton S, Brown P, Catalano R, England SK Blanks AM. The inwardly rectifying K+ channel KIR7.1 controls uterine excitability throughout pregnancy. EMBO Mol. Med. 2014 Jul 23; 6(9):1161-74.

Rada CC Murray G, England SK. The SK3 Channel Promotes Placental Vascularization by Enhancing Secretion of Angiogenic Factors. Am J Physiol Endocrinol Metab. 2014 Nov 15;307(10):E935-43.

Rada CC, Pierce SL, Grotegut, CA, England, SK. Intrauterine Telemetry to Measure Mouse Contractile Pressure in vivo. J. Vis. Exp. (98), e52541, doi:10.3791/52541. 2015.

Grimsey NJ, Narala R, **Rada CC**, Zhang J, Lapek J, Gonzalez DJ, Stephens B, Handel T, Trejo J. A Tyrosine Switch on NEDD4-2 E3 Ligase Transmits GPCR Inflammatory Signaling. Cell Rep. 2018 Sept. 18; 24(12):3312-3323.e5.

Grimsey NJ, Lin Y, Narala R, **Rada CC**, Mejia-Pena H, Trejo J. G protein-coupled receptors activate p38 MAPK via a non-canonical TAB1-TAB2- and TAB1-TAB3-dependent pathway in endothelial cells. JBC. 2019 Apr 12;294(15):5867-5878.

ABSTRACT OF THE DISSERTATION

HSP27 regulation of GPCR-induced vascular inflammation

by

Cara Coleen Rada

Doctor of Philosophy in Biomedical Sciences

University of California San Diego, 2020

Professor JoAnn Trejo, Chair

The vascular endothelium plays a crucial role in maintaining fluid and macromolecule homeostasis through the body as well as propagating inflammatory responses as a result of pathogens and injuries. This process is generally protective and resolves efficiently. However, dysregulation of this process can lead to chronic inflammation in diseases such as diabetes and hypertension, or acute inflammatory conditions as seen in tissue edema or sepsis, in the presence of bacteria, and can lead to death. Understanding the mechanisms that underlie this balanced regulation and re-establishment of tissue homeostasis after inflammation is important to understand as it has a vast array of therapeutic potential for combating inflammation-driven

diseases. G-protein coupled receptors (GPCRs) are often activated by inflammatory mediators in the endothelium and are key modulators leading to endothelial barrier permeability and cytokine production. In this dissertation, I describe a novel mechanism for endothelial GPCR signaling through heat shock protein 27 (HSP27) in the resolution of vascular inflammation after GPCR-induction both *in vitro* and *in vivo*.

Chapter 1

Introduction: GPCR-induced vascular inflammation and its effectors

1.1 Introduction

Vascular inflammation is a tightly regulated process that is responsible for controlling endothelial permeability to plasma proteins into surrounding tissues to maintain tissue homeostasis and protect the body from pathogens and injuries. This process creates inflammatory mediators, many of which act as agonists on the transmembrane G protein-couple receptors (GPCRs) to promote endothelial barrier permeability and cytokine production (Sun and Ye, 2012, Goddard and Iruela-Arispe, 2013). However, the exact mechanism by which GPCRs promotes endothelial barrier permeability through pro-inflammatory signaling is unclear. The non-canonical activation of the major pro-inflammatory mediator, p38 MAPK, by GPCRs has been shown to promote endothelial barrier permeability (Grimsey et al., 2015, Borbiev et al., 2004). Yet despite vast efforts, no p38 inhibitors have progressed beyond phase II clinical trials (Gupta and Nebreda,

2015), indicating a need to better understand p38-dependent inflammatory signaling. Thus, a thorough understanding of how GPCRs-induce p38 mediated pro-inflammatory signaling may reveal new targets for drug development. The focus of this thesis dissertation is to elucidate the mechanism by which GPCR-activated p38 signaling to the heat shock protein 27 (HSP27) promotes vascular inflammation resolution.

1.1.1 Mechanisms of vascular inflammation

Blood vessels are essential physiological structures important for providing nutrients and oxygen throughout the body. The vascular endothelium creates the inner-most lining of blood vessel and provides a semi-permeable membrane to allow fluid and macromolecular homeostasis with the surrounding interstitium (Komarova and Malik, 2010). During inflammation disruption of the endothelial monolayer occurs creating interstitial spaces to allow large movement of fluids into surrounding tissues, leukocyte transmigration, and platelet aggregation (Fig. 1.1) (Mehta and Malik, 2006, Gavard, 2009). These interstitial spaces are created by disassembly of adherens junctions and contraction of acton and myosin crossbridges. In a non-pathophysiological state, vascular inflammation is a transitory state in which resolution of inflammatory mediators and the endothelial barrier occurs in a timely manner. In diseases where vascular inflammation remains in a chronic, sustained state, such as diabetes and acute lung injury, edema and hyperalgesia can occur (Sun and Ye, 2012). Acute failures of vascular inflammation resolution, such as seen sepsis with the presence of bacteria, can even lead to death.

Disruption of the endothelial monolayer through the paracellular pathway is a delicately choreographed event involving rearrangements of proteins involved in cell-cell contact in interendothelial junctions (IEJs). IEJs are comprised of tight junctions, adherens junctions, and

gap junctions that form a paracellular zipperlike structure through homophilic adhesions (Mehta and Malik, 2006, Sukriti et al., 2014). Gap junctions are comprised of two connexins from adjacent cells to create a pore and facilitates signaling molecules and transmembrane potentials (Sukriti et al., 2014). Tight junctions are comprised of occludins, claudins, and junctional adhesion molecules all which interact to provide junctional stability through interactions with zona occluden proteins to connect to the actin cytoskeleton. Tight junctions function more readily as rheostats and increases barrier properties with their increased expression, and thus are expressed most highly in the blood-brain barrier, the vascular bed with tightest barrier properties (Harris and Nelson, 2010). This enhanced function in the cerebral vasculature is recapitulated *in vivo* with the highest expressed tight junction, claudin-5, specific knockout mice having defects in their blood-brain barrier and dying shortly after parturition (Nitta et al., 2003).

Adherens junctions are the workhorse of the IEJs. Adherens junctions are comprised of VE-cadherin which connects calcium-dependent extracellular domains from adjacent cells, and catenins which connect to intracellular domains of VE-cadherin and create a scaffold for connections to the actin cytoskeleton (Dejana et al., 2008, Sukriti et al., 2014). VE-cadherin is required to maintain vascular integrity with gene deficiencies resulting in mouse embryonic lethality (Carmeliet et al., 1999). Adherens junctions are also a major site of cell signaling through post-translation modification, internalization, and transcriptional activators to effect multiple inflammatory pathways (Harris and Nelson, 2010).

While the IEJ proteins are important for disrupting paracellular adhesion, the actin cytoskeleton is required for gap junction formation through tensile forces pulling the endothelial cells away from each other. This is through the polymerization of globular (g)-actin into filamentous (f)- actin creating actin stress fibers. Stress fibers both internalize adherens and tight

junctions, and also cause changes in cell motility through isometric contractile machinery of actin and myosin filaments (Sukriti et al., 2014). It is through both IEJ protein disassembly and actomyosin machinery activation that gap junctions in the endothelial monolayer are created to allow the passage of macromolecules and fluids as well as leukocyte transmigration to promote inflammation. While much is known about the initiation of vascular inflammation, the natural resolution of vascular inflammation has been understudied and a mechanism of GPCR-induced barrier resolution will be addressed in this dissertation.

1.1.2 GPCR-activated endothelial barrier disruption pathways

Well-studied modulators of vascular inflammation are GPCRs. Many vascular inflammatory mediators such as histamine, bradykinin, prostaglandins, platelet activating factor, and thrombin all function as GPCR agonists affecting vascular function (Sun and Ye, 2012, Goddard and Iruela-Arispe, 2013). GRCPs are seven transmembrane receptors representing the largest family of FDA -approved druggable targets and the most abundant signaling receptor in the mammalian genome (Heng et al., 2013, Lappano and Maggiolini, 2011). GPCR activation occurs when a soluble extracellular ligand binds to the receptor causing a conformational change allowing the intracellular domains to engage and activate the intracellular heterotrimeric G protein signaling effectors $\alpha\beta\gamma$. Upon GPCR stimulation the disassociation of the α subunit from the $\beta\gamma$ subunits allow each subunit to have distinct, localized signaling profiles (Oldham and Hamm, 2008).

Activation of endothelial GPCRs by inflammatory mediators function initially to rapidly increase vascular endothelial permeability and secondarily to increase gene transcription of cytokines and chemokines to create a sustained increase in permeability through cytokine sig-

naling (Sun and Ye, 2012, Dejana et al., 2008). GPCR-induced disruption of the endothelial barrier to create gap junctions in the paracellular pathway is primarily mediated by disruption of cell-cell contact in the IEJ through the adherens junctions disassembly and contractility of the actin-myosin machinery (Mehta and Malik, 2006). Adherens junctions disassembly and internalization is initiated by the disassociation of VE-cadherin homophilic dimers through tyrosine phosphorylation (Vestweber, 2008, Dejana et al., 2008). Downstream GPCR effectors Gα13 and RhoA GTPase have been shown to induce VE-cadherin phosphorylation, disassembly, and internalization (Dejana et al., 2008, Gong et al., 2014). Catenins (α,β,γ and p120) are cadherin-associated proteins that provide a linkage from VE-cadherin to the actin cytoskeleton (Gavard, 2009). The GPCR agonists, histamine and thrombin, are both shown to induced catenin phosphorylation and disassociation from VE-cadherin, to destabilize the adherens junctions and a mechanism of GPCR-induced barrier disruption (Gavard, 2009, Parsons et al., 2010).

Modulation of the actin cytoskeleton is another major effector of gap junction formation and endothelial barrier permeability. GPCR-induced changes in actin cytoskeleton are often regulated by small GTPases (Parsons et al., 2010, Marinkovic et al., 2015). The Gα12/13 effector GTPase, RhoA, regulates stress fiber formation during cell contractions (Dejana et al., 2008). Another GTPase, Rac1, often has opposing effects to RhoA and modulates actin polymerization and reinforcement of cortical actin at the adherens junctions to stabilize the endothelial monolayer (Marinkovic et al., 2015). An additional key modulator of GPCR-induced actin modulation is through the myosin light chain phosphorylation to cause myosin to engage in with actin stress fibers to create tensile endothelial forces (Mehta and Malik, 2006) and will be discussed further in PAR1 canonical signaling pathways.

1.1.3 Thrombin generation and PAR1 canonical signaling pathways

One of the early steps of inflammation is the membrane protein, tissue factor—typically kept segregated from the blood—binding to its soluble receptor, factor VIIa, and through a series of zymogen conversions creating the protease thrombin (Levi et al., 2004). Thrombin irreversibly activates the GPCRs protease activated receptors (PAR) 1,2, and 4 through proteolytic cleavage of the N-terminus revealing a tethered ligand to bind intermolecularly on loop 2 of its cognate receptor and activate G protein signaling (Vu et al., 1991). Many cells of the vasculature including monocytes, dendritic cells, platelets, and endothelial cells express tissue factor and the PARs to specifically propagate inflammation (Chen and Dorling, 2009).

PAR1 is the prototype and the most abundantly expressed PAR in the vascular endothelium, and its activation by thrombin by cleaveage of the N-terminus at arginine 41 leads to endothelial barrier permeability, expression of adhesion molecules, and cytokine production (Sun and Ye, 2012). PAR1 has also shown biased agonism through alternative cleavage sites of the N-terminus. APC, for example, is shown to cleave PAR1 at arginine 46 and create cytoprotective effects on the endothelial barrier (Soh and Trejo, 2011). However, the majority of this thesis will focus on canonical cleavage of PAR1 through thrombin. Thrombin cleaved PAR1 has the ability to couple and signal through three distinct heterotrimeric G proteins, Gαq/11, Gαi, and Gα12/13 (Fig. 1.2) (Soh et al., 2010).

The α subunit of G12/13 induces RhoA activation through Rho guanine nucleotide exchange factor (GEFs) (Coughlin, 2000). RhoA can then activate Rho-activated kinases (ROCK) which phosphorylate and inhibit myosin light chain (MLC) phosphatases (Coughlin, 2000). MLC phosphorylation allows MLC to phosphorylate myosin and interact with F-actin creating stress fibers and causes endothelial contraction through the actomyosin contractility (Grimsey and

Trejo, 2016). This actin driven contraction also leads to adherens junction disassembly further disruption endothelial barrier properties (Mehta and Malik, 2006).

The α subunit of Gq/11 also converges on MLC phosphorylation through a different mechanism. This is facilitated through mobilization of phospholipase C-β (PLC-β) generating inositol 1,4,5-triphosphate (IP3) and diacylglycerol (DAG), which activate to increasing intracellular calcium and calmodulin (Grimsey and Trejo, 2016, Mehta and Malik, 2006, Alberelli and De Candia, 2014). Increased intracellular calcium allows protein kinase C (PKC) activation and canonical MAP kinase signaling cascades. Calcium and calmodulin also activate MLC kinase to phosphorylate MLC and again lead to the actomyosin contractility of the endothelial monolayer through stress fiber formation (Grimsey and Trejo, 2016). PKC-dependent kinases can also activate RhoA to affect cytoskeletal changes through ROCK similar to G12/13 pathways (Gavard and Gutkind, 2008).

Gαi inhibits adenylyl cyclase, a response primarily functioning in platelet responses (Coughlin, 2000). The G$\beta\gamma$ subunits activate phosphoinositide-3-kinase (PI3K), G protein-receptor kinases, potassium channels, and non-receptor tyrosine kinases (Alberelli and De Candia, 2014). With PI3K being the main effector by modifying the inner plasma membrane creating scaffolds for actin and signaling complexes (Coughlin, 2000). G$\beta\gamma$ subunits have also been implicated in the resolution of endothelial barrier permeability through focal adhesion kinase activation leading to the recovery of adherens junctions re-assembly (Knezevic et al., 2009).

1.1.4 p38 MAPK canonical and non-canonical activation

The activation of p38 mitogen-activated protein kinase (MAPK) is classically activated by cellular stresses through the three-tiered kinase cascade starting with MAPK kinase ki-

nases (MAPKKKs), activating MAPK kinases (MKKs), and finally activating MAPKs (Cuenda and Rousseau, 2007). Canonical activation of p38 MAPK (p38) occurs specifically by MKK3 and MKK6 phosphorylating the Thr-Gly-Tyr motif of p38 on threonine 180 and tyrosine 182 to cause activation through a conformational change (Fig. 1.3A)(Cuenda and Rousseau, 2007, Yang et al., 2014). GPCR-induces canonical p38 signaling through Gαq coupled signaling pathways by activation of MKK3/6 through either the PLC-DAG-PKC signaling or PLC-IP3-calcium-src signaling pathways (Goldsmith and Dhanasekaran, 2007). There are four mammalian isoforms of p38 α,β,γ,δ and all are activated by the three-tiered kinase cascade and share approximately 60 percent homology (Cuenda and Rousseau, 2007, Cuadrado and Nebreda, 2010).

The p38α isoform is the most abundant isoform and is reported to be activated non-canonically independent of the MKK pathway (Martinez-Limon et al., 2020). The first mechanism is described in T cells through the T cell antigen receptor where a tyrosine kinase, ZAP70, phosphorylates p38 on Tyrosine 323 to causing p38 autoactivation. This autoactivation causes a conformational change allowing phosphorylation of its own Thr-Gly-Tyr motif as well as other downstream effectors (Fig. 1.3B) (Salvador et al., 2005a, Salvador et al., 2005b). The second pathway of autophosphorylation of the p38α isoform can occur by directly binding transforming growth factor β-activated kinase -1 (TAB1) (Cuenda and Rousseau, 2007). TAB1 promotes a conformational change to p38 enabling autophosphorylation in cis and increases p38α affinity toward ATP (DeNicola et al., 2013).

PAR1 has been shown to activate non-canonical p38 activation through the E3 ubiquitin ligase, Nedd4-2. Ubiquitination of the receptor allows TAB2 to bind through a zinc-finger domain to the K63-linked ubiquitin moiety (Grimsey et al., 2015). TAB2 stabilizes TAB1 and allows p38 to bind to the complex and autoactivate (Fig. 1-3C) (Grimsey et al., 2015, Grimsey and Trejo,

2016). TAB3 can act as a functional homolog for TAB2 in this pathway to also stabilize TAB1 and bind to the K63-linked ubiquitin (Fig 1.3C)(Grimsey et al., 2019). Other GPCR agonists such as histamine, prostaglandin E2, and ADP can also activate non-canonical p38 through this mechanism (Grimsey et al., 2019). PAR1 can activate p38 (Borbiev et al., 2004) through this non-canonical pathway to lead to endothelial barrier permeability (Grimsey et al., 2015) and the mechanism in which this occurs is a main focus of this dissertation.

1.1.5 HSP27 activity and phosphorylation

The small heat shock protein 27 (HSP27) is a small ATP-independent chaperone regulating multiple cellular functions including protein folding, cytoskeletal architecture, and cell growth and metabolism (Kostenko and Moens, 2009). HSP27 has a highly conserved α-crystallin domain (ACD), a WDPF N-terminal domain, and a short, flexible C-terminal domain (Fig. 1.4A) (Kostenko and Moens, 2009). HSP27 forms homodimers with the alignment of the β 6 and 7 strands in the ACD of adjacent HSP27 monomers (Haslbeck et al., 2019, Mymrikov et al., 2020, Lambert et al., 1999). HSP27 can form larger homo- and hetero-oligomers up to 800 kDa through a mechanism not completely understood but the use of WDPF domain, ACD, and flexible regions of HSP27 domains are implicated, with the WDPF domain regulating higher order multimers (Kostenko and Moens, 2009, Mymrikov et al., 2020, Lambert et al., 1999).

HSP27 regulates its modulation of the cytoskeleton through oligomerization and can function as an actin capping protein to inhibit F-actin formation (Fig. 1.4B) (Pichon et al., 2004, Rogalla et al., 1999, Benndorf et al., 1994). HSP27 can also prevent action polymerization through globular actin sequestration (During et al., 2007). The phosphorylation of HSP27 causes a conformational change and disrupts large HSP27 oligomeric complexes and releases

its constraints on actin and decreases chaperone function (Rogalla et al., 1999, Salinthone et al., 2008). This disassociation of HSP27 oligomers allows polymerization of F-actin. F-Actin polymerization contributes to endothelial barrier disruption through modulation of actin-myosin contractility by creating tensile forces to pull the endothelial monolayer apart and create gap junctions. Complete dissociation of HSP27 oligomers *in vitro* are regulated by phosphorylation of three serine residues of HSP27: 15, 78, and 82. This was determined through a series of *in vitro* mutagenesis studies, in which a constitutively phosphorylated mutant for one, two, or all three serines were phosphorylated, and oligomerization status assessed through size exclusion gel filtration and confirmed with electron microscopy and light scattering experiments (Rogalla et al., 1999). Serine 15 is found in the WDPF domain while serine 78 and 82 are found in the flexible region immediately prior to the ACD. It is unknown the implication of each phosphosite alone in contributing to endothelial barrier permeability.

The predominate pathway of HSP27 phosphorylation is through p38 regulated mitogen-activated protein kinase-activated protein kinases (MKs), although PKC and PKD have also been shown to phosphorylate HSP27 independent of p38 pathways (Kostenko and Moens, 2009, Evans et al., 2008). Kinase specificity for each of the three HSP27 phosphosites are cell type and stimulation dependent. Endothelial modulations of HSP27-induced microfilament dynamics is generally accepted to be regulated and phosphorylated by the p38-MK2 signaling axis upon stimulation of a stressor such as osmotic stress or UV light (Huot et al., 1997, Kostenko and Moens, 2009). MK3 and MK5, which have a high degree of homology in the catalytic domain to MK2, are also thought to be major regulators of HSP27 phosphorylation and MK2 is exclusively regulated by p38α (Gaestel, 2006). MK5 has been shown to phosphorylate HSP27 in endothelial cells, while MK3 has only phosphorylated HSP27 in *in vitro* settings

(Huot et al., 1997). Thrombin stimulation causes p38-MK2-induced phosphorylation of HSP27 in platelets (Tokuda et al., 2016) and vascular smooth muscle cell lines (Nakajima et al., 2005, Brophy et al., 1998), but endothelial specific GPCR-induced HSP27 phosphorylation is unknown and will be addressed in this thesis.

HSP27 phosphorylation is a reversible process, but dephosphorylation of HSP27 has been studied to a lesser extent. Protein phosphatase 2A (PP2A) has been implicated as the main phosphatase to dephosphorylate HSP27 *in vitro* and *in vivo* with direct activity on HSP27 and indirectly through MK2 dephosphorylation and deactivation (Cairns et al., 1994, Kostenko and Moens, 2009). To a lesser extent, PP2B and protein phosphatase 1 exhibit phosphatase activity with purified proteins *in vitro* but this function is not recapitulated *in vivo* (Cairns et al., 1994, Kostenko and Moens, 2009).

While it is well established HSP27 functionally regulates actin dynamics, little work has been done to examine HSP27's role on endothelial barrier permeability. One study demonstrated endothelial overexpression of HSP27 preserves blood brain barrier integrity after oxygen deprivation *in vitro* and *in vivo*, suggesting a role for HSP27 in regulation of endothelial barrier permeability (Shi et al., 2017). Another study showed specific phosphorylation of HSP27 has a protective response to hyperpermeability after burn serum challenge in the endothelium, implicating the phosphorylation of HSP27 being required for endothelial barrier permeability (Sun et al., 2015). Whether HSP27 and its phosphorylation status mediates GPCR-induced endothelial barrier permeability is not known and will be addressed in this dissertation.

1.1.6 Cytokine response to GPCR stimulation

A second main effect of endothelial GPCR stimulation is transcriptional regulation of genes encoding cytokines, chemokines and adhesion molecules. This creates a prolonged, sustained inflammatory response opposed to the more rapid responses of endothelial barrier permeability through cell signaling to adherens junctions and actomyosin contractility. Endothelial GPCRs coupled to G proteins Gαi and Gαq/11 lead to activation of transcription factors such as CREB, c-Jun, NF-$\kappa\beta$, and STAT3 to translocate to the nucleus to regulation pro-inflammatory gene expression (Sun and Ye, 2012).

Specifically, thrombin has been shown to upregulate the pro-inflammatory genes including interleukin (IL)-1, IL-6, IL-8, vascular cell adhesion molecule 1 (VCAM-1), intercellular adhesion molecule 1 (VCAM1), monocyte chemotactic protein-1 (MCP-1) and P-selectin (Naldini et al., 2000, Ellinghaus et al., 2016, Marin et al., 2001). Increased transcription of these genes leads to cytokine production and leukocyte recruitment, adherence, rolling, and transmigration, all essential for the inflammatory response (Granger and Senchenkova, 2010). IL-6, specifically, is a potent multifunctional pro-inflammatory cytokine that has been shown to be secreted by endothelial cells after thrombin and histamine stimulation and regulated in a p38-dependent manner (Marin et al., 2001, Li et al., 2001). How thrombin-induced non-canonical p38 and HSP27 affect cytokine induction is not known and will be the focus of chapter 4 of this dissertation.

1.2 References

ALBERELLI, M. A. DE CANDIA, E. 2014. Functional role of protease activated receptors in vascular biology. Vascul Pharmacol, 62, 72-81.

BENNDORF, R., HAYESS, K., RYAZANTSEV, S., WIESKE, M., BEHLKE, J. LUTSCH, G. 1994. Phosphorylation and supramolecular organization of murine small heat shock protein HSP25 abolish its actin polymerization-inhibiting activity. J Biol Chem, 269, 20780-4.

BORBIEV, T., BIRUKOVA, A., LIU, F., NURMUKHAMBETOVA, S., GERTHOFFER, W. T., GARCIA, J. G. VERIN, A. D. 2004. p38 MAP kinase-dependent regulation of endothelial cell permeability. Am J Physiol Lung Cell Mol Physiol, 287, L911-8.

BROPHY, C. M., BEALL, A., MANNES, K., LAMB, S., DICKINSON, M., WOODRUM, D. DEVOE, L. D. 1998. Heat shock protein expression in umbilical artery smooth muscle. J Reprod Fertil, 114, 351-5.

CAIRNS, J., QIN, S., PHILP, R., TAN, Y. H. GUY, G. R. 1994. Dephosphorylation of the small heat shock protein Hsp27 in vivo by protein phosphatase 2A. J Biol Chem, 269, 9176-83.

CARMELIET, P., LAMPUGNANI, M. G., MOONS, L., BREVIARIO, F., COMPERNOLLE, V., BONO, F., BALCONI, G., SPAGNUOLO, R., OOSTHUYSE, B., DEWERCHIN, M., ZANETTI, A., ANGELLILO, A., MATTOT, V., NUYENS, D., LUTGENS, E., CLOTMAN, F., DE RUITER, M. C., GITTENBERGER-DE GROOT, A., POELMANN, R., LUPU, F., HERBERT, J. M., COLLEN, D. DEJANA, E. 1999. Targeted deficiency or cytosolic truncation of the VE-cadherin gene in mice impairs VEGF-mediated endothelial survival and angiogenesis. Cell, 98, 147-57.

CHEN, D. DORLING, A. 2009. Critical roles for thrombin in acute and chronic inflammation. J Thromb Haemost, 7 Suppl 1, 122-6.

COUGHLIN, S. R. 2000. Thrombin signalling and protease-activated receptors. Nature, 407, 258-64.

CUADRADO, A. NEBREDA, A. R. 2010. Mechanisms and functions of p38 MAPK signalling. Biochem J, 429, 403-17.

CUENDA, A. ROUSSEAU, S. 2007. p38 MAP-kinases pathway regulation, function and role in human diseases. Biochim Biophys Acta, 1773, 1358-75.

DEJANA, E., ORSENIGO, F. LAMPUGNANI, M. G. 2008. The role of adherens junctions and VE-cadherin in the control of vascular permeability. J Cell Sci, 121, 2115-22.

DENICOLA, G. F., MARTIN, E. D., CHAIKUAD, A., BASSI, R., CLARK, J., MARTINO, L., VERMA, S., SICARD, P., TATA, R., ATKINSON, R. A., KNAPP, S., CONTE, M. R. MARBER, M. S. 2013. Mechanism and consequence of the autoactivation of p38alpha mitogen-activated protein kinase promoted by TAB1. Nat Struct Mol Biol, 20, 1182-90.

DURING, R. L., GIBSON, B. G., LI, W., BISHAI, E. A., SIDHU, G. S., LANDRY, J. SOUTHWICK, F. S. 2007. Anthrax lethal toxin paralyzes actin-based motility by blocking Hsp27 phosphorylation. EMBO J, 26, 2240-50.

ELLINGHAUS, P., PERZBORN, E., HAUENSCHILD, P., GERDES, C., HEITMEIER, S., VISSER, M., SUMMER, H. LAUX, V. 2016. Expression of pro-inflammatory genes in human endothelial cells: Comparison of rivaroxaban and dabigatran. Thromb Res, 142, 44-51.

EVANS, I. M., BRITTON, G. ZACHARY, I. C. 2008. Vascular endothelial growth factor induces heat shock protein (HSP) 27 serine 82 phosphorylation and endothelial tubulogenesis via protein kinase D and independent of p38 kinase. Cell Signal, 20, 1375-84.

GAESTEL, M. 2006. MAPKAP kinases - MKs - two's company, three's a crowd. Nat Rev Mol

Cell Biol, 7, 120-30.

GAVARD, J. 2009. Breaking the VE-cadherin bonds. FEBS Lett, 583, 1-6.

GAVARD, J. GUTKIND, J. S. 2008. Protein kinase C-related kinase and ROCK are required for thrombin-induced endothelial cell permeability downstream from Galpha12/13 and Galpha11/q. J Biol Chem, 283, 29888-96.

GODDARD, L. M. IRUELA-ARISPE, M. L. 2013. Cellular and molecular regulation of vascular permeability. Thromb Haemost, 109, 407-15.

GOLDSMITH, Z. G. DHANASEKARAN, D. N. 2007. G protein regulation of MAPK networks. Oncogene, 26, 3122-42.

GONG, H., GAO, X., FENG, S., SIDDIQUI, M. R., GARCIA, A., BONINI, M. G., KOMAROVA, Y., VOGEL, S. M., MEHTA, D. MALIK, A. B. 2014. Evidence of a common mechanism of disassembly of adherens junctions through Galpha13 targeting of VE-cadherin. J Exp Med, 211, 579-91.

GRANGER, D. N. SENCHENKOVA, E. 2010. Inflammation and the Microcirculation. San Rafael (CA).

GRIMSEY, N. J., AGUILAR, B., SMITH, T. H., LE, P., SOOHOO, A. L., PUTHENVEEDU, M. A., NIZET, V. TREJO, J. 2015. Ubiquitin plays an atypical role in GPCR-induced p38 MAP kinase activation on endosomes. J Cell Biol, 210, 1117-31.

GRIMSEY, N. J., LIN, Y., NARALA, R., RADA, C. C., MEJIA-PENA, H. TREJO, J. 2019. G protein-coupled receptors activate p38 MAPK via a non-canonical TAB1-TAB2- and TAB1-TAB3-dependent pathway in endothelial cells. J Biol Chem, 294, 5867-5878.

GRIMSEY, N. J. TREJO, J. 2016. Integration of endothelial protease-activated receptor-1 inflammatory signaling by ubiquitin. Curr Opin Hematol, 23, 274-9.

GUPTA, J. NEBREDA, A. R. 2015. Roles of p38alpha mitogen-activated protein kinase in mouse models of inflammatory diseases and cancer. FEBS J, 282, 1841-57.

HARRIS, E. S. NELSON, W. J. 2010. VE-cadherin: at the front, center, and sides of endothelial cell organization and function. Curr Opin Cell Biol, 22, 651-8.

HASLBECK, M., WEINKAUF, S. BUCHNER, J. 2019. Small heat shock proteins: Simplicity meets complexity. J Biol Chem, 294, 2121-2132.

HENG, B. C., AUBEL, D. FUSSENEGGER, M. 2013. An overview of the diverse roles of G-protein coupled receptors (GPCRs) in the pathophysiology of various human diseases. Biotechnol Adv, 31, 1676-94.

HUOT, J., HOULE, F., MARCEAU, F. LANDRY, J. 1997. Oxidative stress-induced actin reorganization mediated by the p38 mitogen-activated protein kinase/heat shock protein 27 pathway in vascular endothelial cells. Circ Res, 80, 383-92.

KNEZEVIC, N., TAUSEEF, M., THENNES, T. MEHTA, D. 2009. The G protein betagamma subunit mediates reannealing of adherens junctions to reverse endothelial permeability increase by thrombin. J Exp Med, 206, 2761-77.

KOMAROVA, Y. MALIK, A. B. 2010. Regulation of endothelial permeability via paracellular and transcellular transport pathways. Annu Rev Physiol, 72, 463-93.

KOSTENKO, S. MOENS, U. 2009. Heat shock protein 27 phosphorylation: kinases, phosphatases, functions and pathology. Cell Mol Life Sci, 66, 3289-307.

LAMBERT, H., CHARETTE, S. J., BERNIER, A. F., GUIMOND, A. LANDRY, J. 1999. HSP27 multimerization mediated by phosphorylation-sensitive intermolecular interactions at the amino terminus. J Biol Chem, 274, 9378-85.

LAPPANO, R. MAGGIOLINI, M. 2011. G protein-coupled receptors: novel targets for drug discovery in cancer. Nat Rev Drug Discov, 10, 47-60.

LEVI, M., VAN DER POLL, T. BULLER, H. R. 2004. Bidirectional relation between inflammation and coagulation. Circulation, 109, 2698-704.

LI, Y., CHI, L., STECHSCHULTE, D. J. DILEEPAN, K. N. 2001. Histamine-induced production of interleukin-6 and interleukin-8 by human coronary artery endothelial cells is enhanced by endotoxin and tumor necrosis factor-alpha. Microvasc Res, 61, 253-62.

MARIN, V., FARNARIER, C., GRES, S., KAPLANSKI, S., SU, M. S., DINARELLO, C. A. KAPLANSKI, G. 2001. The p38 mitogen-activated protein kinase pathway plays a critical role in thrombin-induced endothelial chemokine production and leukocyte recruitment. Blood, 98, 667-73.

MARINKOVIC, G., HEEMSKERK, N., VAN BUUL, J. D. DE WAARD, V. 2015. The Ins and Outs of Small GTPase Rac1 in the Vasculature. J Pharmacol Exp Ther, 354, 91-102.

MARTINEZ-LIMON, A., JOAQUIN, M., CABALLERO, M., POSAS, F. DE NADAL, E. 2020. The p38 Pathway: From Biology to Cancer Therapy. Int J Mol Sci, 21.

MEHTA, D. MALIK, A. B. 2006. Signaling mechanisms regulating endothelial permeability. Physiol Rev, 86, 279-367.

MYMRIKOV, E. V., RIEDL, M., PETERS, C., WEINKAUF, S., HASLBECK, M. BUCHNER, J. 2020. Regulation of small heat-shock proteins by hetero-oligomer formation. J Biol Chem, 295,

158-169.

NAKAJIMA, K., HIRADE, K., ISHISAKI, A., MATSUNO, H., SUGA, H., KANNO, Y., SHU, E., KITAJIMA, Y., KATAGIRI, Y. KOZAWA, O. 2005. Akt regulates thrombin-induced HSP27 phosphorylation in aortic smooth muscle cells: function at a point downstream from p38 MAP kinase. Life Sci, 77, 96-107.

NALDINI, A., CARNEY, D. H., PUCCI, A., PASQUALI, A. CARRARO, F. 2000. Thrombin regulates the expression of proangiogenic cytokines via proteolytic activation of protease-activated receptor-1. Gen Pharmacol, 35, 255-9.

NITTA, T., HATA, M., GOTOH, S., SEO, Y., SASAKI, H., HASHIMOTO, N., FURUSE, M. TSUKITA, S. 2003. Size-selective loosening of the blood-brain barrier in claudin-5-deficient mice. J Cell Biol, 161, 653-60.

OLDHAM, W. M. HAMM, H. E. 2008. Heterotrimeric G protein activation by G-protein-coupled receptors. Nat Rev Mol Cell Biol, 9, 60-71.

PARSONS, J. T., HORWITZ, A. R. SCHWARTZ, M. A. 2010. Cell adhesion: integrating cytoskeletal dynamics and cellular tension. Nat Rev Mol Cell Biol, 11, 633-43.

PICHON, S., BRYCKAERT, M. BERROU, E. 2004. Control of actin dynamics by p38 MAP kinase - Hsp27 distribution in the lamellipodium of smooth muscle cells. J Cell Sci, 117, 2569-77.

ROGALLA, T., EHRNSPERGER, M., PREVILLE, X., KOTLYAROV, A., LUTSCH, G., DUCASSE, C., PAUL, C., WIESKE, M., ARRIGO, A. P., BUCHNER, J. GAESTEL, M. 1999. Regulation of Hsp27 oligomerization, chaperone function, and protective activity against oxidative stress tumor necrosis factor alpha by phosphorylation. Journal of Biological Chemistry, 274, 18947-18956.

SALINTHONE, S., TYAGI, M. GERTHOFFER, W. T. 2008. Small heat shock proteins in smooth muscle. Pharmacol Ther, 119, 44-54.

SALVADOR, J. M., MITTELSTADT, P. R., BELOVA, G. I., FORNACE, A. J., JR. ASHWELL, J. D. 2005a. The autoimmune suppressor Gadd45alpha inhibits the T cell alternative p38 activation pathway. Nat Immunol, 6, 396-402.

SALVADOR, J. M., MITTELSTADT, P. R., GUSZCZYNSKI, T., COPELAND, T. D., YAMAGUCHI, H., APPELLA, E., FORNACE, A. J., JR. ASHWELL, J. D. 2005b. Alternative p38 activation pathway mediated by T cell receptor-proximal tyrosine kinases. Nat Immunol, 6, 390-5.

SHI, Y., JIANG, X., ZHANG, L., PU, H., HU, X., ZHANG, W., CAI, W., GAO, Y., LEAK, R. K., KEEP, R. F., BENNETT, M. V. CHEN, J. 2017. Endothelium-targeted overexpression of heat shock protein 27 ameliorates blood-brain barrier disruption after ischemic brain injury. Proc Natl Acad Sci U S A, 114, E1243-E1252.

SOH, U. J., DORES, M. R., CHEN, B. TREJO, J. 2010. Signal transduction by protease-activated receptors. Br J Pharmacol, 160, 191-203.

SOH, U. J. TREJO, J. 2011. Activated protein C promotes protease-activated receptor-1 cyto-protective signaling through beta-arrestin and dishevelled-2 scaffolds. Proc Natl Acad Sci U S A, 108, E1372-80.

SUKRITI, S., TAUSEEF, M., YAZBECK, P. MEHTA, D. 2014. Mechanisms regulating endothelial permeability. Pulm Circ, 4, 535-51.

SUN, H. B., REN, X., LIU, J., GUO, X. W., JIANG, X. P., ZHANG, D. X., HUANG, Y. S. ZHANG, J. P. 2015. HSP27 phosphorylation protects against endothelial barrier dysfunction under burn serum challenge. Biochem Biophys Res Commun, 463, 377-83.

SUN, L. YE, R. D. 2012. Role of G protein-coupled receptors in inflammation. Acta Pharmacol Sin, 33, 342-50.

TOKUDA, H., KUROYANAGI, G., TSUJIMOTO, M., MATSUSHIMA-NISHIWAKI, R., AKAMATSU, S., ENOMOTO, Y., IIDA, H., OTSUKA, T., OGURA, S., IWAMA, T., KOJIMA, K. KOZAWA, O. 2016. Thrombin Receptor-Activating Protein (TRAP)-Activated Akt Is Involved in the Release of Phosphorylated-HSP27 (HSPB1) from Platelets in DM Patients. Int J Mol Sci, 17.

VESTWEBER, D. 2008. VE-cadherin: the major endothelial adhesion molecule controlling cellular junctions and blood vessel formation. Arterioscler Thromb Vasc Biol, 28, 223-32.

VU, T. K., HUNG, D. T., WHEATON, V. I. COUGHLIN, S. R. 1991. Molecular cloning of a functional thrombin receptor reveals a novel proteolytic mechanism of receptor activation. Cell, 64, 1057-68.

YANG, Y., KIM, S. C., YU, T., YI, Y. S., RHEE, M. H., SUNG, G. H., YOO, B. C. CHO, J. Y. 2014. Functional roles of p38 mitogen-activated protein kinase in macrophage-mediated inflammatory responses. Mediators Inflamm, 2014, 352371.

1.3 Figures

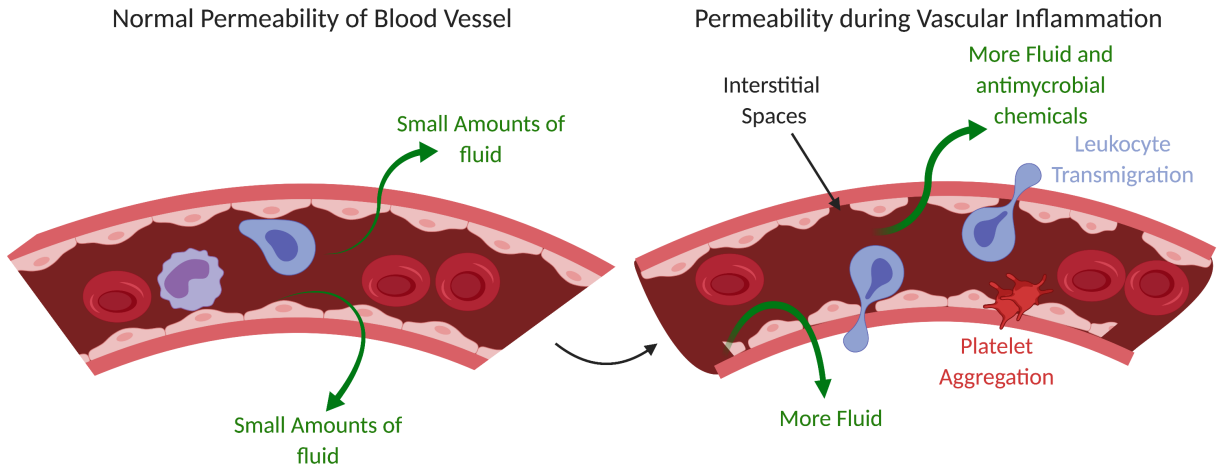

Figure 1.1: Vascular Inflammation. The vascular endothelium creates a semi-permeability membrane with relatively low movement of fluids and macromolecules into surrounding tissues. Vascular inflammation creates interstitial spaces to allow large movement of fluids and antimicrobial chemicals into surrounding tissues. This also facilitates leukocyte transmigration and platelet aggregation.

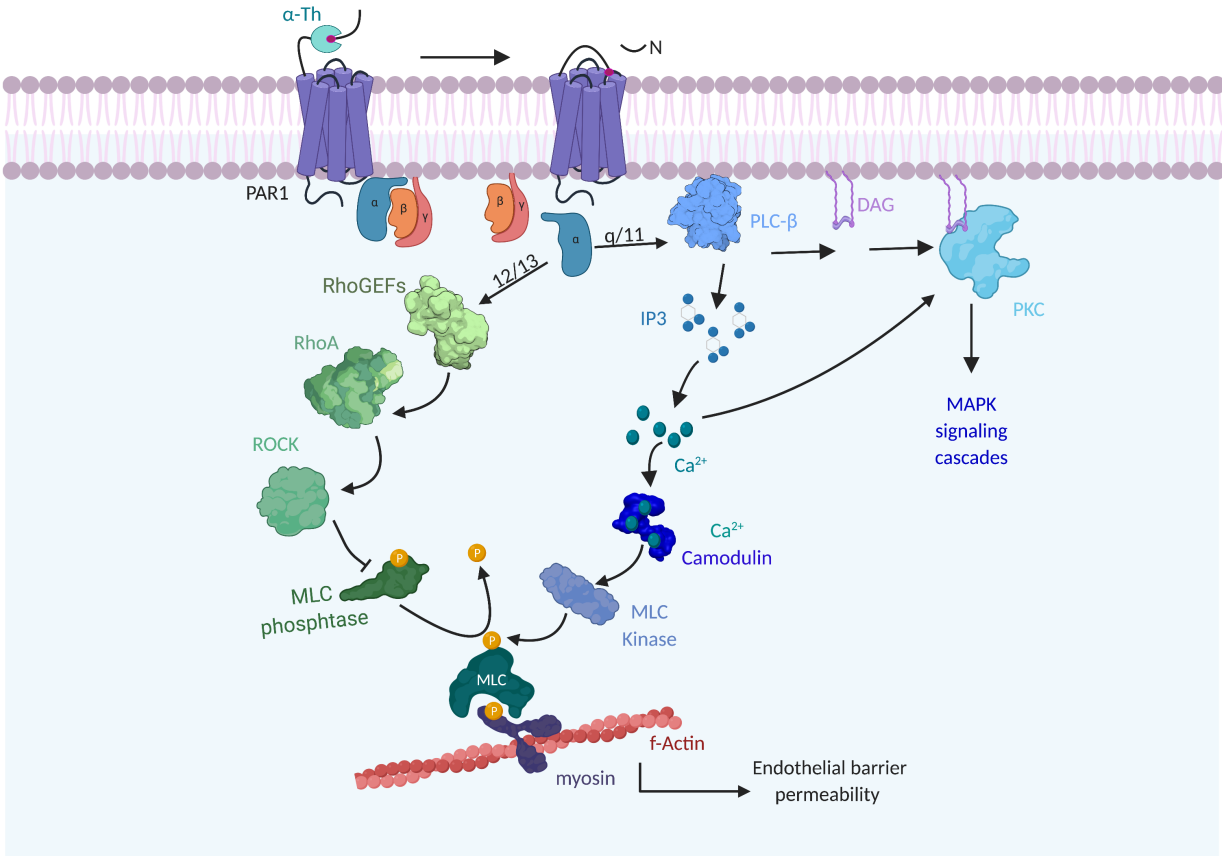

Figure 1.2: Gα12/13 and Gαq/11 signaling upon PAR1 activation. In the endothelium, thrombin-activated PAR1 couples to Gαq which activates and mobilizes phospholipase C-β (PLC-β) generating inositol 1,4,5-triphosphate (IP3) and diacylglycerol (DAG). IP3 generation allows calcium (Ca^{2+}) mobilization. Ca^{2+} can either activate protein kinase C (PKC) with DAG to facilitate canonical MAP kinase signaling cascades, or Ca^{2+} in conjuncture with calmodulin allow myosin light chain (MLC) phosphorylation that initiates actin myosin contractility and pulls the endothelial monolayer apart through interactions with filamentous (f)-actin and producing endothelial permeability. PAR1 also couples to Gα12/13 and activates RhoA through Rho guanine nucleotide exchange factor (GEFs). RhoA then activates Rho-activated kinases (ROCK) which phosphorylate and inhibit MLC phosphatases. Again, phosphorylated MLC can interact with f-actin and produce endothelial permeability.

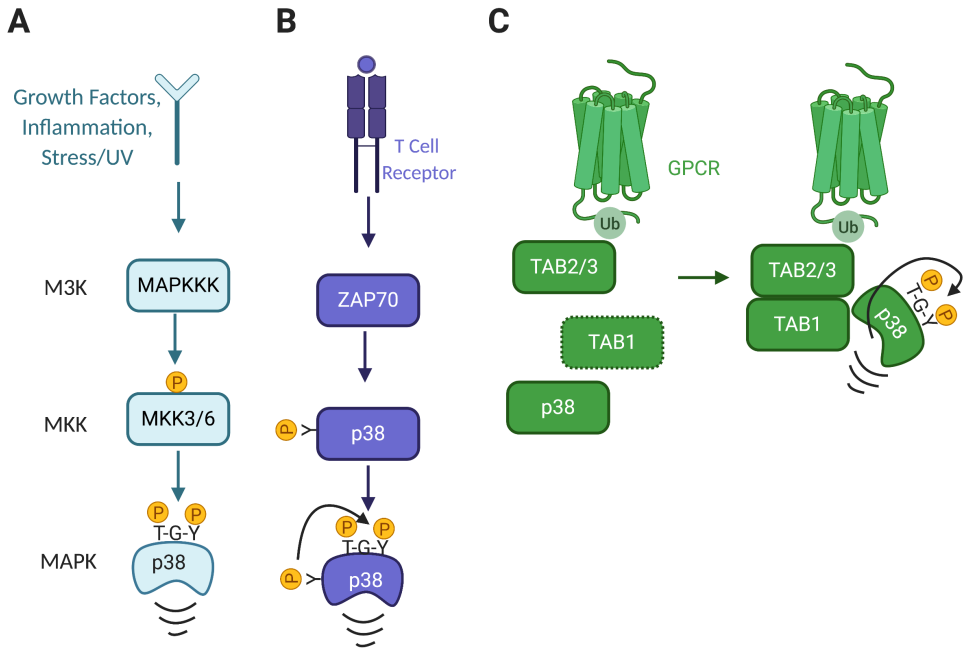

Figure 1.3: p38 MAPK canonical and non-canonical signaling. A.) Classic canonical p38 mitogen-activated protein kinase (MAPK) 3 tier kinase cascade signaling. External stimuli activate MAPK kinase kinases (MAPKKKs) which phosphorylates MAPK kinases (MKKs), and then to phosphorylate p38 MAPKs. B.) Non-canonical p38 activation in T cells, where T cell receptor gets stimulated and activates the kinase ZAP70, which phosphorylates p38 at a non-canonical residue causing a conformational change and autophosphorylation of p38. C.) GPCR-induced p38 non-canonical activation begins with GPCR ubiquitination. TAB2 to associates with the receptor at the site of ubiquitination and allows TAB1 to stabilize and form a complex. p38 bind to the complex causing a conformational change and autoactivates.

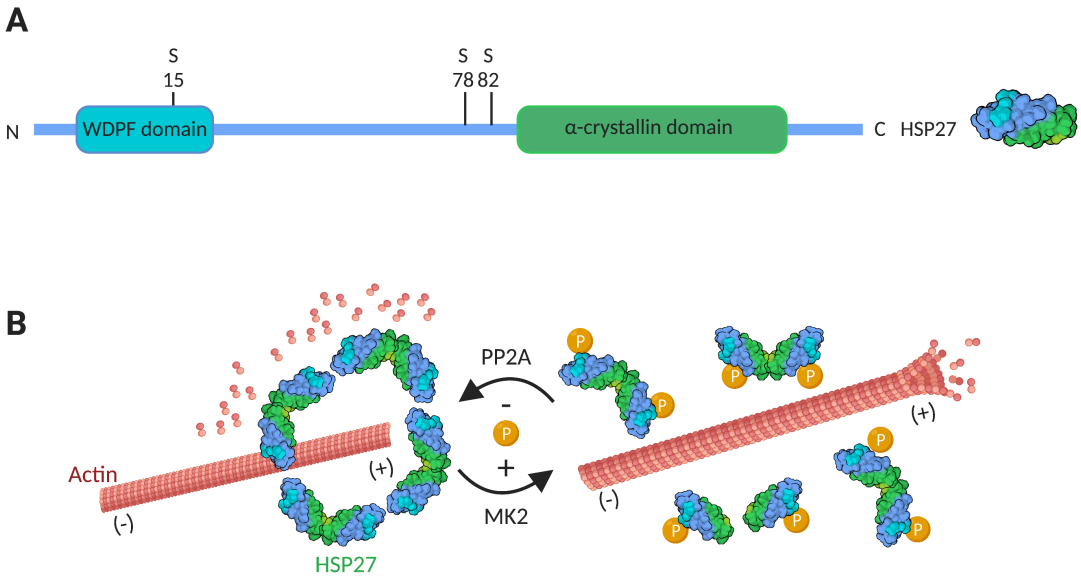

Figure 1.4: HSP27 structure and activity. A.) Heat shock protein (HSP) 27 protein has a highly conserved α-crystallin domain, a WDPF N-terminal domain, and a short, flexible C-terminal domain. The three phosphorylated serines (S) at highlighted with residue of phosphorylation. B.) HSP27 regulation of the cytoskeleton through oligomerization and function as an actin capping protein to inhibit f-actin formation. Phosphorylation of HSP27 by the kinase MAPKAPK2 (MK2) and dephosphorylation of HSP27 by protein phosphatase 2A (PP2A) causing formation and disruption of large HSP27 oligomeric complexes.

Chapter 2

PAR1-induced p38 activation causes specific phosphorylation of HSP27 through kinases MK2 and MK3

Vascular inflammation results in increased endothelial barrier permeability and tissue edema. Protease-activated receptor-1 (PAR1), a G protein-coupled receptor (GPCR) for thrombin, mediates hemostasis, thrombosis, and inflammatory responses including barrier disruption. Thrombin activation of PAR1 stimulates p38 MAPK pro-inflammatory signaling via a non-canonical pathway that promotes endothelial barrier disruption, a process that remains poorly understood. Using mass spectrometry phosphoproteomic analysis, we identified heat shock protein 27 (HSP27), which exists as a large oligomer and binds actin, as a promising candidate for p38-mediated barrier disruption. We confirm HSP27 phosphorylation is sensitive to p38 inhibition in microvascular and macrovascular endothelial cell lines after PAR1 or histamine

stimulation. We further show that MAPKAPK2 (MK2) and MAPKAPK3 (MK3), downstream kinases of p38, differentially phosphorylate HSP27 at three distinct sites Ser15, Ser78, and Ser82. While inhibition of thrombin-stimulated p38 activation ablated HSP27 phosphorylation, blockade of MK2 resulted in only loss of Ser15 and Ser78 phosphorylation, whereas both MK2 and MK3 are required for Ser82 phosphorylation. Moreover, thrombin-initiated disassembly of HSP27 oligomers requires p38 signaling and is dependent on both MK2 and MK3 activity. In this chapter we show GPCR activated p38 signals to MK2 and MK3 to specifically phosphorylate HSP27 and affect its activity through oligomerization.

2.1 Introduction

Vascular endothelial cells form a semi-permeable barrier that is important for normal tissue homeostasis. Disruption of the endothelial barrier by inflammatory mediators can lead to endothelial barrier disruption and cytokine production resulting in increased permeability, tissue edema, and subsequent organ failure (Komarova and Malik, 2010). Many inflammatory mediators act through G protein-coupled receptors (GPCR) to promote endothelial barrier disruption (Sun and Ye, 2012), however, the mechanism by which this occurs is not clearly understood. Protease-activated receptor-1 (PAR1), a GPCR for the protease thrombin, couples to Gαq and Gα12/13 proteins and causes endothelial permeability through increases in Ca^{2+}/PKC and RhoA activation (Komarova and Malik, 2010). These pathways converge on myosin light chain (MLC) phosphorylation, which promotes actin-myosin contractility and adherens junction disassembly resulting in endothelial barrier permeability.

Our group has demonstrated that PAR1 non-canonical activation of p38 MAPK occurs independent of the canonical 3-tier kinase cascade, and instead signals through a TAB1 de-

pendent pathway (Borbiev et al., 2004, Grimsey et al., 2015). We have further characterized multiple other GPCRs, including the H1 histamine receptor, can activate non-canonical p38 (Grimsey et al., 2019). We show non-canonical activation of p38 is an important mediator of PAR1-induced endothelial permeability (Grimsey et al., 2014). Other GPCRs, including the H1 receptor, have also been implicated to act through p38 to disrupt endothelial barrier disruption (Adderley et al., 2015). However, these studies have failed to provide a causative mechanism for how GPCR-activated p38 promotes endothelial barrier disruption.

Heat shock protein 27 (HSP27) is a small molecular chaperone that can oligomerize to function as an actin capping protein to inhibit F-actin formation (Pichon et al., 2004, Rogalla et al., 1999). Phosphorylation of HSP27 disrupts large HSP27 oligomeric complexes and releases its constraints on actin (Rogalla et al., 1999, Salinthone et al., 2008). This allows actin to polymerize, which can contribute to endothelial barrier disruption through modulation of actin-myosin contractility. However, specific regulation of HSP27 in the endothelium to affect its activity has yet to be elucidated.

In this chapter, we show thrombin activated p38 signals independent of known Gαq and Gα12/13 modulators and instead signals through an MK2-MK3-HSP27 signaling axis. Furthermore, we show this signaling axis is conserved for other GPCRs. We further delineate the mechanism of HSP27 regulation on HSP27 activity by showing both MK2 and MK3 are required for differential phosphorylation of HSP27 which affect its oligomerization and enhance oligomer disruption.

2.2 Results

Thrombin-induced p38 signaling is not integrated with the RhoA/MLC pathway and promotes HSP27 phosphorylation

In addition to known RhoA and MLC kinase pathways that perturb endothelial barrier integrity (Bogatcheva et al., 2002), we recently showed that thrombin-activated PAR1-induced p38 activation occurs through a TAB1-mediated non-canonical pathway and promotes endothelial barrier permeability (Grimsey et al., 2015). However, the mechanism by which p38 signaling contributes to barrier disruption is not known. To assess whether thrombin-activated p38 is integrated into known Gαq and Gα12/13 signaling pathways, we tested the effect of p38 blockade on RhoA activation and MLC phosphorylation, downstream effectors of Gαq and Gα12/13 signaling, respectively. Thrombin treatment induced a robust increase in RhoA activation in HUVEC-derived EA.hy926 cells after agonist stimulation in vehicle control cells, whereas inhibition of p38 with SB203580, a p38α and β selective inhibitor, had no effect on RhoA activation (Fig. 2.1A). Phosphorylation of MLC, an MLC kinase substrate regulated by RhoA and Ca^{2+}, peaked after 1 min of thrombin stimulation in HUVECs and then declined, however, a similar change in MLC phosphorylation was observed in cells treated with SB203580, the p38 specific inhibitor (Fig. 2.1B). This suggests thrombin-stimulated p38 signaling affects endothelial barrier disruption independent of known PAR1-stimulated G protein signaling effectors and is likely mediated by unknown proteins.

To identify the unknown mediators of PAR1-activated p38 signaling, we previously performed a quantitative phosphoproteomics analysis on EA.hy926 endothelial cells stimulated with thrombin for 0, 2.5, or 5 min (Lin et al., 2020). Heat shock protein 27 (HSP27), a downstream

substrate of p38, has previously been implicated in regulation of endothelial barrier integrity (Shi et al., 2017, Sun et al., 2015, Sun et al., 2019), emerged from this data set as a promising candidate for further interrogation. However, the role of HSP27 in GPCR regulation of endothelial barrier integrity is not known. Thrombin caused a significant increase in HSP27 phosphorylation at four unique sites including serine (Ser) 15, 78, 82, and 83 (Fig. 2.1C and 2.1D). The Ser15 and Ser82 sites of HSP27 phosphorylation induced by thrombin were detected on single peptides, whereas Ser78 was only detected together with Ser82 or both Ser82 and Ser83 (Fig. 2.1C and 2.1D). HSP27 phosphorylation at Ser15, Ser78, and Ser82 are known to affect HSP27 function (Kostenko and Moens, 2009), but how HSP27 phosphorylation contributes to GPCR-induced endothelial barrier permeability is not known.

GPCR agonists stimulate p38-dependent HSP27 phosphorylation in multiple endothelial cell types

To confirm our phosphoproteomic data and the specificity of PAR1-induced HSP27 phosphorylation, HUVECs were stimulated for 5 or 10 min with the PAR1 specific peptide agonist, TFLLRNPNDK, which mimics the thrombin cleaved tethered ligand of PAR1. Phosphorylation of p38, and HSP27 on Ser15, Ser78, and Ser82 were detected using phospho-specific HSP27 antibodies. The PAR1 peptide agonist caused significant phosphorylation for both 5 and 10 min time points for p38, and on HSP27 at all three serine residues (Fig. 2.2A, lanes 1-3). The PAR1 specific antagonist, Vorapaxar, caused complete ablation of all HSP27 and p38 phosphorylation (Fig. 2.2A, lanes 4-6). These results confirm HSP27 phosphorylation is specific to PAR1 activation.

To understand the activity of HSP27, we employed a prolonged signaling time course

to examine the kinetics of thrombin-induced HSP27 phosphorylation. HUVECS were stimulated with thrombin over a 60 min time-course and phosphorylation of HSP27 on Ser15, Ser78, and Ser82 was detected. Thrombin induced an increase in phosphorylation at all three sites with varying kinetics. A peak in Ser82 phosphorylation was detected at 5 min following thrombin stimulation (Fig. 2.2B, lanes 1-6), whereas Ser78 phosphorylation was detected later at 10 min after thrombin incubation (Fig. 2.2B, lanes 1-6). Thrombin-stimulated Ser15 phosphorylation peaked at 30 min and was sustained (Fig. 2.2B, lanes 1-6). To determine if thrombin induced HSP27 phosphorylation required p38 activity, HUVECs were pretreated with SB203580 or DMSO vehicle control. Inhibition of p38 significantly ablated thrombin stimulated HSP27 phosphorylation at Ser82, Ser78, and Ser15 (Fig. 2.2B, lanes 7-12).

Next, we examined if thrombin-triggered HSP27 phosphorylation is conserved in other endothelial cell types using primary human dermal microvascular endothelial cells (HDMEC). HDMECs were stimulated with thrombin over a 60 min time course and detection of HSP27 Ser15, 78, and 82 phosphorylation measured at various times (Fig. 2.2C, lanes 1-6). Thrombin caused a peak in phosphorylation of HSP27 Ser78 and Ser82 at 5 min and 10 min, respectively, that then declined, whereas Ser15 phosphorylation peaked at 5 min and was sustained after thrombin (Fig. 2.2C, lanes 1-6). Pretreatment with the p38 inhibitor SB203580 significantly inhibited thrombin-induced HSP27 Ser15 and Ser78 phosphorylation, and reduced Ser82 phosphorylation to a lesser extent (Fig. 2.2C, lanes 7-12). HDMECs exhibited similar kinetics of thrombin-induced HSP27 phosphorylation compared to HUVECs at all three phosphorylation sites and retained sensitivity to p38 inhibition.

In previous studies we showed multiple GPCR agonists can activate non-canonical p38 signaling in endothelial cells (Grimsey et al., 2015, Grimsey et al., 2019). Histamine is known

to signal via H1 and H2 GPCR receptors expressed in endothelial cells and promotes barrier disruption (Adderley et al., 2015). To determine if other GPCR agonists induce HSP27 phosphorylation, HUVECs were stimulated with histamine over a 30 min time course. Histamine induced a peak in phosphorylation of Ser15, Ser78, and Ser82 at 10 min (Fig. 2.2D, lanes 1-5), and then declined to baseline by 30 min (Fig. 2D, lanes 1-5). SB203580 pretreatment completely ablated phosphorylation of Ser15, Ser78, and Ser82 (Fig. 2.2D, lanes 6-10). Similar to thrombin, histamine induced p38-dependent HSP27 phosphorylation at all three sites. While thrombin has been shown to phosphorylate HSP27 in platelets (Tokuda et al., 2016) and vascular smooth muscle cell lines (Nakajima et al., 2005, Brophy et al., 1998a), endothelial specific GPCR-induced HSP27 phosphorylation has not been previously reported.

MK2 and MK3 are required for thrombin-induced HSP27 phosphorylation

Although HSP27 phosphorylation is dependent on p38 MAPK, it is not likely a direct substrate. HSP27 is instead a substrate of numerous p38 regulated kinases (Kostenko and Moens, 2009). To determine which p38 regulated kinases mediate thrombin-stimulated HSP27 phosphorylation, we used PHOXTRACK computational software (Weidner et al., 2014) to interrogate the thrombin-induced phosphoproteome (Lin et al., 2020), and identified two candidates, MAPKAPK2 (MK2) and MAPKAPK3 (MK3) as potential HSP27 causal kinases (Fig. 2.2). HSP27 has previously been shown to be a direct substrate of MK2 in platelets (Mendelsohn et al., 1991), vascular smooth muscle cells (Brophy et al., 1998b), and in vitro using purified proteins (Stokoe et al., 1992), while MK3 has only been shown to directly phosphorylate HSP27 in vitro (Kostenko and Moens, 2009, McLaughlin et al., 1996). Neither MK2 nor MK3 have been previously linked to endothelial GPCR-induced HSP27 phosphorylation.

To determine if MK2 is required for thrombin induced HSP27 phosphorylation, HUVECs were pretreated with or without PF3644022, an MK2 specific inhibitor, stimulated with thrombin over a 60 min time-course and HSP27 phosphorylation detected by immunoblotting. Thrombin-stimulated Ser15 and Ser78 phosphorylation was significantly ablated by MK2 inhibition, whereas the agonist-induced Ser82 phosphorylation was not altered in the presence of PF3644022 (Fig. 2.4A, lanes 6-12). Thrombin also induced MK2 phosphorylation at Threonine (Thr) 334 in both vehicle control and PF3644022 treated cells (Fig. 2.4A), indicating that MK2 is activated in the pathway. To confirm HSP27 is a direct substrate of MK2 in human cultured endothelial cells, an *in vitro* MK2 kinase assay was performed using purified HSP27 as a substrate. Endogenous MK2 was immunoprecipitated from cells treated with or without PF3644022 followed by stimulation with thrombin for 5 min. MK2 immunoprecipitates were then incubated with purified recombinant GST-tagged HSP27 and ATP and changes in phosphorylation induced *in vitro* detected by immunoblotting. MK2 immunoprecipitates from control cells stimulated with thrombin for 5 min showed increases in both HSP27 Ser78 and Ser82 phosphorylation (Fig. 2.4B, lanes 1-3). However, in cells treated with the MK2 inhibitor PF3644022 only thrombin-induced HSP27 Ser78 phosphorylation was significantly inhibited (Fig. 2.4B, lanes 4-6). Taken together, both the cellular assays and *in vitro* kinase assays to assess HSP27 phosphorylation indicate that both Ser78 and Ser15 require MK2 activation, while Ser82 does not. These findings further suggest that another kinase present in the MK2 immunoprecipitates is competent to phosphorylate HSP27 at Ser82.

To examine the role of MK3 in thrombin-induced HSP27 phosphorylation, HUVECs were transfected with MK3 specific siRNA or non-specific (NS) siRNA, since there are no specific MK3 inhibitors, and then stimulated with thrombin over a 30 min time-course (Fig. 2.4C, lanes 1-8).

Thrombin-induced significant changes in HSP27 phosphorylation in NS siRNA treated HUVECs, however, in MK3 depleted HUVECs only Ser82 showed a significant decrease in phosphorylation at 10 min, whereas there were no significant effects on Ser15 and Ser78 phosphorylation (Fig. 2.4C, lanes 5-8). To determine if MK2 and MK3 kinases were both necessary to fully phosphorylate HSP27, we used the MK2-specific inhibitor PF3644022 and MK3 siRNA to assess the contribution of both MK3 and MK2 to thrombin-induced HSP27 phosphorylation. Using MK3-specific siRNA and the MK2 inhibitor PF3644022, thrombin-induced HSP27 phosphorylation at all three phosphorylation sites was abolished (Fig. 2.4C, lanes 9-12). These results show differential regulation of thrombin-induced HSP27 phosphorylation, where HSP27 Ser15 and Ser78 phosphorylation depends on MK2 activation, while robust phosphorylation of Ser82 requires both MK2 and MK3 activity, suggesting a complex regulation of Ser82 phosphorylation by both MK2 and MK3.

MK2 and MK3 are known to form a complex with their upstream activator p38α (Ronkina et al., 2008). However, it is not known if MK2 and MK3 co-associate in endothelial cells and if thrombin disrupts this interaction. To determine if MK2 and MK3 co-associate, HUVECs were stimulated with thrombin over a 10 min time-course, lysed and immunoprecipitated with anti-MK2 antibody, and co-associated MK3 detected by immunoblotting. MK2 and MK3 were found to basally co-associate, whereas incubation with thrombin caused significant disassociation of the MK2-MK3 complex after 10 min of agonist stimulation (Fig. 2.4D, lanes 2-4), suggesting that MK2-MK3 co-exist in a complex that is dynamically disassociated by thrombin.

Based on the proximity of Ser78 and Ser82 in the primary structure of HSP27, it was surprising that MK2 mediated phosphorylation of only Ser78 and Ser15 residues and not Ser82, suggesting a more complex orientation in the tertiary structure of HSP27. While there is a

HSP27 crystal structure of the highly ordered α-crystallin domain (Rajagopal et al., 2015), Ser15, Ser78, and Ser82 reside in a highly disordered region that is not present in the published structure. Thus, we used Phyre homology modeling (PDB 2N3J) (Kelley et al., 2015) to predict the location of Ser15, Ser78, and Ser82 residues relative to each other in the unstructured region as illustrated in the ribbon, space-filled and merged diagram with the key residues shown in green (Fig. 2.4E). This region is located in the C-terminal region distal to the α-crystallin β-sheets (Fig. 2.4E) (Rajagopal et al., 2015). The homology modeling further predicts Ser15 and Ser78 are adjacent and localized within a pocket that is clearly evident in the space-filled model, whereas Ser82 is situated behind an α-helical loop in its own pocket (Fig. 2.4E). Thus, Ser78 and Ser82 reside farther apart in the tertiary structure, although they appear in close proximity in the primary structure, whereas Ser15 and Ser78 are predicted to be more proximate in the tertiary structure, which may contribute to the preferential phosphorylation of HSP27 Ser15 and Ser78 residues by MK2 versus MK3.

GPCR-induced HSP27 activity requires p38, MK2 and MK3

Under physiological conditions HSP27 exists as large oligomers that interacts with actin as a barbed-end-capping protein, whereas phosphorylation of HSP27 promotes oligomer disassembly and controls actin polymerization (Salinthone et al., 2008), which is important for regulating endothelial barrier function. To gain mechanistic understanding of how PAR1 regulates HSP27 activity, thrombin-induced changes in HSP27 oligomerization were examined using native non-denaturing polyacrylamide gel electrophoresis to facilitate analysis of oligomer disassembly. In HUVECs, thrombin induced rapid disassembly of large HSP27 oligomers resulting in the formation of smaller HSP27 oligomers that appear as lower bands on the native gel within

minutes (Fig. 2.5A, lanes 1-5). HSP27 disassembly and formation of smaller oligomers peaked at 10 min after thrombin stimulation, whereas reformation of HSP27 larger oligomers occurred by 30 min based on the ratio of small versus large oligomers detected (Fig. 2.5A, lanes 1-5). However, in cells pretreated with SB203580, the p38 inhibitor, thrombin-stimulated disassembly of HSP27 larger oligomers was significantly inhibited (Fig. 2.5A, lanes 6-10), indicating that p38 enhances HSP27 disassembly. Histamine stimulation also caused disassembly of large HSP27 oligomers resulting in the formation of smaller HSP27 oligomers (Fig. 2.5B, lanes 1-5) that was blocked by the p38 inhibitor SB203580 (Fig. 2.5B, lanes 6-10), similar to that observed with thrombin, suggesting multiple GPCR agonists induce HSP27 activity through p38 signaling.

To determine if disassembly of large HSP27 oligomers required MK2 function, HUVECs were pretreated with the MK2-specific inhibitor PF3644022 followed by thrombin stimulation. Inhibition of MK2 failed to block thrombin-induced disassembly of HSP27 oligomer disruption and re-formation (Fig. 2.5C, lanes 1-5 versus 6-10). Similarly, depletion of MK3 by siRNA alone failed to inhibit disassembly of large HSP27 oligomers induced by thrombin (Fig. 2.5D, lanes 5-8), compared to NS siRNA transfected control cells (Fig. 2.5D, lanes 1-4). These findings indicate that neither MK2 nor MK3 function alone is sufficient to mediate disassembly of HSP27 oligomers. However, inhibition of both MK2 and MK3 using PF3644022 combined with MK3-specific siRNAs caused a significant decrease in thrombin-induced HSP27 disassembly, where the presence of the large HSP27 oligomers were retained after 5 min and 30 min of agonist stimulation compared to control HUVECs treated with DMSO and NS siRNA (Fig. 2.5D, lanes 1-4 versus 9-12), suggesting alteration of both disassembly and recovery of HSP27 large oligomers. These data suggest that the thrombin-induced p38-MK2-MK3 signaling axis is required for HSP27 phosphorylation at Ser15, Ser78, and Ser82 sites, and mediates disassembly

of HSP27 large oligomers.

2.3 Conclusion and Discussion

In this chapter we define a GPCR signaling pathway that is distinct from the classically known Gαq or Gα12/13 RhoA and MLC effector pathways in which GPCR-activated p38 induces MK2-MK3 signaling to differentially phosphorylate HSP27 that controls the initiation of HSP27 oligomer disruption. We demonstrate that GPCR-induced phosphorylation of HSP27 by p38 is critical for disassembly of HSP27 large oligomers, whereas both MK2 and MK3 are required for HSP27 disassembly following thrombin stimulation. Taken together, this study provides a mechanistic delineation of the p38-MK-MK3 signaling axis to specifically phosphorylate and activate HSP27 after GPCR stimulation. These findings are summarized in Fig. 2.6 schematic.

An important finding of this study is thrombin activation of p38 signaling is independent of effectors of the Gαq or Gα12/13 RhoA and MLC signaling pathways. Both Gαq and Gα12/13 pathways converge on MLC phosphorylation by different mechanisms which increases interactions with F-actin causing actomyosin contractility and opening of the endothelial barrier (Komarova et al., 2007), however, our data suggest thrombin activated p38 is working through HSP27 modulation of the barrier in lieu of MLC. Thrombin has been previously shown to phosphorylate HSP27 in various cell types such as vascular smooth muscle cells and platelets (Hirade et al., 2002, Nakajima et al., 2005); however, this study is the first to report thrombin-induced HSP27 phosphorylation by p38 and to affect HSP27 activity. A recent study showed HSP27 overexpression mediates blood brain barrier preservation (Shi et al., 2017), but how GPCR-stimulated p38 modulation of HSP27 affects barrier integrity has not been determined. Thus, we sought to define the signaling link between HSP27 function and the GPCR-p38 signal-

ing axis that promotes endothelial barrier disruption. We identified four different combinations of HSP27 phosphorylation sites induced by thrombin using mass spectrometry. Two of the HSP27 phosphosites have also been identified in a phosphoproteomic screen in an endothelial derived cell line when giving the PAR1 peptide agonist (van den Eshof et al., 2017), supporting our data in which we identified 2 additional specific HSP27 phosphorylation sites after thrombin addition in endothelial cells. While Ser82 and Ser15 appear to be phosphorylated alone, phosphorylated Ser78 phosphorylation was only detected in combination with Ser82 or Ser83, suggesting there may be a specific order in which HSP27 is phosphorylated on each site. We could speculate one site may be a "priming site" and must be phosphorylated first, but we do not have sufficient evidence to support this in our results.

p38 and HSP27 exhibits delayed signaling kinetics, peaking around 5-10 min of thrombin stimulation, as opposed to MLC and RhoA activation, which peaks at 1 and 2.5 min respectively. This suggests that a temporally distinct GPCR-p38 signaling pathway may contribute not only the opening of the barrier, but potentially the initiation of barrier recovery. Importantly, we show this pathway is conserved for other barrier disrupting GPCR agonists, such as histamine, indicating that the pathway is relevant to GPCRs activated by inflammatory mediators. Another locally produced inflammatory mediator of vascular permeability is bradykinin for allergy-induced responses. Although we did not directly test bradykinin B1/B2 receptors, we would expect the kinin peptide to illicit a response similar to histamine or PAR1 stimulation and also to mediate barrier recovery through HSP27 modulation.

In this work, we also provide detailed mechanistic insight into how p38 causes PAR1-induced HSP27 phosphorylation via the MK2-MK3 signaling pathway. *In vitro* systems have clearly established both MK2 and MK3 are capable of specifically phosphorylating Ser15, Ser78,

and Ser82 of HSP27 (Zakowski et al., 2004, Stokoe et al., 1992). Based on these studies, MK2 and MK3 are thought to have potentially redundant or compensatory effects on HSP27 phosphorylation (Ronkina et al., 2007). However, we show in a native endothelial cell system that thrombin-activated MK2 specifically phosphorylates HSP27 at sites Ser78 and Ser15, and not Ser82, whereas thrombin-activated MK3 prefers the Ser82 site of HSP27. MK2 and MK3 have been shown to exhibit differential functions on gene expression (Ehlting et al., 2019), however, this is the first report to show that MK2 and MK3 differentially phosphorylate HSP27. Phyre homology analysis provides a plausible explanation for how differential phosphorylation of HSP27 mediated by two different kinases might occur. The Phyre model indicates that Ser78 and Ser15 are located more proximal to each other and reside in the same pocket, whereas Ser82 is located at the posterior face of the α-helical loop and in a distinct pocket. Thus, it is conceivable the distinct pockets accommodate two different kinases that bind to and phosphorylate HSP27 at distinct sites. This is also supported by our finding that MK2 and MK3 complex disassociates after thrombin stimulation, permitting the kinases to bind to and phosphorylate specific sites located in the two spatially distinct HSP27 pockets.

While the previous literature using purified proteins *in vitro* has shown HSP27 activity is regulated by its oligomeric state in a phosphorylation-dependent manner (Rogalla et al., 1999), this study utilized a newly developed approach to examine endogenous HSP27 activity through oligomerization in a native cell system. Here, we show that direct modulation of endogenous HSP27 activity by alteration of HSP27 oligomerization state can be disrupted by GPCRs. In fact, both thrombin- and histamine-induced changes in HSP27 phosphorylation correlates with a change in activity, with peak in HSP27 phosphorylation and de-oligomerization occurring between 5-10 min and return to higher order oligomerization around 30 min. Inhibition of p38

blocks GPCR-induced HSP27 disassembly, suggesting that p38 is critical for the initiation of HSP27 activity. However, neither inhibition of MK2 or MK3 alone is sufficient to block oligomer disassembly, suggesting that all three phosphorylation sites are necessary for the re-formation of the larger oligomer. Blockade of MK2 and MK3 together, cause significant inhibition of the HSP27 de-oligomerization, although to a lesser extent than occurs with p38 alone. This suggest that p38 has additional functions such as regulating another effector kinase or phosphatase to decrease or increase HSP27 activity. The phosphatase PP2A is known to dephosphorylate HSP27 *in vitro* (Cairns et al., 1994); it was not tested in these experiments, yet provides a potential avenue for further investigation. In summary, this chapter mechanistically profiles differential phosphorylation of HSP27 after thrombin induction and the role of the p38-MK2-MK3 signaling axis in affecting HSP27 activity after GPCR induction.

2.4 Materials and Methods

Immunoprecipitation and *in vitro* kinase assay

Cells were stimulated with α-thrombin (10 nM) for indicated times and processed as described (Grimsey et al., 2015) with Triton lysis buffer. HUVEC cells were grown in 6 cm dishes for 3 days, serum starved for 2 h, and lysed in Triton lysis buffer containing 200 mM Tris-HCl pH 7.0, 1.5 mM NaCl, 10% Triton X-100, 10 mM EDTA, 10 mM EGTA, 10 mM β-glycerophosphate, 25 mM NaPP, 10 mM $NaVO_4$, 10 μg/ml leupeptin, 10 μg/ml aprotinin, 10 μg/ml trypsin protease inhibitor, 10 μg/ml pepstatin, and 10 μg/ml PMSF. Cell lysates were homogenized, cleared by centrifugation. Protein concentrations determined by bicinchoninic acid assay and equal amounts of lysates were used for immunoprecipitations using the anti-MK2

antibody , samples were eluted with 2X Laemmli sample buffer containing 200 mM dithiothreitol (DTT), resolved by SDS-PAGE and developed by chemiluminescence. *In vitro* kinase assays were performed on immunoprecipitated MK2 in the presence of 200 μM ATP and purified kinase substrate GST-HSP27 for 30 min at 30°C in kinase buffer containing 250 mM Tris-HCl pH 7.0, 20 mM DTT, 50 mM β-glycerophosphate, 1mM $NaVO_4$, and 100 mM $MgCl_2$. Samples were eluted in 3X Laemmli sample buffer and resolved by SDS-PAGE. Aliquots of cell lysates were also immunoblotted with specific antibodies as indicated.

HSP27 phosphorylation assays

HUVECs or HDMECs were serum-starved for 2 hr and were treated under various conditions. Samples were collected in 2X SDS Laemmli sample buffer containing 200 mM DTT. Equivalent amounts of cell lysates were resolved by SDS-PAGE, transferred to membranes and probed with anti-HSP27 phospho-specific and HSP27 antibodies. Membranes were developed by chemiluminescence and quantified by densitometry with Image J (National Institute of Health).

Transfections and siRNA

HUVECs were transfected with siRNAs using TransIT-X2 according to manufacturer's instructions (Mirus Bio). MAPKAPK3 (5'-CCAGATAGTAATAAACACCAT-3') used at 25 nM and nonspecific (ns) All Stars Negative Control siRNA (5'-GGCUACGUCCAGGAGCGCACC-3') were all obtained from Qiagen.

Native gel electrophoresis

HUVECs were serum-starved and treated under various conditions and time courses. Samples were collected in 2X Laemmli sample buffer in the absence of DTT and heat and supplemented with 10 μg/ml leupeptin, 10 μg/ml aprotinin, 10 μg/ml trypsin protease inhibitor, 10 μg/ml pepstatin, and 10 μg/ml PMSF. Samples were resolved on a native PAGE gel in non-denaturing running buffer (25mM Tris-HCl and 192 mM glycine), transferred to PDVF membranes and immunoblotted with anti-HSP27 antibody. Membranes were developed by chemiluminescence and quantified by densitometry.

RhoA Activity Assay

RhoA activity was measured as described in (Soh and Trejo, 2011). Briefly, GST-rhotekin Rho-binding domain (RBD) fusion protein was transformed into BL21 (DE3) Escherichia coli; fusion proteins were induced and purified using standard techniques. Endothelial EA.hy926 cells were serum starved, incubated with p38 inhibitor, SB203580, for 1 hr and treated with thrombin for 2.5 min at 37°C. Cells were lysed in buffer containing 50 mM Tris-HCl pH 7.4, 100 mM sodium chloride, 2 mM $MgCl_2$, 1% Triton X-100, 10% glycerol containing 1 mM DTT, and protease inhibitors. Equivalent amounts of lysates were used in pull-down assays with GST Rhotekin-RBD bound to glutathione Sepharose beads for 45 min at 4°C. Beads were washed with lysis buffer, and RhoA was eluted in 2X SDS Laemmli sample buffer containing 200 mM DTT, resolved by SDS PAGE, transferred to PVDF membranes, and immunoblotted with anti-RhoA antibody. Immunoblots were developed with enhanced chemiluminescence and analyzed by densitometry.

Mass Spectrometry Based Proteomics Analysis

Thrombin-induced phosphorylation of HSP27 was detected in a previous multiplexed, quantitative, phosphoproteomic experiment performed by our lab (Lin et al., 2020). Briefly, cells were serum starved and then stimulated with thrombin for 2.5 and 5 min. Phosphopeptide abundances were grouped using k-means clustering, yielding thrombin-induced clusters. Within a thrombin-induced cluster, we noted a drastic increase in a number of HSP27 phospho-sites in response to thrombin. Formal statistical analysis (one-way ANOVA) of these phospho-sites demonstrated a significant increase from basal levels.

PHOXTRACK computational software

Results selecting MAPKAPK2 (MK2) and MAPKAPK3 (MK3) as causal HSPB1 (HSP27) kinases from our phosphoproteomic dataset input. Graphs show the likelihood of each HSP27 phosphorylation site, Ser15, Ser78, and Ser82 by MK3 and MK2 kinases. Kinases were selected from Human Protein Reference Dataset (HPRD).

Cell culture

Pooled-primary human umbilical vein endothelial cells (HUVEC) or human dermal microvascular endothelial cells (HDMEC) were purchased from Lonza and used up to passage 6. HUVECs were grown in EGM-2 (Lonza). HDMECs were grown in EGM-2MV (Lonza). EA.hy926, HUVEC derived immortalized endothelial cells, were grown in DMEM/F12 with 10% FBS. All cells were cultured in a 37°C incubator with 5% CO_2.

Antibodies and reagents

α-Thrombin was purchased from Enzyme Research Laboratories. Histamine dihydrochloride was from Tocris Bio-Techne. Rabbit IgG antibody and purified GST-HSP27 are from Rockland Immunochemicals. PF3644022 was from Tocris. SB203580 was from LC laboratories. Polyclonal rabbit anti-p38, polyclonal rabbit anti-MK2, polyclonal rabbit anti-MK3, polyclonal rabbit phospho-MK2 (Thr334), polyclonal rabbit anti-MLC, monoclonal mouse anti-phospho-MLC, monoclonal mouse anti-HSP27, and polyclonal rabbit phospho-HSP27 (Ser15, Ser78, and Ser82) antibodies were from Cell Signaling Technology. Monoclonal mouse anti-GAPDH antibody was from GeneTex. Monoclonal mouse anti-Anti-RhoA was from Santa Cruz. HRP-conjugated goat–anti rabbit and goat–anti mouse antibodies were from Bio-Rad Laboratories.

Statistical Analysis and Replications

Statistical significance between datasets with three or more experimental groups was determined using one-way analysis of variance (ANOVA) including a Tukey's test for multiple comparisons. Statistical difference between two experimental groups was determined using a two-tailed unpaired t-test. For all tests, a p-value of 0.05 was used as the cutoff to determine significance. All experiments were repeated a least three times, and p-values are indicated in each figure. All statistical analysis was performed using GraphPad prism 7.

2.5 Acknowledgements

This research was funded by National Institutes of Health (R35 GM127121), a pre-doctoral fellowship by Tobacco-Related Disease Research Program (TRDRP 27DT-0009), as well as a training grant by NIH/NIGMS (T32 GM007752).

Chapter 2 in part is a reprint of material to be submitted to be published in: **Rada CC**, Mejia-Pena H, Grimsey NJ, Canto-Cordova I, Olson J, Wozniak JM, Gonzalez DJ, Nizet V, Trejo J. “Heat Shock Protein 27 activity is linked to endothelial barrier recovery induced by GPCR pro-inflammatory mediator.” The dissertation author was the primary author.

2.6 References

ADDERLEY, S. P., ZHANG, X. E. BRESLIN, J. W. 2015. Involvement of the H1 Histamine Receptor, p38 MAP Kinase, Myosin Light Chains Kinase, and Rho/ROCK in Histamine-Induced Endothelial Barrier Dysfunction. Microcirculation, 22, 237-48.

BOGATCHEVA, N. V., GARCIA, J. G. VERIN, A. D. 2002. Molecular mechanisms of thrombin-induced endothelial cell permeability. Biochemistry (Mosc), 67, 75-84.

BORBIEV, T., BIRUKOVA, A., LIU, F., NURMUKHAMBETOVA, S., GERTHOFFER, W. T., GARCIA, J. G. VERIN, A. D. 2004. p38 MAP kinase-dependent regulation of endothelial cell permeability. Am J Physiol Lung Cell Mol Physiol, 287, L911-8.

BROPHY, C. M., BEALL, A., MANNES, K., LAMB, S., DICKINSON, M., WOODRUM, D. DEVOE, L. D. 1998a. Heat shock protein expression in umbilical artery smooth muscle. J Reprod Fertil, 114, 351-5.

BROPHY, C. M., WOODRUM, D., DICKINSON, M. BEALL, A. 1998b. Thrombin activates MAPKAP2 kinase in vascular smooth muscle. J Vasc Surg, 27, 963-9. CAIRNS, J., QIN, S., PHILP, R., TAN, Y. H. GUY, G. R. 1994. Dephosphorylation of the small heat shock protein Hsp27 in vivo by protein phosphatase 2A. J Biol Chem, 269, 9176-83.

CLAESSON-WELSH, L. 2015. Vascular permeability–the essentials. Ups J Med Sci, 120, 135-43.

EHLTING, C., REX, J., ALBRECHT, U., DEENEN, R., TIEDJE, C., KOHRER, K., SAWODNY, O., GAESTEL, M., HAUSSINGER, D. BODE, J. G. 2019. Cooperative and distinct functions of MK2 and MK3 in the regulation of the macrophage transcriptional response to lipopolysaccharide. Sci Rep, 9, 11021.

GRIMSEY, N., LIN, H. TREJO, J. 2014. Endosomal signaling by protease-activated receptors. Methods Enzymol, 535, 389-401.

GRIMSEY, N. J., AGUILAR, B., SMITH, T. H., LE, P., SOOHOO, A. L., PUTHENVEEDU, M. A., NIZET, V. TREJO, J. 2015. Ubiquitin plays an atypical role in GPCR-induced p38 MAP kinase activation on endosomes. J Cell Biol, 210, 1117-31.

GRIMSEY, N. J., LIN, Y., NARALA, R., RADA, C. C., MEJIA-PENA, H. TREJO, J. 2019. G protein-coupled receptors activate p38 MAPK via a non-canonical TAB1-TAB2- and TAB1-TAB3-dependent pathway in endothelial cells. J Biol Chem, 294, 5867-5878.

HIRADE, K., KOZAWA, O., TANABE, K., NIWA, M., MATSUNO, H., OISO, Y., AKAMATSU, S., ITO, H., KATO, K., KATAGIRI, Y. UEMATSU, T. 2002. Thrombin stimulates dissociation and induction of HSP27 via p38 MAPK in vascular smooth muscle cells. Am J Physiol Heart Circ Physiol, 283, H941-8.

KELLEY, L. A., MEZULIS, S., YATES, C. M., WASS, M. N. STERNBERG, M. J. 2015. The Phyre2 web portal for protein modeling, prediction and analysis. Nat Protoc, 10, 845-58.

KOMAROVA, Y. MALIK, A. B. 2010. Regulation of endothelial permeability via paracellular and transcellular transport pathways. Annu Rev Physiol, 72, 463-93.

KOMAROVA, Y. A., MEHTA, D. MALIK, A. B. 2007. Dual regulation of endothelial junctional permeability. Sci STKE, 2007, re8.

KOSTENKO, S. MOENS, U. 2009. Heat shock protein 27 phosphorylation: kinases, phosphatases, functions and pathology. Cell Mol Life Sci, 66, 3289-307.

LIN, Y., WOZNIAK, J. M., GRIMSEY, N. J., GIRADA, S., PATWARDHAN, A., MOLINAR-INGLIS, O., SMITH, T. H., LAPEK, J. D., GONZALEZ, D. J. TREJO, J. 2020. Phosphoproteomic anal-

ysis of protease-activated receptor-1 biased signaling reveals unique modulators of endothelial barrier function. Proc Natl Acad Sci U S A.

MCLAUGHLIN, M. M., KUMAR, S., MCDONNELL, P. C., VAN HORN, S., LEE, J. C., LIVI, G. P. YOUNG, P. R. 1996. Identification of mitogen-activated protein (MAP) kinase-activated protein kinase-3, a novel substrate of CSBP p38 MAP kinase. J Biol Chem, 271, 8488-92.

MENDELSOHN, M. E., ZHU, Y. O'NEILL, S. 1991. The 29-kDa proteins phosphorylated in thrombin-activated human platelets are forms of the estrogen receptor-related 27-kDa heat shock protein. Proc Natl Acad Sci U S A, 88, 11212-6.

NAKAJIMA, K., HIRADE, K., ISHISAKI, A., MATSUNO, H., SUGA, H., KANNO, Y., SHU, E., KITAJIMA, Y., KATAGIRI, Y. KOZAWA, O. 2005. Akt regulates thrombin-induced HSP27 phosphorylation in aortic smooth muscle cells: function at a point downstream from p38 MAP kinase. Life Sci, 77, 96-107.

PICHON, S., BRYCKAERT, M. BERROU, E. 2004. Control of actin dynamics by p38 MAP kinase - Hsp27 distribution in the lamellipodium of smooth muscle cells. J Cell Sci, 117, 2569-77.

RAJAGOPAL, P., LIU, Y., SHI, L., CLOUSER, A. F. KLEVIT, R. E. 2015. Structure of the alpha-crystallin domain from the redox-sensitive chaperone, HSPB1. J Biomol NMR, 63, 223-8.

ROGALLA, T., EHRNSPERGER, M., PREVILLE, X., KOTLYAROV, A., LUTSCH, G., DUCASSE, C., PAUL, C., WIESKE, M., ARRIGO, A. P., BUCHNER, J. GAESTEL, M. 1999. Regulation of Hsp27 oligomerization, chaperone function, and protective activity against oxidative stress tumor necrosis factor alpha by phosphorylation. Journal of Biological Chemistry, 274, 18947-18956.

RONKINA, N., KOTLYAROV, A., DITTRICH-BREIHOLZ, O., KRACHT, M., HITTI, E., MILARSKI, K., ASKEW, R., MARUSIC, S., LIN, L. L., GAESTEL, M. TELLIEZ, J. B. 2007. The mitogen-

activated protein kinase (MAPK)-activated protein kinases MK2 and MK3 cooperate in stimulation of tumor necrosis factor biosynthesis and stabilization of p38 MAPK. Mol Cell Biol, 27, 170-81.

RONKINA, N., KOTLYAROV, A. GAESTEL, M. 2008. MK2 and MK3–a pair of isoenzymes? Front Biosci, 13, 5511-21.

SALINTHONE, S., TYAGI, M. GERTHOFFER, W. T. 2008. Small heat shock proteins in smooth muscle. Pharmacol Ther, 119, 44-54.

SHI, Y., JIANG, X., ZHANG, L., PU, H., HU, X., ZHANG, W., CAI, W., GAO, Y., LEAK, R. K., KEEP, R. F., BENNETT, M. V. CHEN, J. 2017.Endothelium-targeted overexpression of heat shock protein 27 ameliorates blood-brain barrier disruption after ischemic brain injury. Proc Natl Acad Sci U S A, 114, E1243-E1252.

SOH, U. J. TREJO, J. 2011. Activated protein C promotes protease-activated receptor-1 cytoprotective signaling through beta-arrestin and dishevelled-2 scaffolds. Proc Natl Acad Sci U S A, 108, E1372-80.

STOKOE, D., ENGEL, K., CAMPBELL, D. G., COHEN, P. GAESTEL, M. 1992. Identification of MAPKAP kinase 2 as a major enzyme responsible for the phosphorylation of the small mammalian heat shock proteins. FEBS Lett, 313, 307-13.

SUN, H. B., REN, X., LIU, J., GUO, X. W., JIANG, X. P., ZHANG, D. X., HUANG, Y. S. ZHANG, J. P. 2015. HSP27 phosphorylation protects against endothelial barrier dysfunction under burn serum challenge. Biochem Biophys Res Commun, 463, 377-83.

SUN, L. YE, R. D. 2012. Role of G protein-coupled receptors in inflammation. Acta Pharmacol Sin, 33, 342-50.

SUN, X., YIN, Y., KONG, L., CHEN, W., MIAO, C. CHEN, J. 2019. The effect of propofol on hypoxia-modulated expression of heat shock proteins: potential mechanism in modulating blood-brain barrier permeability. Mol Cell Biochem, 462, 85-96.

TOKUDA, H., KUROYANAGI, G., TSUJIMOTO, M., MATSUSHIMA-NISHIWAKI, R., AKAMATSU, S., ENOMOTO, Y., IIDA, H., OTSUKA, T., OGURA, S., IWAMA, T., KOJIMA, K. KOZAWA, O. 2016. Thrombin Receptor-Activating Protein (TRAP)-Activated Akt Is Involved in the Release of Phosphorylated-HSP27 (HSPB1) from Platelets in DM Patients. Int J Mol Sci, 17.

VAN DEN ESHOF, B. L., HOOGENDIJK, A. J., SIMPSON, P. J., VAN ALPHEN, F. P. J., ZANIVAN, S., MERTENS, K., MEIJER, A. B. VAN DEN BIGGELAAR, M. 2017. Paradigm of Biased PAR1 (Protease-Activated Receptor-1) Activation and Inhibition in Endothelial Cells Dissected by Phosphoproteomics. Arterioscler Thromb Vasc Biol, 37, 1891-1902.

WEIDNER, C., FISCHER, C. SAUER, S. 2014. PHOXTRACK-a tool for interpreting comprehensive datasets of post-translational modifications of proteins. Bioinformatics, 30, 3410-1.

ZAKOWSKI, V., KERAMAS, G., KILIAN, K., RAPP, U. R. LUDWIG, S. 2004. Mitogen-activated 3p kinase is active in the nucleus. Exp Cell Res, 299, 101-9.

2.7 Figures

Figure 2.1: Thrombin-induced p38 signaling is not integrated with the RhoA/MLC pathway and promotes HSP27 phosphorylation. A.)α-Thrombin (10 nM) stimulated RhoA activity assay measured in EA.hy926 cells in the presence and absence of p38 inhibitor, SB203580 (3 μM). Cell lysates were immunoblotted for RhoA, phospho-p38 and p38 as indicated. B.) HUVECs were pretreated with p38 inhibitor, SB203580 for 1 hr and stimulated with α-Th, and phosphorylation of MLC determined. The data (mean $\pm$ S.D., n = 3) were analyzed using a Student's t test were not significant. C.) Heat map of each phosphopeptide of HSP27 discovered from phosphoproteomic dataset from 2.5 and 5 min α-Th stimulation. The data (mean $\pm$ S.D., n=2) were analyzed by 2-way ANOVA (*, P$\leq$0.05; **, P$\leq$0.01; ***, P$\leq$0.001). D.) Schematic of HSP27 phosphopeptides identified in mass spec screen. Red "s" indicates phosphorylated serines.

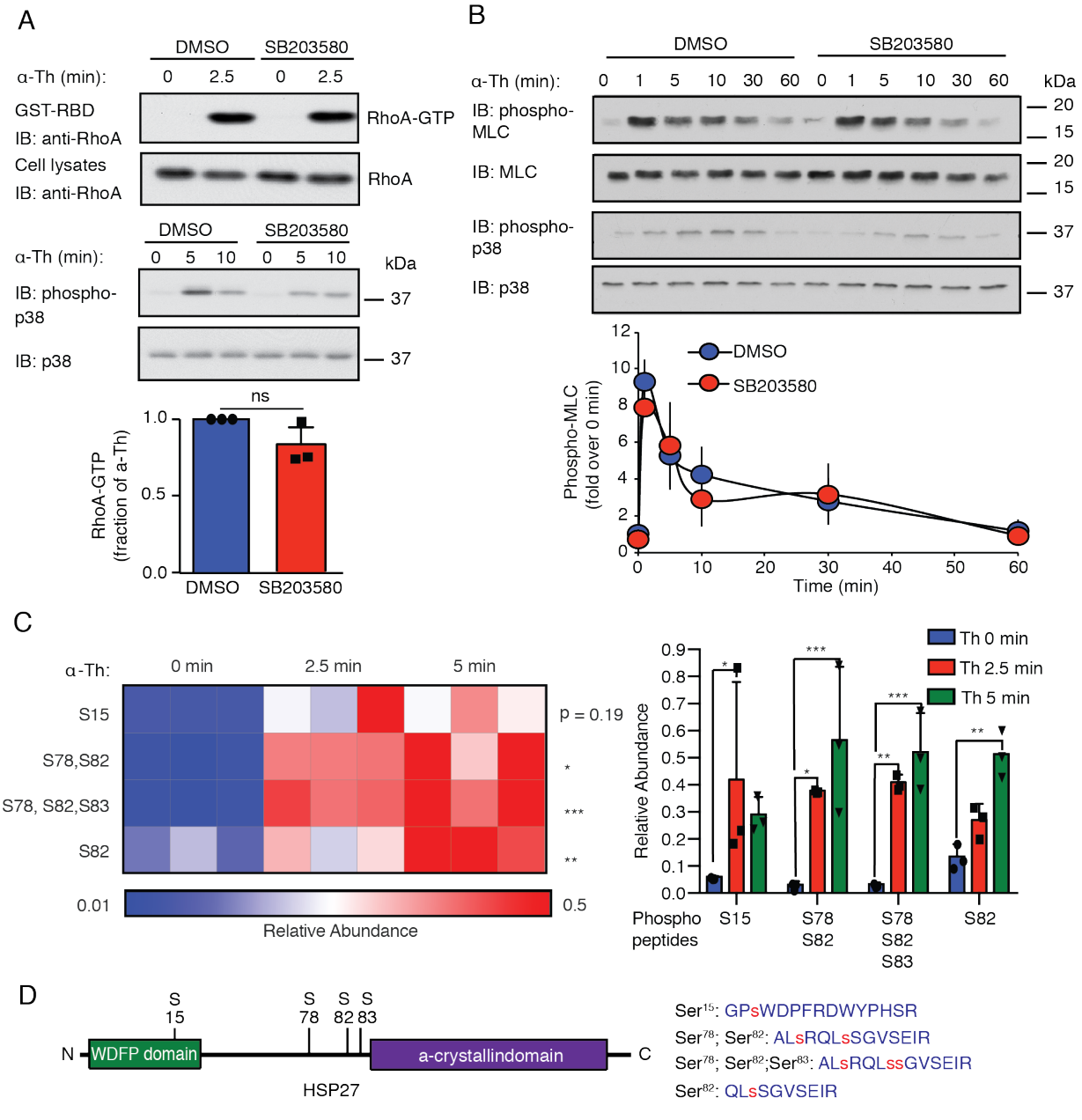
A
DMSO
SB203580
α-Th (min):
0
2.5
0
2.5
GST-RBD
IB: anti-RhoA
RhoA-GTP
Cell lysates
IB: anti-RhoA
RhoA
DMSO
SB203580
α-Th (min):
0
5
10
0
5
10
kDa
IB: phospho-p38
37
IB: p38
37
ns
RhoA-GTP (fraction of a-Th)
1.0
0.5
0.0
DMSO
SB203580
B
DMSO
SB203580
α-Th (min):
0
1
5
10
30
60
0
1
5
10
30
60
kDa
IB: phospho-MLC
20
15
IB: MLC
20
15
IB: phospho-p38
37
IB: p38
37
Phospho-MLC (fold over 0 min)
DMSO
SB203580
Time (min)
C
α-Th:
0 min
2.5 min
5 min
S15
S78,S82
S78, S82,S83
S82
p = 0.19
*
***
**
0.01
0.5
Relative Abundance
Th 0 min
Th 2.5 min
Th 5 min
Relative Abundance
Phospho peptides
S15
S78 S82
S78 S82 S83
S82
D
S 15
S 78
S 82
S 83
N
WDFP domain
a-crystallindomain
C
HSP27
Ser15: GPsWDPFRDWYPHSR
Ser78; Ser82: ALsRQLsSGVSEIR
Ser78; Ser82;Ser83: ALsRQLssGVSEIR
Ser82: QLsSGVSEIR

Figure 2.2: GPCR agonists stimulate p38-dependent HSP27 phosphorylation in multiple endothelial cell types. A.)HUVECs pretreated with 100 μM PAR1 specific antagonist, vorapaxar, for 1 hr and stimulated with 100 μM TFLLRNPNDK for 5 or 10 min and phosphorylation of S15, S78, and S82 of HSP27 was determined by immunoblotting. B.) HUVECs and C.) HDMECs were pretreated with p38 inhibitor, SB203580 (3 μM) for 1 hr and stimulated with 10 nM α-Th for various times, and phosphorylation of Ser15, Ser78, and Ser82 of HSP27 was determined by immunoblotting. A.) HUVECs stimulated with 10 μM histamine pretreated with SB203580 and phosphorylation of HSP27 was determined. The data (mean $\pm$ S.D., n = 4) were analyzed using a Student's t test (*, P $\leq$ 0.05; **, P$\leq$ 0.01; ***, P$\leq$0.001).

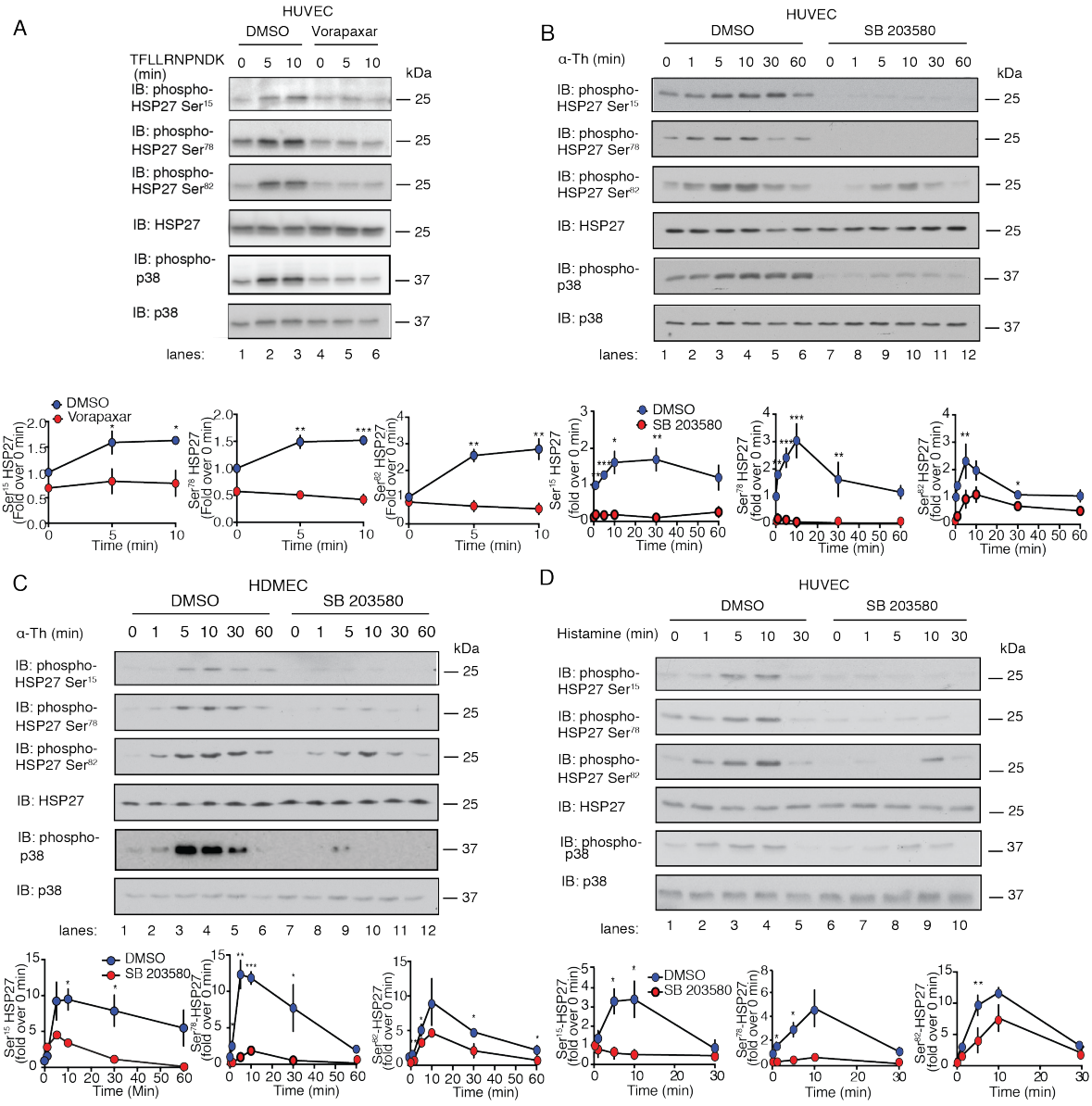
A
HUVEC
DMSO
Vorapaxar
TFLLRNPNDK
(min)
0 5 10 0 5 10
kDa
IB: phospho-HSP27 Ser15
IB: phospho-HSP27 Ser78
IB: phospho-HSP27 Ser82
IB: HSP27
IB: phospho-p38
IB: p38
25
25
25
25
37
37
lanes: 1 2 3 4 5 6
B
HUVEC
DMSO
SB 203580
α-Th (min)
0 1 5 10 30 60 0 1 5 10 30 60
kDa
IB: phospho-HSP27 Ser15
IB: phospho-HSP27 Ser78
IB: phospho-HSP27 Ser82
IB: HSP27
IB: phospho-p38
IB: p38
25
25
25
25
37
37
lanes: 1 2 3 4 5 6 7 8 9 10 11 12
DMSO
Vorapaxar
Ser15 HSP27 (Fold over 0 min)
Ser78 HSP27 (Fold over 0 min)
Ser82 HSP27 (Fold over 0 min)
Time (min)
DMSO
SB 203580
Ser15 HSP27 (fold over 0 min)
Ser78 HSP27 (fold over 0 min)
Ser82 HSP27 (fold over 0 min)
Time (min)
C
HDMEC
DMSO
SB 203580
α-Th (min)
0 1 5 10 30 60 0 1 5 10 30 60
kDa
IB: phospho-HSP27 Ser15
IB: phospho-HSP27 Ser78
IB: phospho-HSP27 Ser82
IB: HSP27
IB: phospho-p38
IB: p38
25
25
25
25
37
37
lanes: 1 2 3 4 5 6 7 8 9 10 11 12
DMSO
SB 203580
Ser15 HSP27 (fold over 0 min)
Ser78 HSP27 (fold over 0 min)
Ser82 HSP27 (fold over 0 min)
Time (Min)
Time (min)
Time (min)
D
HUVEC
DMSO
SB 203580
Histamine (min)
0 1 5 10 30 0 1 5 10 30
kDa
IB: phospho-HSP27 Ser15
IB: phospho-HSP27 Ser78
IB: phospho-HSP27 Ser82
IB: HSP27
IB: phospho-p38
IB: p38
25
25
25
25
37
37
lanes: 1 2 3 4 5 6 7 8 9 10
DMSO
SB 203580
Ser15-HSP27 (fold over 0 min)
Ser78-HSP27 (fold over 0 min)
Ser82-HSP27 (fold over 0 min)
Time (min)
Time (min)
Time (min)

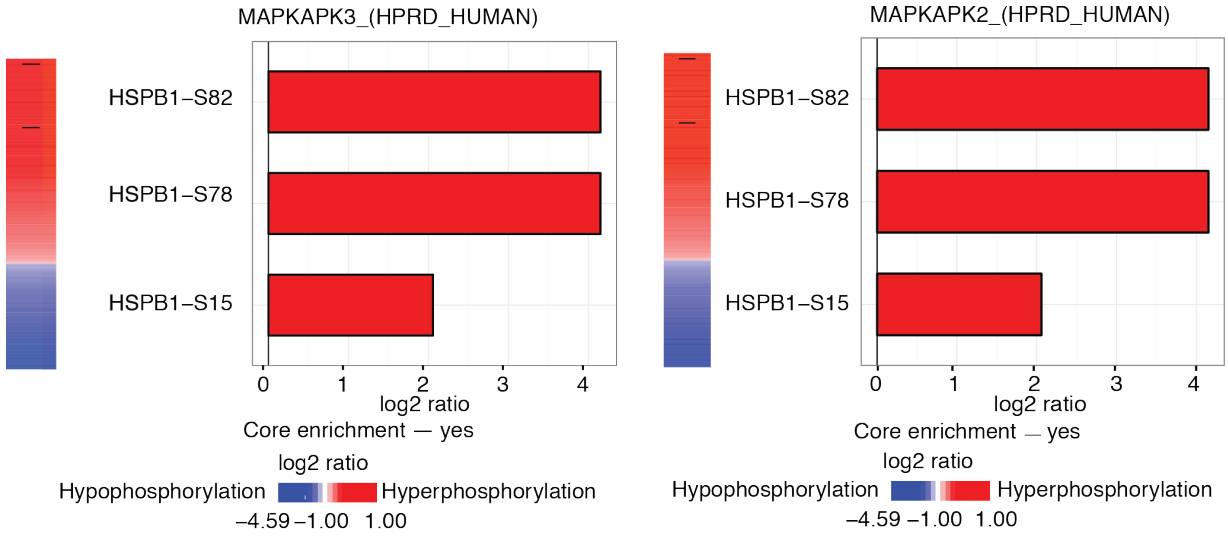

Figure 2.3: PHOXTRACK computational software results selecting MAPKAPK2 (MK2) and MAPKAPK3 (MK3) as causal HSPB1 (HSP27) kinases from our phosphoproteomic dataset input. Graphs show the likelihood of each HSP27 phosphorylation site, Ser15, Ser78, and Ser82 by MK3 and MK2 kinases. Kinases were selected from Human Protein Reference Dataset (HPRD).

Figure 2.4: MK2 and MK3 are required for thrombin-induced HSP27 phosphorylation. A.) HUVECs were pretreated with MK2 inhibitor, PF3644022 (300 nM) for 1 hr and stimulated with 10 nM α-Th, and phosphorylation of Ser15, Ser78, and Ser82 of HSP27 was determined. The data (mean $\pm$ S.D., n = 4) were analyzed using a Student's t-test (*, P $\leq$ 0.05; **, P $\leq$ 0.01; ***, P $\leq$ 0.001). B.) MK2 *in vitro* kinase activity was determined for specific phosphorylation of HSP27 on S78 and S82 in HUVECs pretreated with PF3644022 and stimulated with 10 nM α-Th. The data (mean $\pm$ S.D., n = 4) were analyzed using a Student's t-test (*, P $\leq$ 0.05). C.) HUVECs transiently transfected with non-specific (NS) or MK3 siRNA in addition to pretreatment of DMSO or PF3644022 were stimulated with α-Th and phosphorylation of all three HSP27 sites measured. The data (mean $\pm$ S.D., n = 4) were analyzed using a 2-way ANOVA (*, P $\leq$ 0.05; **, P $\leq$ 0.01). D.) HUVECs were stimulated with α-Th and immunoprecipitated with MK2 to examine co-association with MK3. The data (mean $\pm$ S.D., n = 3) were analyzed using a Student's t-test (**, P $\leq$ 0.01). E.) Homology stick, space filling, and transparent model of HSP27 with Ser15, Ser78, and Ser82 highlighted in green.

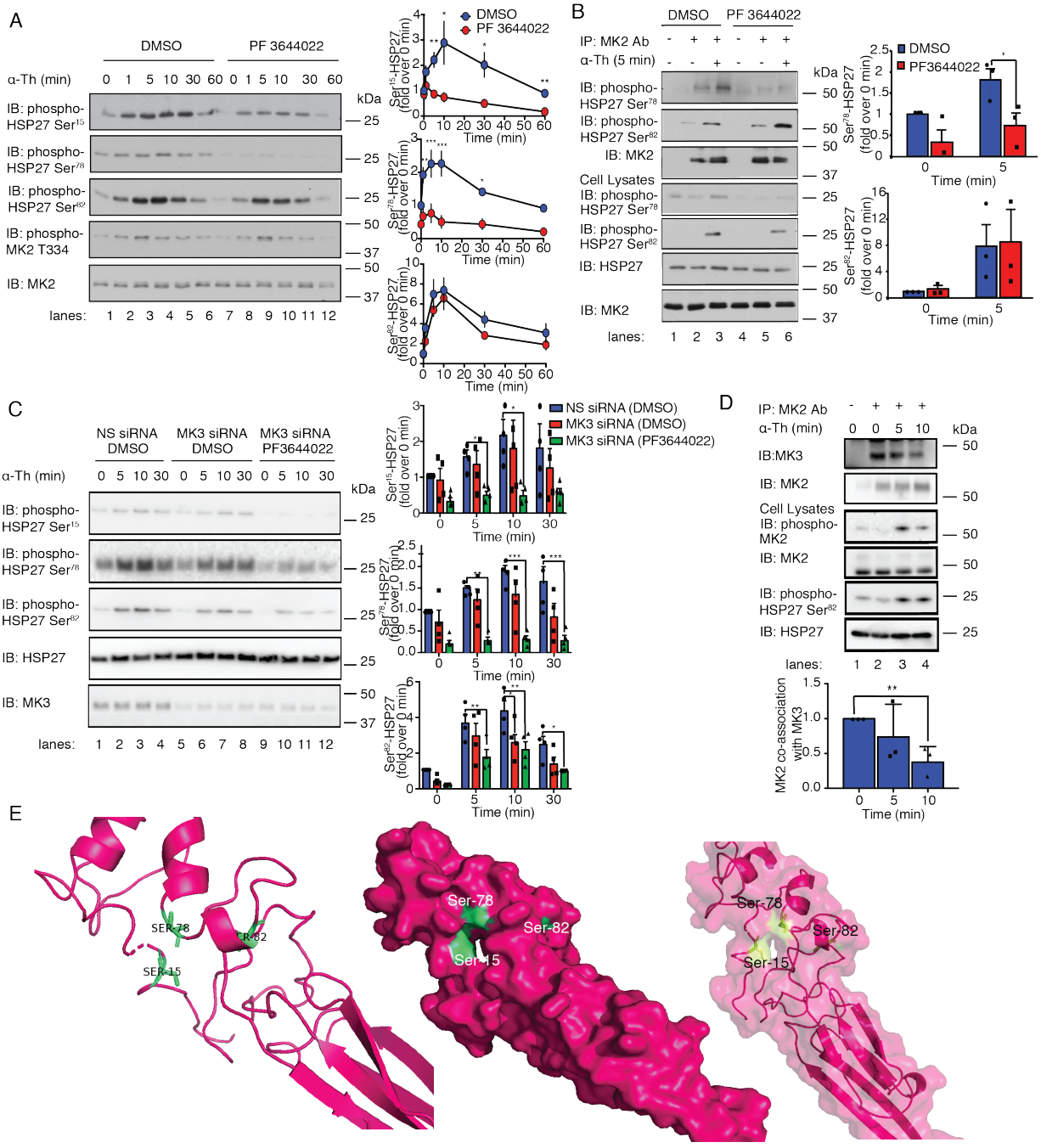
A
DMSO
PF 3644022
α-Th (min)
0 1 5 10 30 60 0 1 5 10 30 60
IB: phospho-HSP27 Ser15
IB: phospho-HSP27 Ser78
IB: phospho-HSP27 Ser82
IB: phospho-MK2 T334
IB: MK2
kDa
lanes: 1 2 3 4 5 6 7 8 9 10 11 12
Ser15-HSP27 (fold over 0 min)
Ser78-HSP27 (fold over 0 min)
Ser82-HSP27 (fold over 0 min)
Time (min)
B
DMSO
PF 3644022
IP: MK2 Ab
α-Th (5 min)
IB: phospho-HSP27 Ser78
IB: phospho-HSP27 Ser82
IB: MK2
Cell Lysates
IB: HSP27
lanes: 1 2 3 4 5 6
C
NS siRNA DMSO
MK3 siRNA DMSO
MK3 siRNA PF3644022
α-Th (min)
0 5 10 30 0 5 10 30 0 5 10 30
IB: HSP27
IB: MK3
lanes: 1 2 3 4 5 6 7 8 9 10 11 12
NS siRNA (DMSO)
MK3 siRNA (DMSO)
MK3 siRNA (PF3644022)
D
IP: MK2 Ab
α-Th (min)
0 0 5 10
IB:MK3
IB: MK2
Cell Lysates
IB: phospho-MK2
IB: phospho-HSP27 Ser82
IB: HSP27
lanes: 1 2 3 4
MK2 co-association with MK3
E
SER-78
SER-82
SER-15
Ser-78
Ser-82
Ser-15

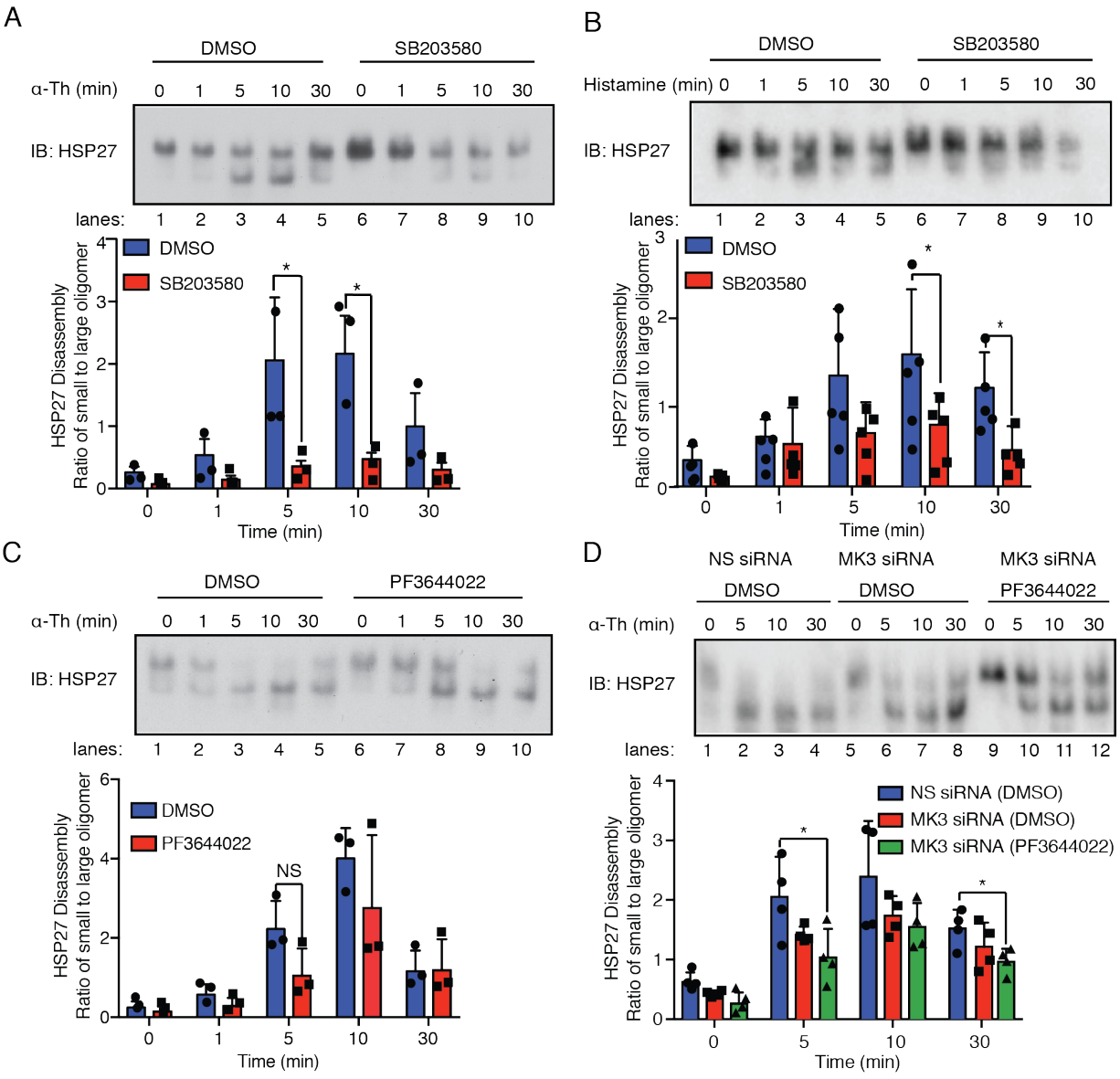

Figure 2.5: GPCR-induced HSP27 activity requires p38, MK2 and MK3. HUVECs pretreated with 3 μM SB203580 and stimulated with A.) 10nM α-Th or B.) 10 μM histamine and resolved on a native non-denaturing gel and immunoblotted for HSP27. C.) HUVECs pretreated with 300 nM PF3644022, MK2 specific inhibitor, and stimulated with thrombin and resolved on a native gel and examine HSP27. D.) HUVECs transiently transfected with non-specific (NS) or MK3 (25 nM) siRNA in addition to pretreatment with DMSO or PF3644022 and stimulated with thrombin and resolved on a native gel and immunoblotted for HSP27. The data (mean $\pm$ S.D., n = 3) were analyzed using a Student's t-test or 2-way ANOVA (*, P $\leq$ 0.05; ns, not significant).

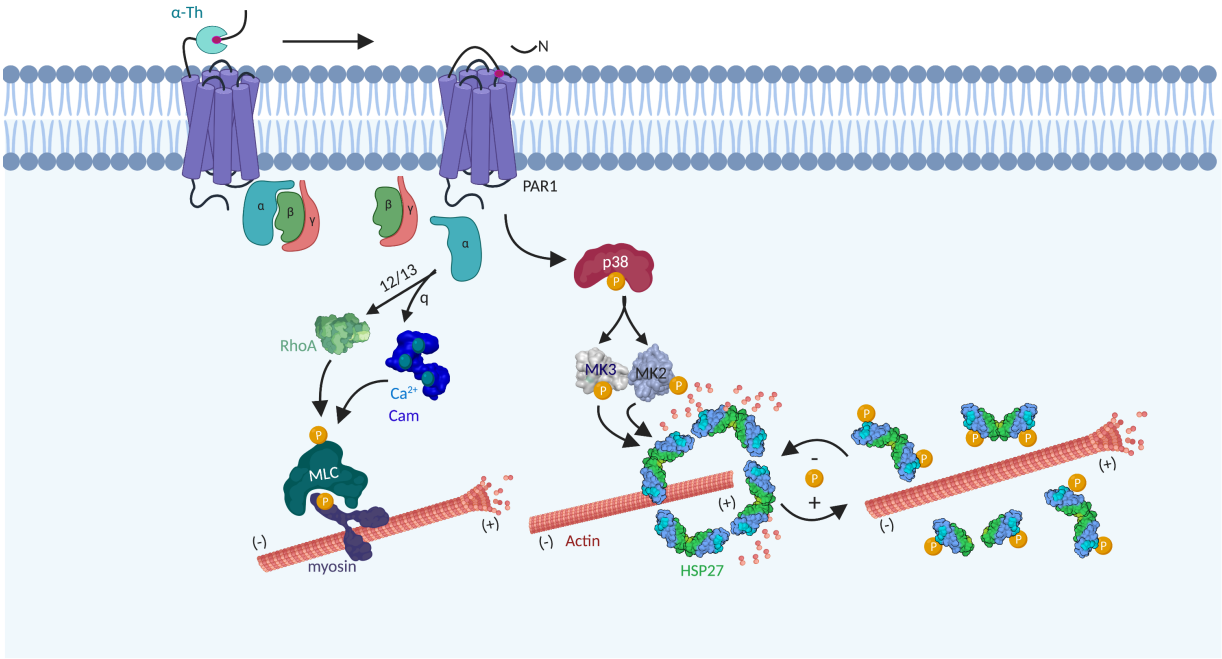

Figure 2.6: PAR1 signaling pathway through HSP27. Thrombin activated PAR1 couples to Gαq to allow calcium (Ca^{2+}) mobilization through calmodulin to allow myosin light chain (MLC) phosphorylation that initiates actin myosin contractility and pulls the endothelial monolayer apart creating endothelial permeability. PAR1 also couples to Gα12/13 and activates RhoA activation and through an alternative pathway also enhances MLC phosphorylation and barrier permeability. PAR1 activation also causes p38 activation which increases HSP27 phosphorylation through two co-associated downstream kinases MK2 and MK3. Phosphorylation of HSP27 disrupts its oligomeric complex and its constraints on actin. The dephosphorylation of HSP27 is important to allow the large HSP27 oligomers to re-form.

Chapter 3

PAR1 induced endothelial barrier recovery is mediated by HSP27

Endothelial cells line the lumen of blood vessels and create a semi-permeable barrier that is disrupted during vascular inflammation resulting in increased permeability, tissue edema, and subsequent organ failure. Protease-activated Receptor-1 (PAR1) is a G protein-coupled receptor (GPCR) for the coagulant protease thrombin and mediates hemostasis, thrombosis, and inflammatory response to vascular injury. However, the distinct mechanism of how endothelial PAR1 promotes vascular pro-inflammatory responses remains poorly understood. We show the protein heat shock protein 27 (HSP27), which functions as a large oligomer to chaperone actin, as a promising candidate for p38-mediated barrier disruption. Indeed, depletion of HSP27 by siRNA *in vitro* enhances barrier permeability and slowed recovery following thrombin stimulation. In contrast, a phospho-deficient HSP27 mutant completely attenuates HSP27 oligomer disruption induced by thrombin and enhances the kinetics of barrier recovery. Inhibition

of thrombin-induced alterations in HSP27 oligomerization using the J2, HSP27 specific inhibitor, increased endothelial barrier permeability *in vitro* and vascular leakage *in vivo*. In this chapter, we show HSP27 function is required for initiating the recovery of the endothelial barrier through phosphorylation of HSP27 after PAR1 stimulation.

3.1 Introduction

Vascular endothelial cells form a semi-permeable barrier that is important for normal tissue homeostasis. During times of inflammation from pathogen or injury, a temporary disruption of the endothelial monolayer occurs to allow movement of fluids and macromolecules to surrounding tissues, leukocyte transmigration, and platelet aggregation (Komarova and Malik, 2010). After resolution of inflammation, a return to homeostasis occurs and the endothelial monolayer returns to its normal, low permeability state. Acute dysregulation of this process can lead to tissue edema and in the presence of pathogens, sepsis, which can ultimately lead to death. Many inflammatory mediators act through GPCRs to promote endothelial barrier disruption (Sun and Ye, 2012), however, the mechanism by which resolution occurs is not clearly understood.

One of the early steps of inflammation is the generation of the protease, thrombin, through a series of zymogen conversion in the blood (Levi et al., 2004). Thrombin irreversibly actives the GPCR, Protease-activated Receptor-1 (PAR1) to promote G protein signaling leading to endothelial barrier permeability through disruption of adherens junction and actin-myosin contractility (Coughlin, 2000). Recently, p38 has been described to regulate PAR1-induced endothelial barrier permeability (Grimsey et al., 2015, Borbiev et al., 2004). In chapter 2 of this dissertation we describe a novel signaling pathway of PAR1-activated p38 through the heat shock

protein (HSP)27 independent of classical G protein signaling effectors RhoA and myosin light chain. In this chapter, we describe the functional consequences of HSP27 on PAR1-induced endothelial barrier permeability.

Endothelial overexpression of HSP27 preserves blood brain barrier integrity, further suggesting a role for HSP27 in regulation of endothelial barrier permeability (Shi et al., 2017). Chapter 2 of this dissertations shows phosphorylation of HSP27 by p38, MK2, and MK3 kinases disrupts large HSP27 oligomeric complexes. Previous studies implicate that phosphorylated HSP27 releases its constraints on actin and allows actin to polymerize (Rogalla et al., 1999, Salinthone et al., 2008), which can contribute to changes in endothelial barrier permeability. In this chapter we will examine the functional consequences of PAR1-activated HSP27 on endothelial barrier permeability both *in vitro* and *in vivo* using both protein depletion and pharmacological inhibition. Furthermore, we examine the role phosphorylation of HSP27 has on endothelial barrier recovery.

3.2 Results

HSP27 mediates thrombin-induced endothelial barrier permeability *in vitro*

We previously demonstrated p38 signaling mediates thrombin-stimulated endothelial permeability *in vitro* and PAR1-induced vascular leakage *in vivo* (Grimsey et al., 2015). HSP27, a substrate phosphorylated by p38 signaling, has also been reported to enhance endothelial barrier *in vitro* (Sun et al., 2015) and *in vivo* (Shi et al., 2017). However, the role of HSP27 in regulation of thrombin-induced endothelial barrier permeability is not known. To examine the thrombin-induced function of HSP27, endothelial cells were transfected with HSP27-specific

siRNAs and endothelial barrier disruption measured *in vitro*. A monolayer of HUVECs were stimulated with thrombin for 10 min and Evans blue-bound albumin flux was quantified for 1 hr. In non-specific (NS) siRNA transfected HUVECs, thrombin-induced a rapid increase in endothelial barrier permeability compared to cells not treated with thrombin (Fig. 3.1A and 3.1B), consistent with previous reports (Grimsey et al., 2015, Knezevic et al., 2009). However, in HUVECs depleted of HSP27 expression, thrombin-induced endothelial barrier permeability was unexpectedly significantly enhanced, resulting in 2.5-fold greater increase in permeability compared to NS siRNA control cells measured at 30 min (Fig. 3.1A and 3.1B). These findings indicate that HSP27 function is important for modulation of thrombin-induced endothelial barrier permeability.

Thrombin induces transient reversible barrier disruption, which recovers to prevent persistent permeability. To understand how loss of HSP27 expression perturbs the dynamics of endothelial barrier permeability, we utilized real-time electric cell-substrate impedance sensing (ECIS) to monitor barrier disruption including the maximum change in impedance or barrier function, time to maximum change in impedance, and time to barrier recovery in HDMECs. HDMECs form strong cell-cell junctions that recapitulates the primary endothelial barrier and were used to examine loss HSP27 function on endothelial barrier dynamics. In NS siRNA transfected HDMECs, the addition of thrombin caused a rapid 20% reduction in impedance or barrier function that peaked at ˜ 4 min (Fig. 3.1C, 3.1D and 3.1E), followed by a rapid recovery that returned to baseline by 40 min (Fig. 3.1C and 3.1F). In contrast, HDMECs deficient in HSP27 expression exhibited a much greater 30% reduction in impedance from baseline after thrombin stimulation and with the maximum loss of barrier function occurred at ˜10 min (Fig. 3.1C, 3.1D and 3.1E). Moreover, in HSP27 depleted HDMECs the time to recovery was much more prolonged, occurring ˜60 min after thrombin stimulation, compared to NS siRNA transfected control cells (Fig.

3.1C and 3.1F). The data also indicate that depletion of HSP27 expression has no significant effect on the baseline or basal barrier function (Fig. 3.1B and 3.1C). However, thrombin stimulation caused a significantly greater reduction in impedance or alteration in barrier function in HSP27 deficient cells, as well as slower recovery time (Fig. 3.1C-F). This is also reflected by enhanced and more prolonged barrier permeability induced by thrombin in HSP27 deficient cells observed in Fig. 3.1A and 3.1B. Given that loss of HSP27 function does not alter the capacity of thrombin to initiate barrier disruption, we hypothesize that HSP27 functions primarily in controlling the magnitude of barrier disruption as well as recovery of barrier function after thrombin stimulation.

HSP27 phosphorylation is required for endothelial barrier recovery

Because HSP27 large oligomer disruption is attenuated by inhibition of p38 as well as inhibition of both MK2 and MK3 which affect all three HSP27 phosphorylation sites, this suggests that Ser15, Ser78, and Ser82 sites are all required to disrupt large HSP27 oligomers. To determine the impact of thrombin-induced phosphorylation of Ser15, Ser78, and Ser82 on endothelial barrier function, we performed knockdown-rescue studies with HSP27 siRNA resistant wildtype (WT) and phosphorylation-deficient mutant in which HSP27 Ser15, Ser78, and Ser82 were converted to alanine, termed triple alanine (TriA) (Fig. 3.2A). HSP27 constructs resistance to siRNA was confirmed by knocking down endogenous HSP27 and rescuing expression with a GFP empty vector or HSP27 siRNA resistant WT or TriA plasmids (Fig. 3.2A and 3.2B). A slight mobility shift can be seen with the re-expression of FLAG-tagged WT and TriA compared to the endogenous HSP27 in the non-specific siRNA control (Fig. 3.2B, lanes 3-4 vs lane 1).

To determine the impact of the phosphorylation sites on HSP27 oligomerization, WT

and TriA constructs were transfected into HUVECs and stimulated with thrombin and resolved using native non-denaturing polyacrylamide gel electrophoresis. Similar to endogenous HSP27, thrombin induced disruption of the large FLAG-tagged WT HSP27 oligomer into smaller oligomers with almost all the large oligomers being disrupted by the 10 min time point (Fig. 3.2C lanes 1-3). In contrast, thrombin failed to cause disassembly of the large FLAG-tagged HSP27 TriA mutant as no changes in mobility were observed after 10 min of stimulation (Fig. 3.2C lanes 4-6). These data suggest that Ser15, Ser78, and Ser82 are required for HSP27 large oligomer disruption induced by thrombin.

To determine the impact of thrombin-induced HSP27 oligomer disruption on endothelial barrier function we performed knockdown-rescue studies with HSP27-siRNA resistant WT and TriA phosphorylation-deficient mutant using ECIS. HDMECs transfected with siRNA to deplete cells of endogenous HSP27 were electroporated with either siRNA-resistant HSP27 WT or TriA mutant or GFP empty vector control. As expected, expression of HSP27 WT significantly reduced the pronounced alterations in thrombin-induced maximal change in impedance and recovery time observed in HDMECs deficient in endogenous HSP27 expression (Fig. 3.2D, 3.2E, and 3.2G). Expression of HSP27 phosphorylation-deficient TriA also significantly reduced maximal thrombin-induced impedance change and barrier recovery time alterations induced by loss of HSP27 function (Fig. 3.2D, 3.2E, and 3.2G), in addition to significantly decreasing time to peak impedance compared to GFP rescue (Fig, 3.2D and 3.2F). This suggests that phosphorylation of Ser15, Ser78, and Ser82 are important for initiating the resolution of the endothelial barrier. Taken together this data suggest that thrombin-induced HSP27 Ser15, Ser78, and Ser82 phosphorylation are required for disassembly of large HSP27 oligomers, which appears to function primarily in recovery of the endothelial barrier.

Disruption of HSP27 oligomerization enhances PAR1-induced vascular leakage *in vitro* and *in vivo*

To determine the role of phosphorylation-independent effects of HSP27 on PAR1-induced barrier disruption, we examined the function of HSP27 using the J2 HSP27 inhibitor and assessed vascular leakage *in vivo*. The J2 inhibitor has been described previously to induce abnormal HSP27 dimer formation, preventing the re-formation of large HSP27 oligomers (Hwang et al., 2017), which is important for modulation of the actin cytoskeleton. To determine the effects of J2 on HSP27 oligomerization, HUVECs were pretreated with J2 and then stimulated with thrombin. While J2 failed to block disassembly of HSP27 large oligomer compared to control cells (Fig. 3.3A, lanes 1-4 versus 6-9), the inhibitor significantly prevented HSP27 small oligomers re-formation into large HSP27 oligomer complexes at the 30 min timepoint (Fig. 3.3A, lane 5 versus 8). We further demonstrate the J2 inhibitor fails to block thrombin-induced changes in HSP27 phosphorylation at Ser15, Ser78, and Ser82 (Fig. 3.3B). Thus, the J2 inhibitor disrupts HSP27 oligomerization in a phosphorylation-independent manner and prevents re-formation of a large oligomeric complex.

To assess if disruption of HSP27 oligomerization affects PAR1-induced endothelial permeability, a monolayer of HUVECs were pretreated with and without the J2 inhibitor, stimulated with thrombin, and measurement of Evans blue-bound albumin flux was quantified. HUVECs pretreated with the J2 inhibitor had a significant 2.5-fold increase in thrombin-induced endothelial permeability at 30 min compared to DMSO control (Fig. 3.3C). No significant changes in baseline permeability were observed in the presence of the J2 inhibitor, indicating that alterations are specific to thrombin effects on endothelial barrier permeability. HSP27 blockade by J2 portrayed a similar enhanced PAR1-dependent barrier permeability phenotype to HUVECs

depleted of HSP27 with siRNA in Fig. 3.1A and 3.1B, suggesting that the J2 inhibitor mimics the HSP27 loss of function phenotype.

To determine if disruption of the HSP27 oligomerization affects PAR1-induced vascular leakage, mice were treated with the J2 inhibitor or DMSO control and vascular leakage measured by the Miles assay (Hwang et al., 2017, Kim et al., 2018). In these studies, mice were stimulated with the PAR1-specific synthetic peptide TFLLRN rather than thrombin, since thrombin activates murine platelet PAR4 resulting in activation and aggregation (Kahn et al., 1999). Mice were pretreated with either high (15 mg/ml) or low (1.5 mg/ml) doses of the J2 inhibitor by IP injection, and then stimulated with TFLLRN, vascular endothelial growth factor (VEGF), or PBS control and vascular leakage measured. Under basal PBS conditions, vascular leakage was not altered by the J2 inhibitor compared to DMSO vehicle control (Fig. 3.3D). Intradermal injections of PAR1-specific peptide agonist, TFLLRN, induced a marked increase in Evans blue-bound albumin leakage compared to the PBS injected control in DMSO treated mice (Fig. 3.3D). However, vascular leakage induced by TFLLRN-activation of PAR1 was significantly enhanced in J2 inhibitor pretreated mice (Fig. 3.3D), consistent with enhanced thrombin-induced barrier permeability observed in HSP27 depleted cells and J2 preincubated cells *in vitro* (Fig. 3.1A and 3.3C). Unlike PAR1-stimulated vascular leakage, inhibition of HSP27 by J2 inhibitor failed to affect VEGF-induced vascular leakage, indicating that HSP27 function is specific to GPCR pro-inflammatory signaling. These results strongly suggest HSP27 is critical for regulating activated PAR1-induced endothelial barrier permeability *in vitro* and *in vivo*.

3.3 Conclusion and Discussion

In this chapter we show HSP27 enhances GPCR-induced endothelial barrier permeability recovery *in vitro* rather than initiating barrier disruption, and HSP27 functions to dampen vascular leakage *in vivo*. We further demonstrate that PAR1-induced phosphorylation of HSP27 is critical for disassembly of HSP27 large oligomers and initiating resolution of the endothelial barrier.

This illustrates an unexpected finding of HSP27 depletion enhancing endothelial barrier leakage. Whereas knockdown of p38 MAPK causes loss of thrombin-induced barrier disruption (Grimsey et al., 2015), our studies show that depletion of HSP27, a target of the p38 signaling axis, results in an opposite effect and enhances thrombin-induced barrier permeability. These differences may be caused by the broad actions of p38 on numerous downstream substrates (Cuenda and Rousseau, 2007) that disrupt barrier integrity including modulation of adherens junction destabilization (Khanna et al., 2010) and actomyosin contractility (Mirzapoiazova et al., 2005). Moreover, HSP27 appears to function in barrier recovery in an agonist-dependent manner following thrombin stimulation, since loss of HSP27 protein does not affect baseline barrier permeability. Although thrombin is known to transiently disrupt barrier permeability through disruption of adherens junction and actin myosin contractility (Rabiet et al., 1996, Bogatcheva et al., 2002), there is limited understanding of the mechanism responsible for resolution of the endothelial barrier. A previous study showed G$\beta\gamma$ signaling through FAK modulates adherens junctions reassembly and is important for thrombin / PAR1 induced barrier recovery (Knezevic et al., 2009). Our study shows thrombin / PAR1 endothelial barrier recovery functions through HSP27, an actin binding protein.

Furthermore, we show that the initiation of barrier recovery is dependent on HSP27

phosphorylation using knockdown-rescue ECIS experiments. It has previously been reported that an imbalance of both phosphorylation and dephosphorylation of HSP27 can lead to inadequate or excessive actin filaments and affect actin motility (Gurgis et al., 2014). This suggests that by inhibiting HSP27 phosphorylation with our phospho-deficient mutant, TriA, there is a dysregulation in actin regulating the endothelial barrier, although we cannot definitively state if too much or too little actin is being polymerized in our studies.

In summary, this chapter provides evidence that HSP27 is required for the resolution of GPCR-induced barrier recovery *in vitro* and for PAR1-induced vascular leakage *in vivo*. The J2 inhibitor alters HSP27 oligomerization consistent with a loss of function in which it does not allow the HSP27 oligomer to reanneal. J2 is unique as it disrupts HSP27 activity but is phosphorylation-independent so the functionality of the protein can be assessed in the smaller oligomer state, recapitulating a loss of function protein. We show HSP27 activity is agonist dependent and appears to be specific to GPCR regulation as VEGF had no change in vascular permeability with the J2 inhibitor. This study demonstrates HSP27 as a target for localized control of vascular leakage and a potential candidate for therapeutic intervention in vascular diseases.

3.4 Materials and Methods

Endothelial barrier permeability assay

Endothelial barrier permeability was quantified by measuring the flux of Evans blue-bound BSA as previously described (Grimsey et al., 2018). HUVEC cells were seeded onto collagen-coated 3.0 μM transwell permeability support chambers (Corning) and grown for 5

days until confluent. The cells were serum starved for 2 hr and treated with 10 nM thrombin. Evans blue conjugated to BSA was added to the upper chamber after 10 or 30 min of thrombin stimulation. Samples were removed from the lower chamber at the indicated time points and the amount of Evans blue diffusion was quantified by measuring the absorbance at 605 nm using a microplate reader (SpectraMax Plus, Molecular Devices).

Vascular permeability assays

Vascular permeability was measured *in vivo* as described with minor modifications (Korhonen et al., 2009). Briefly, 8-week old CD1/CD1 female mice were injected intraperitoneally with 100 μl of DMSO in PBS, 1.5 mg/kg, or 15 mg/kg of J2 HSP27 inhibitor. After 24 hr, mice were anesthetized and injected in the tail-vein with 200 μl of 1.0% Evan's blue-0.1% BSA diluted in PBS. After 1 min, 50 μl of 0.1% BSA in PBS, 4 ng/μl VEGF or 1μg/μl TFLLRN peptide were injected intradermally into separate areas of the shaved back skin of the mouse. The mice were sacrificed 10 min post injection and 8 mm punch biopsy of skin containing the site of injection was removed. The skin biopsies were incubated in 500 μl of formamide at 65°C for 24 hr, and the amount of extracted Evan's blue dye was measured using a microplate reader at O.D. 595 nm. Animal studies were performed in accordance with the recommendations in the Guide for the Care and Use of Laboratory Animals of the National Institutes of Health under protocols approved by the Institutional Animal Care and Use Committee (IACUC) at the University of California San Diego.

Native gel electrophoresis

HUVECs were serum-starved, incubated 10 μM J2 for 16 hr or no pretreatment with HSP27 constructs, and treated with 10 nM thrombin over a 10 or 30 min time courses. Samples were collected in 2X Laemmli sample buffer in the absence of DTT and heat and supplemented with 10 μg/ml leupeptin, 10 μg/ml aprotinin, 10 μg/ml trypsin protease inhibitor, 10 μg/ml pepstatin, and 10 μg/ml PMSF. Samples were resolved on a native PAGE gel in non-denaturing running buffer (25mM Tris-HCl and 192 mM glycine), transferred to PDVF membranes and immunoblotted with anti-HSP27 antibody. Membranes were developed by chemiluminescence and quantified by densitometry.

Transfections and siRNA

HUVECs and HDMECs were transfected with siRNAs using TransIT-X2 according to manufacturer's instructions (Mirus Bio). HSPPB1 siRNA (5'-AAGGACGAGCATGGCTACATC-3') used at 12.5 nM in HUVEC and 25 nM in HDMECs; and nonspecific (ns) All Stars Negative Control siRNA (5'-GGCUACGUCCAGGAGCGCACC-3') were all obtained from Qiagen. HDMEC knockdown rescue experiments were performed by transfecting HSP27 siRNA for 5 days and then rescuing with siRNA resistant HSP27 constructs by electroporation on ECIS machine for 36 hr.

Electrical cell impedance sensing (ECIS)

Following siHSP27/control knockdown, HDMECs were seeded on to cysteine/collagen-coated gold microwell 8W10E+ ECIS array (Applied Biophysics, MA) and allowed to reach confluence for 48-72 hr until impedance reached 3000 ohms. Baseline barrier was recorded and

established using multiple frequency/time (MFT). Permeability was measured following 10 nM thrombin treatment and recording continued until barrier recovered to baseline impedance. For knockdown recovery experiments, cells were electroporated with 0.2 μg of plasmid DNA on ECIS array electrodes at 36 hr and allowed 36 hr to recovery before adding thrombin.

HSP27 phosphorylation assays and Western Immunoblots

HUVECs incubated 10 μM J2 for 16 hr, serum-starved for 2 hr, and were treated with α-thrombin over a 30 min time course. Samples were collected in 2X SDS Laemmli sample buffer containing 200 mM DTT and heated at 95°C for 10 min. Equivalent amounts of cell lysates were resolved by SDS-PAGE, transferred to PDVF membranes and probed with anti-GAPDH, anti-HSP27, phospho-specific HSP27, anti-p38, and phospho-specific p38 antibodies. Membranes were developed by chemiluminescence and quantified by densitometry with Image J (National Institute of Health).

Cell culture and Plasmids

Pooled-primary human umbilical vein endothelial cells (HUVEC) or human dermal microvascular endothelial cells (HDMEC) were purchased from Lonza and used up to passage 6. HUVECs were grown in EGM-2 (Lonza). HDMECs were grown in EGM-2MV (Lonza). PAR1 expressing Hela cells and EA.hy926, HUVEC derived immortalized endothelial cells, were grown in DMEM/F12 with 10% FBS. All cells were cultured in a 37°C incubator with 5% CO_2. N-terminal FLAG-tagged human pcDNA of HSP27 WT and TriA mutant were generous gifts provided by the Gary Brewer Lab (Rutger's University, Newark, NJ). HSP27 siRNA resistance was generated with QuikChange site-directed mutagenesis (Agilent Technologies) of 5 silent point mutations

at the site of siRNA binding to residues c387t, g390a, t393c, c396t, c399t. All plasmids were confirmed with sequencing.

Antibodies and reagents

α-Thrombin was purchased from Enzyme Research Laboratories. Murine PAR1 agonist peptide (TFLLRN) was synthesized and purified by reverse-phase high-pressure liquid chromatography at Tufts University Core Facility. VEGF was purchased from PeproTech. HSP27 specific inhibitor J2 was synthesized and purchased from ProbChem. PF3644022 was purchased from Tocris. SB203580 was from LC laboratories. Polyclonal rabbit anti-p38, monoclonal mouse anti-HSP27, and polyclonal rabbit phospho-HSP27 (Ser15, Ser78, and Ser82) antibodies were from Cell Signaling Technology. Monoclonal mouse anti-GAPDH antibody was from GeneTex. HRP-conjugated goat–anti rabbit and goat–anti mouse antibodies were from Bio-Rad Laboratories.

Statistical Analysis and Replications

Statistical significance between datasets with three or more experimental groups was determined using one-way analysis of variance (ANOVA) including a Tukey's test for multiple comparisons. Statistical difference between two experimental groups was determined using a two-tailed unpaired t-test. For all tests, a p-value of 0.05 was used as the cutoff to determine significance. All experiments were repeated a least three times, and p-values are indicated in each figure. All statistical analysis was performed using GraphPad prism 7.

3.5 Acknowledgements

This research was funded by National Institutes of Health (R35 GM127121), a pre-doctoral fellowship by Tobacco-Related Disease Research Program (TRDRP 27DT-0009), as well as a training grant by NIH/NIGMS (T32 GM007752).

Chapter 3 in part is a reprint of material to be submitted to be published in: **Rada CC**, Mejia-Pena H, Grimsey NJ, Canto-Cordova I, Olson J, Wozniak JM, Gonzalez DJ, Nizet V, Trejo J. “Heat Shock Protein 27 activity is linked to endothelial barrier recovery induced by GPCR pro-inflammatory mediator.” The dissertation author was the primary author.

3.6 References

BOGATCHEVA, N. V., GARCIA, J. G. VERIN, A. D. 2002. Molecular mechanisms of thrombin-induced endothelial cell permeability. Biochemistry (Mosc), 67, 75-84.

BORBIEV, T., BIRUKOVA, A., LIU, F., NURMUKHAMBETOVA, S., GERTHOFFER, W. T., GARCIA, J. G. VERIN, A. D. 2004. p38 MAP kinase-dependent regulation of endothelial cell permeability. Am J Physiol Lung Cell Mol Physiol, 287, L911-8.

COUGHLIN, S. R. 2000. Thrombin signalling and protease-activated receptors. Nature, 407, 258-64.

CUENDA, A. ROUSSEAU, S. 2007. p38 MAP-kinases pathway regulation, function and role in human diseases. Biochim Biophys Acta, 1773, 1358-75.

GRIMSEY, N. J., AGUILAR, B., SMITH, T. H., LE, P., SOOHOO, A. L., PUTHENVEEDU, M. A., NIZET, V. TREJO, J. 2015. Ubiquitin plays an atypical role in GPCR-induced p38 MAP kinase activation on endosomes. J Cell Biol, 210, 1117-31.

GRIMSEY, N. J., NARALA, R., RADA, C. C., MEHTA, S., STEPHENS, B. S., KUFAREVA, I., LAPEK, J., GONZALEZ, D. J., HANDEL, T. M., ZHANG, J. TREJO, J. 2018. A Tyrosine Switch on NEDD4-2 E3 Ligase Transmits GPCR Inflammatory Signaling. Cell Rep, 24, 3312-3323 e5.

GURGIS, F. M., ZIAZIARIS, W. MUNOZ, L. 2014. Mitogen-activated protein kinase-activated protein kinase 2 in neuroinflammation, heat shock protein 27 phosphorylation, and cell cycle: role and targeting. Mol Pharmacol, 85, 345-56.

HWANG, S. Y., KWAK, S. Y., KWON, Y., LEE, Y. S. NA, Y. 2017. Synthesis and biological effect of chrom-4-one derivatives as functional inhibitors of heat shock protein 27. Eur J Med Chem,

139, 892-900.

KAHN, M. L., NAKANISHI-MATSUI, M., SHAPIRO, M. J., ISHIHARA, H. COUGHLIN, S. R. 1999. Protease-activated receptors 1 and 4 mediate activation of human platelets by thrombin. J Clin Invest, 103, 879-87.

KHANNA, P., YUNKUNIS, T., MUDDANA, H. S., PENG, H. H., AUGUST, A. DONG, C. 2010. p38 MAP kinase is necessary for melanoma-mediated regulation of VE-cadherin disassembly. Am J Physiol Cell Physiol, 298, C1140-50.

KIM, J. Y., AN, Y. M., YOO, B. R., KIM, J. M., HAN, S. Y., NA, Y., LEE, Y. S. CHO, J. 2018. HSP27 inhibitor attenuates radiation-induced pulmonary inflammation. Sci Rep, 8, 4189.

KNEZEVIC, N., TAUSEEF, M., THENNES, T. MEHTA, D. 2009. The G protein betagamma subunit mediates reannealing of adherens junctions to reverse endothelial permeability increase by thrombin. J Exp Med, 206, 2761-77.

KOMAROVA, Y. MALIK, A. B. 2010. Regulation of endothelial permeability via paracellular and transcellular transport pathways. Annu Rev Physiol, 72, 463-93.

KORHONEN, H., FISSLTHALER, B., MOERS, A., WIRTH, A., HABERMEHL, D., WIELAND, T., SCHUTZ, G., WETTSCHURECK, N., FLEMING, I. OFFERMANNS, S. 2009. Anaphylactic shock depends on endothelial Gq/G11. J Exp Med, 206, 411-20.

MIRZAPOIAZOVA, T., KOLOSOVA, I. A., ROMER, L., GARCIA, J. G. VERIN, A. D. 2005. The role of caldesmon in the regulation of endothelial cytoskeleton and migration. J Cell Physiol, 203, 520-8.

RABIET, M. J., PLANTIER, J. L., RIVAL, Y., GENOUX, Y., LAMPUGNANI, M. G. DEJANA, E. 1996. Thrombin-induced increase in endothelial permeability is associated with changes in

cell-to-cell junction organization. Arterioscler Thromb Vasc Biol, 16, 488-96.

RENNA, M., SCHAFFNER, C., BROWN, K., SHANG, S., TAMAYO, M. H., HEGYI, K., GRIMSEY, N. J., CUSENS, D., COULTER, S., COOPER, J., BOWDEN, A. R., NEWTON, S. M., KAMPMANN, B., HELM, J., JONES, A., HAWORTH, C. S., BASARABA, R. J., DEGROOTE, M. A., ORDWAY, D. J., RUBINSZTEIN, D. C. FLOTO, R. A. 2011. Azithromycin blocks autophagy and may predispose cystic fibrosis patients to mycobacterial infection. J Clin Invest, 121, 3554-63.

ROGALLA, T., EHRNSPERGER, M., PREVILLE, X., KOTLYAROV, A., LUTSCH, G., DUCASSE, C., PAUL, C., WIESKE, M., ARRIGO, A. P., BUCHNER, J. GAESTEL, M. 1999. Regulation of Hsp27 oligomerization, chaperone function, and protective activity against oxidative stress tumor necrosis factor alpha by phosphorylation. Journal of Biological Chemistry, 274, 18947-18956.

SALINTHONE, S., TYAGI, M. GERTHOFFER, W. T. 2008. Small heat shock proteins in smooth muscle. Pharmacol Ther, 119, 44-54.

SHI, Y., JIANG, X., ZHANG, L., PU, H., HU, X., ZHANG, W., CAI, W., GAO, Y., LEAK, R. K., KEEP, R. F., BENNETT, M. V. CHEN, J. 2017. Endothelium-targeted overexpression of heat shock protein 27 ameliorates blood-brain barrier disruption after ischemic brain injury. Proc Natl Acad Sci U S A, 114, E1243-E1252.

SUN, H. B., REN, X., LIU, J., GUO, X. W., JIANG, X. P., ZHANG, D. X., HUANG, Y. S. ZHANG, J. P. 2015. HSP27 phosphorylation protects against endothelial barrier dysfunction under burn serum challenge. Biochem Biophys Res Commun, 463, 377-83.

SUN, L. YE, R. D. 2012. Role of G protein-coupled receptors in inflammation. Acta Pharmacol Sin, 33, 342-50.

3.7 Figures

Figure 3.1: Loss of HSP27 enhances thrombin-induced endothelial barrier permeability *in vitro*. A.) Representative tracing of HUVECs transfected with HSP27 siRNA or non-specific (NS) siRNA were stimulated with or without 10 nM α-Th for 10 min and endothelial cell (EC) barrier permeability measured by quantifying Evan's blue albumin diffusion. Inset, shows siRNA-mediated depletion of HSP27. B.) α-Th induced EC permeability was quantified at 30 min. The data (mean $\pm$ S.E.M., n=4) and analyzed by a Student's t-test (**, P$\leq$0.01). C.) Representative tracing of HDMECs transfected with NS and HSP27 siRNA were stimulated with α-Th and reduction in endothelial barrier impedance or function was determined by ECIS measurement. The data normalized at time of thrombin addition (0 min) were quantified for maximum (max) thrombin-induced change in impedance (D), time to max impedance (E), and time to barrier recovery (F), performed in duplicate and the data (mean $\pm$ S.E.M, n=4) and analyzed by a 2-way ANOVA (*, P$\leq$0.05).

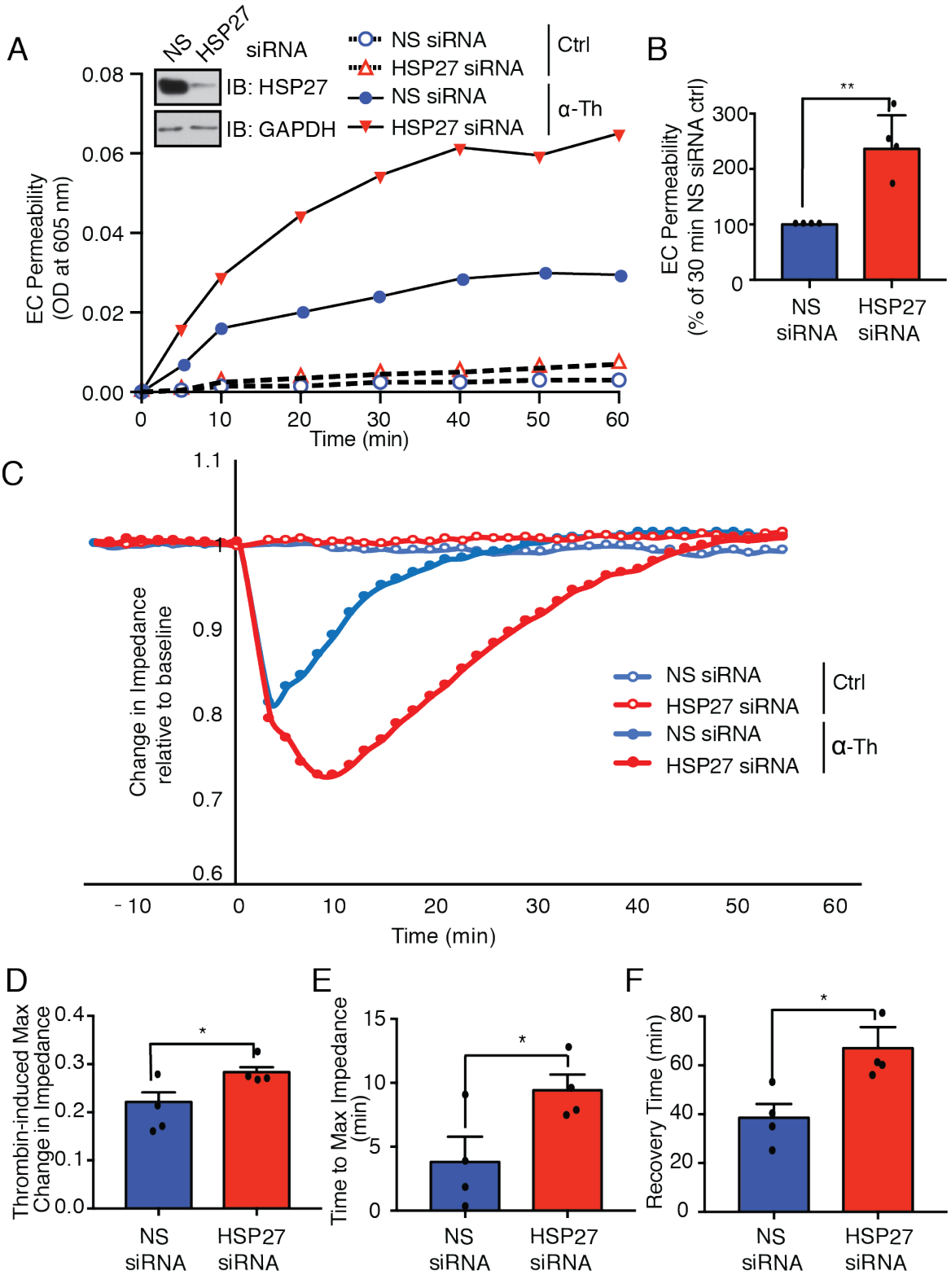
A
NS
HSP27
siRNA
IB: HSP27
IB: GAPDH
NS siRNA
HSP27 siRNA
NS siRNA
HSP27 siRNA
Ctrl
α-Th
EC Permeability (OD at 605 nm)
Time (min)
B
EC Permeability (% of 30 min NS siRNA ctrl)
**
NS siRNA
HSP27 siRNA
C
Change in Impedance relative to baseline
NS siRNA
HSP27 siRNA
NS siRNA
HSP27 siRNA
Ctrl
α-Th
Time (min)
D
Thrombin-induced Max Change in Impedance
*
NS siRNA
HSP27 siRNA
E
Time to Max Impedance (min)
*
NS siRNA
HSP27 siRNA
F
Recovery Time (min)
*
NS siRNA
HSP27 siRNA

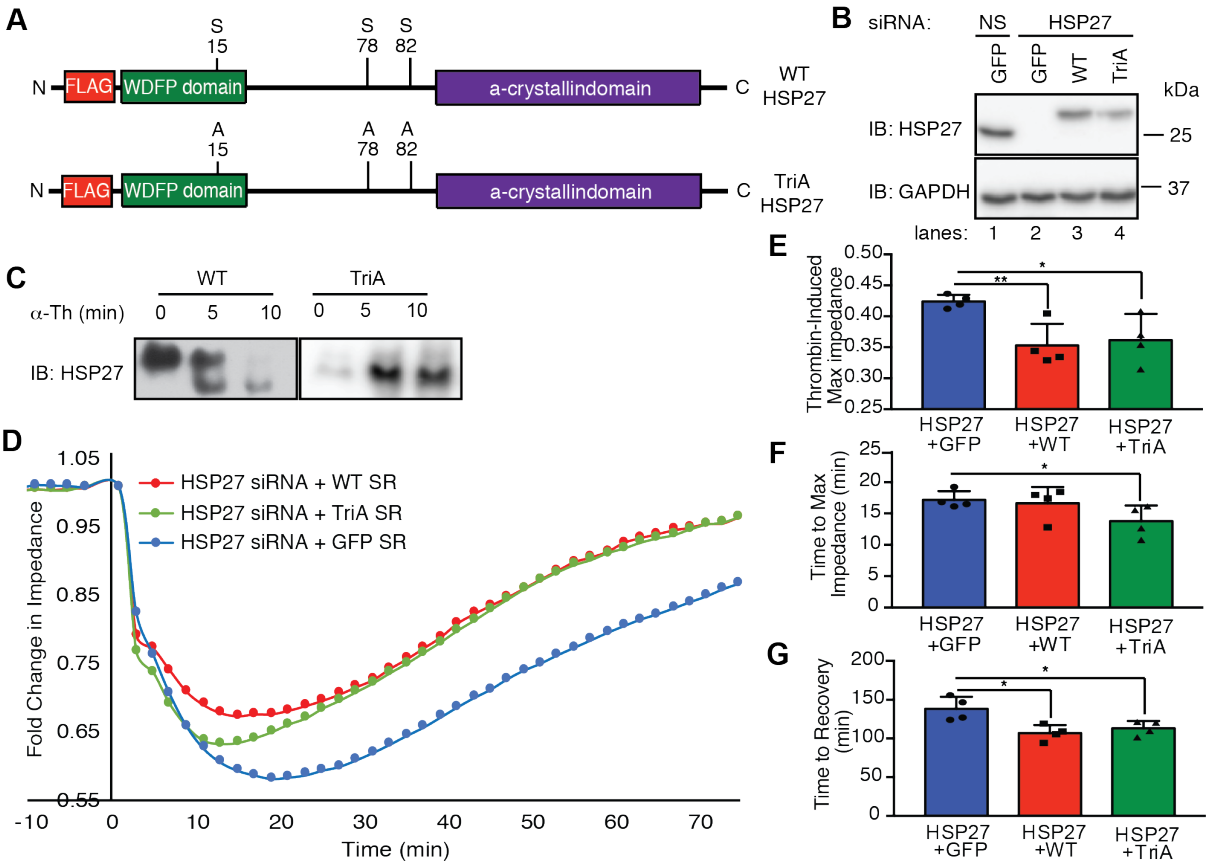

Figure 3.2: HSP27 phosphorylation is required for endothelial barrier recovery. A.) Map of N-terminal flag-tagged HSP27 wildtype (WT) and triple alanine substitution (TriA) constructs. B.) Immunoblot confirmation of HSP27 siRNA resistance for HSP27 WT and TriA constructs, but not GFP empty vector in PAR1 expressing Hela cells. C.) HUVECs transfected with WT or TriA HSP27 plasmid and stimulated with 10nM α-Th and resolved on a native non-denaturing gel and immunoblotted for HSP27. D.) Representative ECIS tracing of HDMECs depleted of HSP27 with siRNA and re-expression of GFP or siRNA resistant HSP27 WT or TriA plasmids. Addition of 10nM α-Th is at 0 min. Quantified data of E.) maximum (max) thrombin-induced change in impedance, time to F.) max impedance and G.) barrier recovery. The data ran in duplicate (mean $\pm$ S.E.M., n=4) and analyzed by a 2-way ANOVA (*, P$\leq$0.05; **, P$\leq$0.01).

Figure 3.3: Disruption of HSP27 oligomerization enhances PAR1-induced vascular leakage in vivo. A.) HUVECs pretreated with 10 μM J2, HSP27 specific inhibitor, and stimulated with 10 nM α-Th resolved on a native non-denaturing gel and immunoblotted for HSP27. B.) HUVECs were pretreated with HSP27 inhibitor, J2 (10 μM) for 16 hr and stimulated with 10 nM α-Th for various times, and phosphorylation of p38 and S15, S78, and S82 of HSP27 was determined by immunoblotting. C.) Representative tracing of HUVECs pretreated with HSP27 inhibitor, J2 or DMSO were stimulated with or without 10 nM α-Th for 30 min and endothelial cell (EC) barrier permeability measured by quantifying Evan's blue albumin diffusion. α-Th induced EC permeability was quantified at 30 min. The data (mean $\pm$ S.D., n=3) were analyzed by a Student's t-test (*, P$\leq$0.05) D.) The Miles Assay in which mice received intraperitoneal injection of PBS or low or high doses of J2 24 hr before injection of PBS, 4 ng/μl VEGF, or 1 μg/μl TFLLRN. The data (mean $\pm$ S.E.M., n = 24 mice) from four independent experiments were analyzed using a 2-way ANOVA (*, P$\leq$0.05; **, P$\leq$0.01; ***, P$\leq$ 0.001).

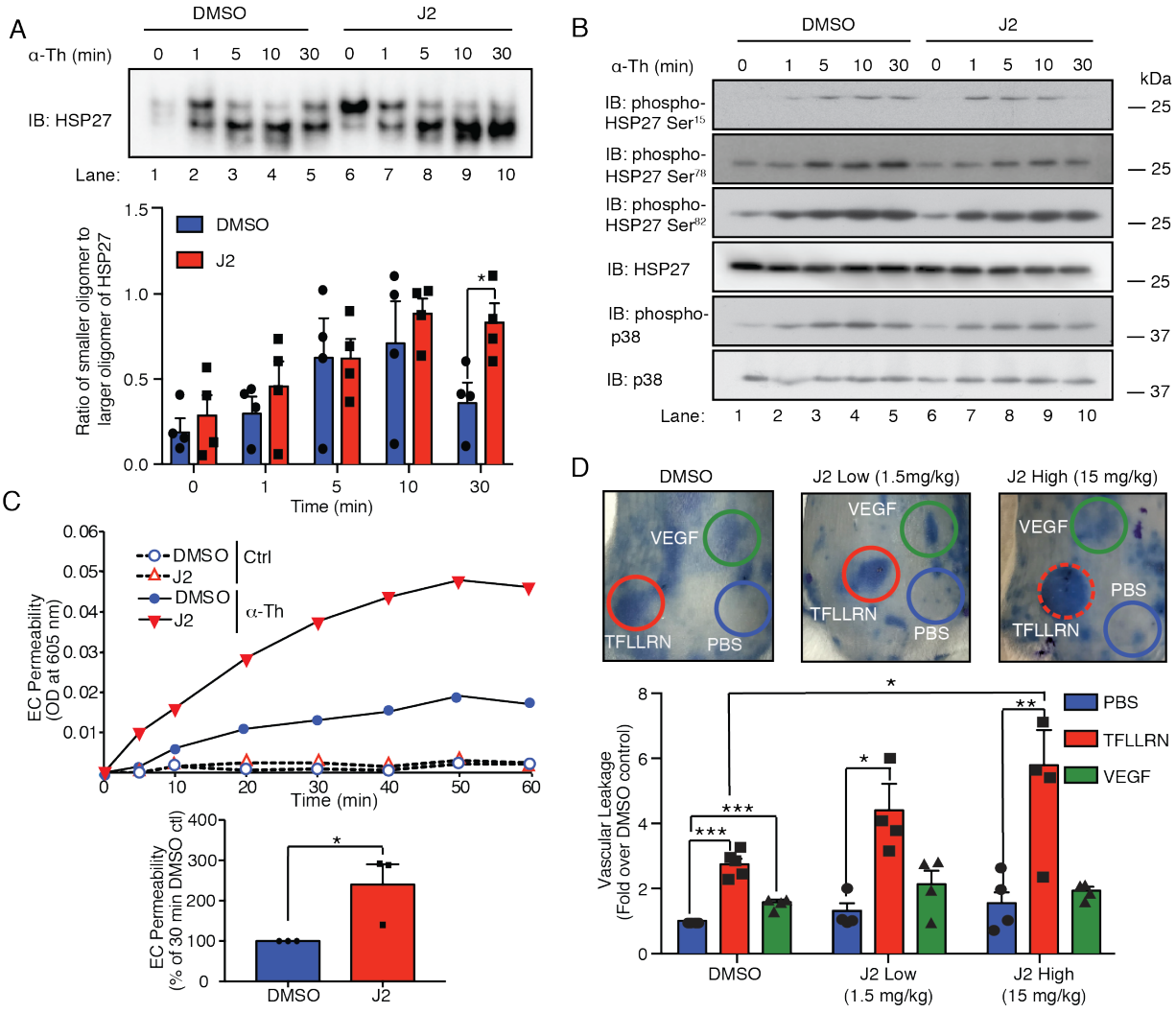
A
DMSO
J2
α-Th (min)
0 1 5 10 30 0 1 5 10 30
IB: HSP27
Lane: 1 2 3 4 5 6 7 8 9 10
Ratio of smaller oligomer to larger oligomer of HSP27
DMSO
J2
Time (min)
B
DMSO
J2
α-Th (min)
0 1 5 10 30 0 1 5 10 30
kDa
IB: phospho-HSP27 Ser15
IB: phospho-HSP27 Ser78
IB: phospho-HSP27 Ser82
IB: HSP27
IB: phospho-p38
IB: p38
25
25
25
25
37
37
Lane: 1 2 3 4 5 6 7 8 9 10
C
EC Permeability (OD at 605 nm)
DMSO Ctrl
J2
DMSO α-Th
J2
Time (min)
EC Permeability (% of 30 min DMSO ctl)
DMSO
J2
D
DMSO
J2 Low (1.5mg/kg)
J2 High (15 mg/kg)
VEGF
TFLLRN
PBS
Vascular Leakage (Fold over DMSO control)
PBS
TFLLRN
VEGF
DMSO
J2 Low (1.5 mg/kg)
J2 High (15 mg/kg)

Chapter 4

GPCR regulation of non-canonical p38 and HSP27 IL-6 cytokine production

The vascular endothelium plays a key role in the inflammatory response. Eliciting both an immediate response to injury and pathogens, as well as a secondary sustain response to thoroughly clear the body of infection and resolve injury before returning to fluid and macromolecule homeostasis. This secondary response is often through upregulation of chemokine and cytokines, however, the mechanism through which this occurs after GPCR activation is unclear. In this chapter we provide a plausible mechanism for how GPCR-activated non-canonical p38 signaling regulate IL-6 production in primary endothelial cells. We also show PAR1-induced IL-6 production requires HSP27, suggesting PAR1 activated non-canonical p38 signals through HSP27 for both endothelial barrier permeability as well as through the secondary inflammatory response of cytokine upregulation.

4.1 Introduction

Key hallmarks of vascular inflammation include endothelial barrier disruption and cytokine production resulting in increased permeability, tissue edema, and subsequent organ failure if unresolved. Many vasoactive factors produced during inflammation signal through GPCRs (Sprague and Khalil, 2009). Generation of the coagulant protease thrombin, during tissue injury and inflammation can trigger inflammatory responses including endothelial barrier disruption (Marin et al., 2001, ç et al., 2016) and cytokine production. Endothelial disruption is a rapid inflammatory response, while a secondary more sustained inflammatory response is the induction of cytokine production. Cytokine production initiates for the recruitment of leukocytes to sites of inflammation and helps in tissue resolution (Sun and Ye, 2012).

p38 has been shown to mediate GPCR induction of cytokine production (Cuenda and Rousseau, 2007, Li et al., 2001, Kotlyarov et al., 2002, Marin et al., 2001). Classically p38 is activated by a 3-tiered kinase cascade, however, PAR1-induced p38 activation has been shown to promote pro-inflammatory signaling through p38α after TAB2 or TAB3 binding through a zinc finger domain on the ubiquitinated PAR1 receptor allowing the stabilization of TAB1 to form a complex and autoactivation of p38 through a conformational change allowing p38α to have a higher affinity for ATP (Grimsey et al., 2015, DeNicola et al., 2013). However, it is unknown if non-canonical p38 activators TAB1 and TAB2 or TAB3 regulate GPCR induced cytokine production or if p38 induced cytokine production is from the classical 3-tiered kinase cascade and will be determined in this chapter.

Mice with global knockout of the HSP27 gene, HSPB1, exhibit increased pro-inflammatory cytokine generation (Crowe et al., 2013), suggesting a potential role for HSP27 in GPCR-induced cytokine regulation *in vivo*. *In vitro* studies have shown HSP27 is required

for production of the pro-inflammatory mediators: IL-6, IL-8, and COX-2 after IL-1β stimulation (Alford et al., 2007). However, it is not known if HSP27 has a role in GPCR-stimulated cytokine generation and will be examined in chapter 4.

4.2 Results

Thrombin and histamine induced IL-6 production requires non-canonical p38

IL-6 is a pro-inflammatory cytokine secreted by endothelial cells following stimulation by various GPCRs agonists including thrombin and histamine (Marin et al., 2001, Li et al., 2001). However, the role and relevance of GPCR-stimulated TAB1–dependent p38 activation in IL-6 production has not been determined and was examined by measuring IL-6 production in HUVECs transfected with siRNAs targeting TAB1 and TAB2 or TAB1 and TAB3. Thrombin induced a ˜2-fold increase in IL-6 production that was significantly reduced in endothelial cells co-depleted of TAB1–TAB3 (Fig. 4.1A), consistent with thrombin-induced TAB1–TAB3–dependent activation of p38 in HUVEC protein (Grimsey et al., 2019). Despite the apparent decrease in IL-6 production stimulated by thrombin in HUVECs co-depleted of TAB1–TAB2, the results were variable and not significant (Fig. 4.1A). In contrast, co-depletion of either TAB1–TAB2 or TAB1–TAB3 resulted in a marked and significant decrease in IL-6 production stimulated by histamine compared with nonspecific siRNA-transfected control cells (Fig. 4.1B). These findings are also consistent with a role for both TAB1–TAB2 and TAB1–TAB3 in histamine-stimulated p38 activation in HUVEC protein (Grimsey et al., 2019). Together, these findings indicate that GPCR agonists induce p38 proinflammatory signaling in various endothelial cell types via a non-canonical TAB1–dependent pathway.

Thrombin induced IL-6 production requires HSP27

Chapters 2 and 3 of this dissertation show GPCR-activated p38 signals through HSP27 to regulate pro-inflammatory signaling leading to endothelial barrier recovery. However, it is unknown if HSP27 regulates PAR1-induced IL-6 production. Previous studies have shown HSP27 regulates IL-6 induction in endothelial cells after IL-1β induction (Alford et al., 2007), but it is unknown if HSP27 regulates GPCR-induced IL-6 production. To determine the impact of HSP27 on PAR1-activated IL-6 production, HUVECs depleted of endogenous HSP27 with siRNA or NS siRNA were stimulated with α-Th for 2 hr and IL-6 transcript levels measured by qPCR. The longer α-Th stimulated time course produced 6-fold increase in IL-6 production compared to non-stimulated HUVECs (Fig. 4.2). This thrombin-induced upregulation of IL-6 was significantly dampened by depletion of HSP27. This finding suggests HSP27 is required for Thrombin-induced IL-6 production in primary endothelial cells.

4.3 Conclusion and Discussion

MAPKs exist as distinct signaling cascades, comprised of three evolutionarily conserved, sequential acting kinases including a MAPK, MAP2K, and MAP3K (Cuenda and Rousseau, 2007). MAP3Ks are typically activated by phosphorylation mediated by upstream MAP2Ks. In contrast to canonical MAPK cascades, the p38α isoform can also be autoactivated through its interaction with TAB1 or through phosphorylation facilitated by the tyrosine kinase Zap70 (Ge et al., 2002, Salvador et al., 2005). Although MKK3 and MKK6 are the major upstream MAP2Ks for p38α activation in response to cytokines or stress, we found that co-depletion of either TAB1–TAB2 or TAB1–TAB3 caused a significant loss of GPCR-induced cytokine production

of IL-6.

Although activation of p38α by the three-tiered kinase cascade is the presumed major pathway for many inflammatory mediators, our data provide compelling evidence that TAB1-mediated p38α autoactivation is the predominate pathway utilized by mammalian GPCRs in human primary endothelial cells and reveal a new paradigm by which GPCRs stimulate p38 inflammatory signaling through HSP27 to regulate IL-6 transcription. In addition, the mechanisms by which GPCR-stimulated TAB1-induced p38 signaling controls various inflammatory responses including induction of cytokine production remains poorly understood. We provide HSP27 as a plausible explanation for the mechanism by which PAR1 induces IL-6 production base on HSP27 siRNA depletion significantly attenuating thrombin-induce IL-6 cytokine transcription. What effect HSP27 phosphorylation has on IL-6 production is also a question that warrants further exploration.

In this chapter we provide evidence for a plausible pathway of GPCR-induced pro-inflammatory signaling for cytokine production through non-canonical activation of p38 to activate HSP27 and regulation IL-6 production. Depletion of the p38α upstream non-canonical activators TAB1 and TAB2 or TAB3 or HSP27 dampen PAR1 and histamine induced IL-6 upregulation affecting sustained pro-inflammatory responses.

4.4 Materials and Methods

Transfections and siRNAs

HUVECs and HDMECs were transfected with siRNAs using TransIT-X2 according to manufacturer's instructions (Mirus Bio). HSPPB1 siRNA (5'-

AAGGACGAGCATGGCTACATC-3'); TAB1 siRNA (5-CGGCUAUGAUGGCAACCGATT-3); TAB2 siRNA (5'-GUCAAUAGCCAGACCUUAATT-3); and TAB3 siRNA (5'-CGGUAUAGUACAAAUCCAATT-3); and nonspecific (ns) All Stars Negative Control siRNA (5'-GGCUACGUCCAGGAGCGCACC-3') used at 12.5 nM in HUVEC and 25 nM in HDMECs and were all obtained from Qiagen.

Antibodies and reagents

α-Thrombin was purchased from Enzyme Research Laboratories. SYBR Green master mix and TRIzol were purchased from Thermo Fisher Scientific, Direct-zolTM RNA MiniPrep Plus was purchased from Zymo Research, iScript gDNA Clear cDNA Synthesis kit purchased from Bio-Rad. Histamine dihydrochloride was from Tocris Bio-Techne.

qPCR

The cDNA was generated from mRNA extracted from confluent cell cultures using Direct-zolTM RNA MiniPrep Plus (Zymo), cDNA synthesis was carried out using iScriptTM gDNA Clear cDNA Synthesis kit (Bio-Rad). Reverse transcription-qPCRs were performed using iTAQTM Universal SYBR Green Supermix (Bio-Rad). The following gene-specific primers were used:β-actin (forward 5-CAAGCAGGAGTATGACGAGTC-3, reverse 5-GCCATGCCAATCTCATCTTG-3); and IL-6 (forward 5-GGAGACTTGCCTGGTGAAA-3, reverse 5-CTGGCTTGTTCCTCACTACTC-3). The number of cycles until threshold (Ct) was determined using an Eppendorf Mastercycler RealPlex2. To normalize for variation in the total number of cells and the efficiency of the mRNA extraction, the Ct value for β-actin was subtracted from the Ct values for each target. The change in expression for each target was then determined relative to cells transfected with nonspecific

siRNA using the $\delta\delta$CT method. All experiments were performed in triplicate.

Cell culture

Pooled-primary human umbilical vein endothelial cells (HUVEC) were purchased from Lonza and used up to passage 6. HUVECs were grown in EGM-2 (Lonza). All cells were cultured in a 37°C incubator with 5% CO_2.

Statistical analyses

Statistical significance between datasets with three or more experimental groups was determined using one-way analysis of variance (ANOVA) including a Tukey's test for multiple comparisons. Statistical difference between two experimental groups was determined using a two-tailed unpaired t-test. For all tests, a p-value of 0.05 was used as the cutoff to determine significance. All experiments were repeated a least three times, and p-values are indicated in each figure. All statistical analysis was performed using GraphPad prism 7.

4.5 Acknowledgements

This research was funded by National Institutes of Health (R35 GM127121), a pre-doctoral fellowship by Tobacco-Related Disease Research Program (TRDRP 27DT-0009), as well as a training grant by NIH/NIGMS (T32 GM007752).

A portion of chapter 4 figures are published as: Grimsey NJ, Lin Y, Narala R, **Rada CC**, Mejia-Pena H, Trejo J. "G protein-coupled receptors activate p38 MAPK via a non-canonical TAB1-TAB2- and TAB1-TAB3-dependent pathway in endothelial cells." Journal of Biological

Chemistry. 2019 Apr 12;294(15):5867-5878. This dissertation author is a co-author of the manuscript and performed and designed experiments used in this dissertation.

4.6 References

ALFORD, K. A., GLENNIE, S., TURRELL, B. R., RAWLINSON, L., SAKLATVALA, J. DEAN, J. L. 2007. Heat shock protein 27 functions in inflammatory gene expression and transforming growth factor-beta-activated kinase-1 (TAK1)-mediated signaling. J Biol Chem, 282, 6232-41.

Ç, K., SAVANT, S., GIRI, H., GHOSH, A., FISSLTHALER, B., FLEMING, I., RAM, U., BERA, A. K., AUGUSTIN, H. G. DIXIT, M. 2016. Angiopoietin-2 mediates thrombin-induced monocyte adhesion and endothelial permeability. J Thromb Haemost.

CROWE, J., AUBAREDA, A., MCNAMEE, K., PRZYBYCIEN, P. M., LU, X., WILLIAMS, R. O., BOU-GHARIOS, G., SAKLATVALA, J. DEAN, J. L. 2013. Heat shock protein B1-deficient mice display impaired wound healing. PLoS One, 8, e77383.

CUENDA, A. ROUSSEAU, S. 2007. p38 MAP-kinases pathway regulation, function and role in human diseases. Biochim Biophys Acta, 1773, 1358-75.

DENICOLA, G. F., MARTIN, E. D., CHAIKUAD, A., BASSI, R., CLARK, J., MARTINO, L., VERMA, S., SICARD, P., TATA, R., ATKINSON, R. A., KNAPP, S., CONTE, M. R. MARBER, M. S. 2013. Mechanism and consequence of the autoactivation of p38alpha mitogen-activated protein kinase promoted by TAB1. Nat Struct Mol Biol, 20, 1182-90.

GE, B., GRAM, H., DI PADOVA, F., HUANG, B., NEW, L., ULEVITCH, R. J., LUO, Y. HAN, J. 2002. MAPKK-independent activation of p38alpha mediated by TAB1-dependent autophosphorylation of p38alpha. Science, 295, 1291-4.

GRIMSEY, N. J., AGUILAR, B., SMITH, T. H., LE, P., SOOHOO, A. L., PUTHENVEEDU, M. A., NIZET, V. TREJO, J. 2015. Ubiquitin plays an atypical role in GPCR-induced p38 MAP kinase activation on endosomes. J Cell Biol, 210, 1117-31.

GRIMSEY, N. J., LIN, Y., NARALA, R., RADA, C. C., MEJIA-PENA, H. TREJO, J. 2019. G protein-coupled receptors activate p38 MAPK via a non-canonical TAB1-TAB2- and TAB1-TAB3-dependent pathway in endothelial cells. J Biol Chem, 294, 5867-5878.

KOTLYAROV, A., YANNONI, Y., FRITZ, S., LAASS, K., TELLIEZ, J. B., PITMAN, D., LIN, L. L. GAESTEL, M. 2002. Distinct Cellular Functions of MK2. Molecular and Cellular Biology, 22, 4827-4835.

LI, Y., CHI, L., STECHSCHULTE, D. J. DILEEPAN, K. N. 2001. Histamine-induced production of interleukin-6 and interleukin-8 by human coronary artery endothelial cells is enhanced by endotoxin and tumor necrosis factor-alpha. Microvasc Res, 61, 253-62.

MARIN, V., FARNARIER, C., GRES, S., KAPLANSKI, S., SU, M. S., DINARELLO, C. A. KAPLANSKI, G. 2001. The p38 mitogen-activated protein kinase pathway plays a critical role in thrombin-induced endothelial chemokine production and leukocyte recruitment. Blood, 98, 667-73.

SALVADOR, J. M., MITTELSTADT, P. R., GUSZCZYNSKI, T., COPELAND, T. D., YAMAGUCHI, H., APPELLA, E., FORNACE, A. J., JR. ASHWELL, J. D. 2005. Alternative p38 activation pathway mediated by T cell receptor-proximal tyrosine kinases. Nat Immunol, 6, 390-5.

SPRAGUE, A. H. KHALIL, R. A. 2009. Inflammatory cytokines in vascular dysfunction and vascular disease. Biochem Pharmacol, 78, 539-52. SUN, L. YE, R. D. 2012. Role of G protein-coupled receptors in inflammation. Acta Pharmacol Sin, 33, 342-50.

4.7 Figures

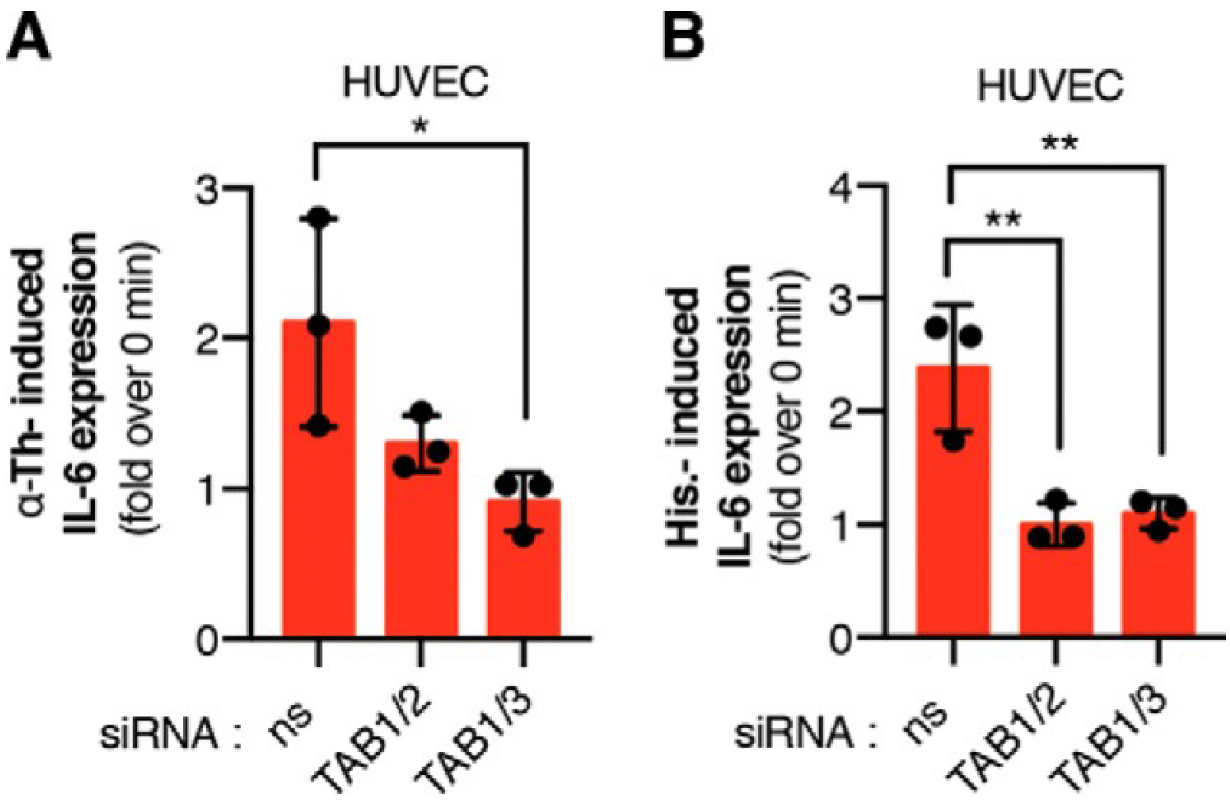

Figure 4.1: Thrombin and histamine induced IL-6 production requires non-canonical p38.HUVEC transfected with nonspecific (ns), TAB1 and TAB2 (TAB1/2), or TAB1 and TAB3 (TAB1/3) siRNAs and were stimulated with (A) 10 nm α-thrombin (α-Th) for 5 min or (B) 1 μm histamine (His.) for 7.5 min and lysed, and total RNA was isolated for qPCR as described above. The data (mean $\pm$ S.D., n = 3) are representative of three independent experiments expressed as the fold over 0 min control and analyzed by Student's t test (*, $p \leq 0.05$; **, $p \leq 0.01$).

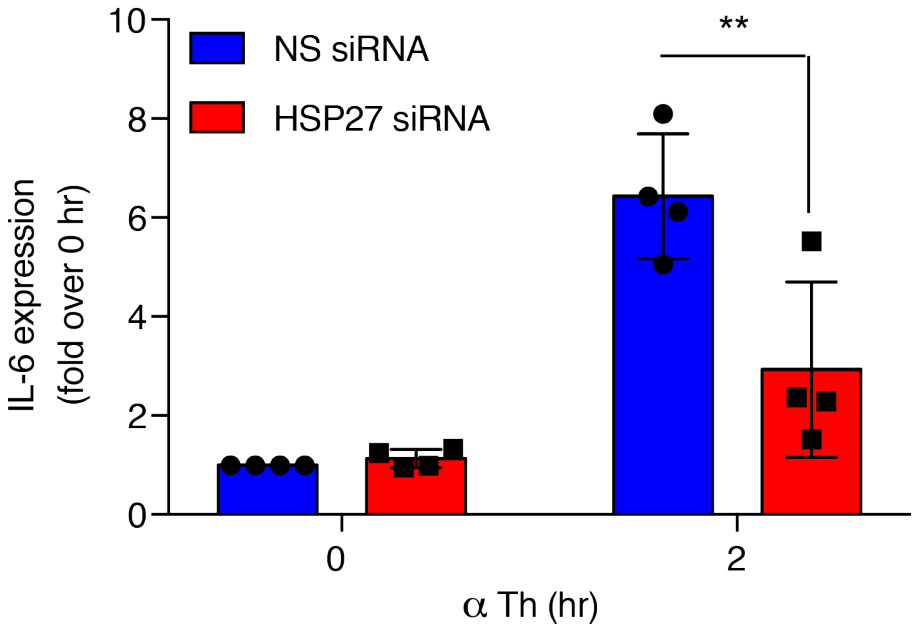

Figure 4.2: Thrombin induced IL-6 production requires HSP27. HUVEC transfected with non-specific (ns) or HSP27 siRNA and were stimulated with 10 nm α-thrombin (α-Th) for 2 hrs and lysed, and total RNA was isolated for qPCR as described above. The data (mean $\pm$ S.D., n = 3) are representative of three independent experiments and analyzed by Student's t test ($p \leq 0.01$).

Chapter 5

Conclusion: Impact of GPCR-induced vascular inflammation resolution for therapeutic potential.

Vascular inflammation is a highly regulated complex process that involves not only the opening of the endothelial barrier, but also a timely resolution of the inflammatory state. GPCRs provided an exceptionally attractive drug targets for their ability to translate an external stimulus (ligand) to an intracellular response, and over a third of FDA-approved drugs on the market target GPCRs. Decades of research on pro-inflammatory endothelial GPCRs have translated into numerous therapeutic interventions for the treatment of diseases associated with vascular permeability, such as the blockbuster drug that blocks the histamine receptor in the treatment of allergic responses. However, the mechanistic details of how resolution of the endothelial barrier to the re-establishment of tissue homeostasis after inflammation have been understud-

ied. My dissertation work has focused on detailed mechanistic understanding in elucidating the transient signaling pathways of GPCR barrier resolution after agonist disruption and identifying and characterizing the key modulator, HSP27. In the remainder of this chapter I will discuss the impact my work has on the vascular inflammation field and how HSP27 could be targeted therapeutically, as well as potential future directions of this project.

5.1 Delineation of novel GPCR signaling pathway

Much of the work on GPCRs in the vascular endothelium have examined the mechanisms of how the endothelial barrier opens, but the mechanisms of resolution have been severely neglected. HSP27 provides a novel target for therapeutic intervention as a key temporal regulator to dampen barrier opening and initiate the return to a homeostatic baseline of minimal fluid, macromolecule, and leukocyte transmigration. The dynamic regulation of HSP27 by dual kinase activity of MK2 and MK3 provides a unique tool to target specific HSP27 phosphorylation by inhibiting each upstream kinase. Inhibition of p38 has the ability to stop phosphorylation on all three phosphorylation sites, while MK2 or MK3 inhibitors alone affect specific phosphorylation giving an added level of regulation for HSP27. While I do not specifically delineate the role of each individual phosphosite on HSP27 alone, further work could be done to determine if each of the three highlighted Serine phosphorylation sites has a specific function in the vascular endothelium. My work in delineating the kinases responsible for HSP27 phosphorylation provides a much more attractive drug target than targeting the chaperone itself as kinase active sites have been pursued in the pharmaceutical industry for over 20 years (Cohen and Alessi, 2013) and provide a specific pocket for blockade. Although p38 affects all three phosphorylation sites on HSP27 and would be an ideal kinase to inhibit to affect HSP27 activity, p38 inhibitors

have not made it through stage II of clinical trials due to off target effects (Martinez-Limon et al., 2020). Thus, MK2 and MK3, which are expressed much less ubiquitously, would provide a more attractive target for drug development for HSP27 activity inhibition.

5.2 HSP27 function in controlling endothelial barrier properties

The ability of HSP27 inhibition to open the endothelial barrier after GPCR agonist stimulation could also play a unique role in hijacking the vascular system to open specific vascular beds for localized drug delivery. Thrombin is a potential, yet localized inducer of vascular leakage. If HSP27 depletion has no effect on baseline permeability, an inhibitor such as the J2 compound could be used in conjunction with the PAR1 activating peptide (or other permeability inducing GPCR agonists such as histamine or bradykinin) and selectively open a specific vascular bed on command to a greater extent that thrombin alone. This could provide a wide array of therapeutic potential to specifically open the vascular beds of specific organs to deliver drugs that would not normally be permissible due to their structure.

In a study that overexpressed HSP27 in the brain microvascular cells, an increase in blood brain barrier properties were observed with the overexpression of HSP27 (Shi et al., 2017). PAR1 is also expressed in the brain microvascular (Brailoiu et al., 2017). This suggests that PAR1-activated HSP27 function could potentially be leveraged in the notoriously fickle blood brain barrier to allow selective drug delivery to the brain. One major pitfall of drugs for diseases such as Parkinson's and Alzheimer's are their ineffectiveness to pass the blood brain barrier due to their chemical structure and are thus unable to treat the brain pathophysiology. The potential of HSP27 and PAR1 activation to provide a means of drug delivery could have large implications in the field of neurodegenerative diseases. And the blood brain barrier is but a single

example of a potential vascular bed that HSP27 and GPCR agonism could hijack for therapeutic intervention.

5.3 Future Directions of HSP27 regulation of Barrier Resolution

Future directions of this project would include the impact HSP27 has on actin dynamics. HSP27 has been described to function as an actin capping protein to inhibit filamentous (F)-actin formation (Rogalla et al., 1999, Pichon et al., 2004, Benndorf et al., 1994) although we do not specifically test that assumption in our work. Thrombin is also well known to cause actin stress fibers to pull the endothelial monolayer apart through actin myosin contractility (Coughlin, 2000, Mehta and Malik, 2006). However, the work of this thesis suggests that HSP27 may be a key mediator to stop actin polymerization and creation of F-actin after thrombin induction and be a temporal modulator to stop barrier opening and signal for the initiation of barrier resolution and return to homeostasis.

It is also feasible to suggest that HSP27 is modulating a stabilizing pool of actin such as cortical actin for barrier recovery after agonist induction more similar to what is seen in the barrier stabilizing GPCR, S1PR1, through Rac1 activation (Marinkovic et al., 2015, Komarova et al., 2007). We show this PAR1-p38 pathway does not affect the small GTPase RhoA but did not asses the function of the barrier stabilizing GTPase Rac1. Rac1 has been shown to signal through PAR1 after APC cleavage of the N-terminus at arginine 46 instead of canonical thrombin cleavage of the receptor at arginine 41 (Ludeman et al., 2005). Since HSP27 phosphorylation status controls the initiation of barrier resolution, it would be interesting to determine if Rac1 activation affects HSP27 phosphorylation status or activity.

5.4 Final thoughts

Throughout my dissertation work I have had the opportunity to learn and grow as a scientist while making contributions to the fields of vascular biology, pharmacology, and cell signaling. I hope the findings of this dissertation advance each of these fields to lay groundwork for further investigations of HSP27 in regulating vascular permeability and provide sufficient evidence to lead to the development of therapeutic targets to treat the numerous diseases of both chronic and acute vascular inflammation.

5.5 References

BENNDORF, R., HAYESS, K., RYAZANTSEV, S., WIESKE, M., BEHLKE, J. LUTSCH, G. 1994. Phosphorylation and supramolecular organization of murine small heat shock protein HSP25 abolish its actin polymerization-inhibiting activity. J Biol Chem, 269, 20780-4.

BRAILOIU, E., SHIPSKY, M. M., YAN, G., ABOOD, M. E. BRAILOIU, G. C. 2017. Mechanisms of modulation of brain microvascular endothelial cells function by thrombin. Brain Res, 1657, 167-175.

COHEN, P. ALESSI, D. R. 2013. Kinase drug discovery–what's next in the field? ACS Chem Biol, 8, 96-104.

COUGHLIN, S. R. 2000. Thrombin signalling and protease-activated receptors. Nature, 407, 258-64.

HAUSER, A. S., ATTWOOD, M. M., RASK-ANDERSEN, M., SCHIOTH, H. B. GLORIAM, D. E. 2017. Trends in GPCR drug discovery: new agents, targets and indications. Nat Rev Drug Discov, 16, 829-842.

KOMAROVA, Y. A., MEHTA, D. MALIK, A. B. 2007. Dual regulation of endothelial junctional permeability. Sci STKE, 2007, re8.

LUDEMAN, M. J., KATAOKA, H., SRINIVASAN, Y., ESMON, N. L., ESMON, C. T. COUGHLIN, S. R. 2005. PAR1 cleavage and signaling in response to activated protein C and thrombin. J Biol Chem, 280, 13122-8.

MARINKOVIC, G., HEEMSKERK, N., VAN BUUL, J. D. DE WAARD, V. 2015. The Ins and Outs of Small GTPase Rac1 in the Vasculature. J Pharmacol Exp Ther, 354, 91-102.

MARTINEZ-LIMON, A., JOAQUIN, M., CABALLERO, M., POSAS, F. DE NADAL, E. 2020. The p38 Pathway: From Biology to Cancer Therapy. Int J Mol Sci, 21.

MEHTA, D. MALIK, A. B. 2006. Signaling mechanisms regulating endothelial permeability. Physiol Rev, 86, 279-367.

PARSONS, M. E. GANELLIN, C. R. 2006. Histamine and its receptors. Br J Pharmacol, 147 Suppl 1, S127-35.

PICHON, S., BRYCKAERT, M. BERROU, E. 2004. Control of actin dynamics by p38 MAP kinase - Hsp27 distribution in the lamellipodium of smooth muscle cells. J Cell Sci, 117, 2569-77.

ROGALLA, T., EHRNSPERGER, M., PREVILLE, X., KOTLYAROV, A., LUTSCH, G., DUCASSE, C., PAUL, C., WIESKE, M., ARRIGO, A. P., BUCHNER, J. GAESTEL, M. 1999. Regulation of Hsp27 oligomerization, chaperone function, and protective activity against oxidative stress tumor necrosis factor alpha by phosphorylation. Journal of Biological Chemistry, 274, 18947-18956.

SHI, Y., JIANG, X., ZHANG, L., PU, H., HU, X., ZHANG, W., CAI, W., GAO, Y., LEAK, R. K., KEEP, R. F., BENNETT, M. V. CHEN, J. 2017. Endothelium-targeted overexpression of heat shock protein 27 ameliorates blood-brain barrier disruption after ischemic brain injury. Proc Natl Acad Sci U S A, 114, E1243-E1252.